Functional polymer brush-coating to prevent biomaterial associated infections

Muszanska, Agnieska Karolina

Functional Polymer Brush-Coating to Prevent Biomaterial Associated Infections

Agnieszka Karolina Muszanska

Functional Polymer Brush-Coating to Prevent Biomaterial Associated Infections

University Medical Center Groningen, University of Groningen
Groningen, The Netherlands

Cover design by Ed Rochford

Printed by Off Page, Amsterdam, The Netherlands

ISBN (printed version): 978-90-367-6493-3

ISBN (electronic version): 978-90-367-6494-0

rijksuniversiteit groningen

Functional Polymer Brush-Coating to Prevent Biomaterial Associated Infections

Proefschrift

ter verkrijging van de graad van doctor aan de
Rijksuniversiteit Groningen
op gezag van de
rector magnificus, prof. dr. E. Sterken,
en volgens besluit van het College voor Promoties

De openbare verdediging zal plaatsvinden op
woensdag 27 november 2013
om 14.30 uur

door

Agnieszka Karolina Muszanska
geboren op 14 september 1982
te Rymanów, Polen

Promotores:	Prof. dr. ir. W. Norde
	Prof. dr. ir. H.J. Busscher
	Prof. dr. H.C. van der Mei
Beoordelingscommissie :	Prof. dr. A. Herrmann
	Prof. dr. J.A. Loontjens
	Prof. dr. S.K. Bulstra

Paranimfen: Lucja Jarosz

Agnieszka Gruszka

The important thing is not to stop questioning. Curiosity has its own reason for existing."

Albert Einstein

Contents

Chapter 1

General introduction

In the rapidly ageing Western societies, the use of biomaterial implants and devices for regenerative medicine is instantly growing. Moreover, the expectations for better quality of life become higher and higher along with improved and more affordable health care. Nowadays, technologies in the field of biomaterials offer impressive solutions to promote tissue restoration and regeneration [1]. A wide range of biomaterials used for medical implants including ceramics, metals, biocompatible polymers and composites is currently being used in the clinic to approach various medical challenges, from prosthetic devices for trauma patients or plastic surgery implants to daily used contact lenses [2,3]. Advanced technologies, based on different scientific disciplines, are currently aimed to develop materials with improved biocompatibility and reduced risk of causing biomaterials-associated infection [4-6].

SILICONE RUBBER BASED IMPLANTS

Polydimethylsiloxane, better known as silicone rubber, is a non-biodegradable, biocompatible polymeric material widely used as a soft tissue implant, like voice prostheses, breast implants, finger joints, testicular implants, maxillofacial reconstructive implants, urinary catheters, hearth valves and contact lenses [7,8]. Presence of Si–O–Si linkages in the polymer backbone (structure presented in Figure 1) determines important properties, such as good thermal and chemical stability, resistance to oxygen, ozone and UV light, low chemical reactivity, elastic nature and low surface tension [9]. Because of these physico-chemical properties, silicone rubber (a) has a very good biostability necessary for long term implantation, (b) can be easily sterilized and shaped, (c) is non-allergic and (d) has low thrombogenicity. However, when silicone rubber comes into direct contact with body fluids proteins may adhere strongly to its surface within a few minutes. The proteinaceous conditioning film thus formed attracts different micro-

organisms like *Candida*, *Staphylococci* or *Pseudomonas* which is a first step in biofilm formation that may lead to infection of an implant [10].

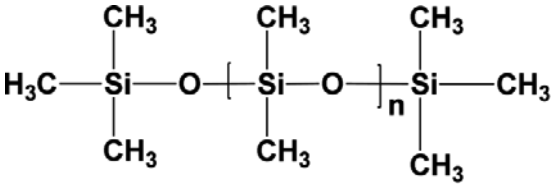

Figure 1. Chemical structure of silicone rubber (polydimethylsiloxane).

BIOMATERIALS-ASSOCIATED INFECTIONS

Biomaterials-associated infections (BAI) remain the number one cause of failure of biomaterial implants or devices despite the development of various strategies to control microbial contamination during implantation, like modern, ventilated operating theatres and impermeable personnel clothing [11]. The occurrence of BAI has serious clinical and economic consequences. In case of cardiovascular implants BAI is associated with a high mortality risk [12], and in case of orthopedic or plastic surgery implants, may result in serious disabilities or psychological trauma [13]. Infection starts with the adhesion of microorganisms to the surface of a biomaterial. The adhering microorganisms may grow into a biofilm, a complex structure where the microorganisms embed themselves in a matrix of extracellular polymeric substances (EPS) containing polysaccharides, proteins, teichoic acids and extracellular DNA [14]. This self-produced matrix provides the microorganisms protection against antibiotics, disinfectants and against the components of the immune defense system of the host [15,16]. Common treatment procedures for patients suffering from BAI include intravenous and oral antibiotic therapy for several weeks or months. Nevertheless, treatments often fail and then the fate of an infected implant or device is usually replacement at

great discomfort for the patient and several-fold greater infection risk of the secondary implant due to the presence of bacteria in the tissue surrounding the implant [13,17].

STRATEGIES TO PREVENT IMPLANT INFECTIONS

Since bacterial adhesion to the surface of a biomaterial is the first step in biofilm formation, various surface modifications have been developed that aim at reducing the contact with approaching bacteria. Coatings based on hydrophilic poly(ethylene oxide) polymer brushes [18-21], polyamidoamine dendrimers [22] coatings of poly(2-methyl-2-oxazoline) [23], zwitterionic structures such as sulfobetaine [24] or phospholipid polymers [25] are already known in the literature for their good anti-adhesive properties. Another strategy to prevent BAI is immobilizing the surface of a biomaterial with various bactericidal agents that are proven to kill bacteria upon contact such as antibiotics [26], bioactive antibodies [27], nitric oxide [28], metal nanoparticles [29,30], furanones [31], cationic antimicrobial peptides [32,33] or chitosan and its quaternized derivatives [34].

POLYMER BRUSH COATINGS

Polymer brush coatings are currently the most promising non-adhesive coatings as they reduce the adhesion of bacteria by orders of magnitude [20,35]. A polymer brush in an aqueous environment is formed when hydrophilic polymer chains end-grafted to a surface in a high packing density are forced to stretch away from the surface into the adjacent medium [18,36]. Polymer chains can be covalently attached to the surface or simply physically adsorbed. Chemical attachment is often assumed to provide better stability than physi-sorption. Control of the brush density requires a more complex, time-consuming procedure

[37]. In case of block copolymers the physical immobilization of polymer chains is a very easy spontaneous process based on hydrophobic or electrostatic attraction with the surface. The conformation of the adsorbed polymer layer depends on the grafting density. At low grafting densities, the polymer chains are coiled attaining a mushroom conformation. With increasing grafting density, the polymer chains stretch out into the medium attaining a brush conformation, as presented in Figure 2 [38]. The basic criterion to obtain the brush conformation is that the distance between two anchoring points should be less than two times the radius of a coiled polymer chain [18,39].

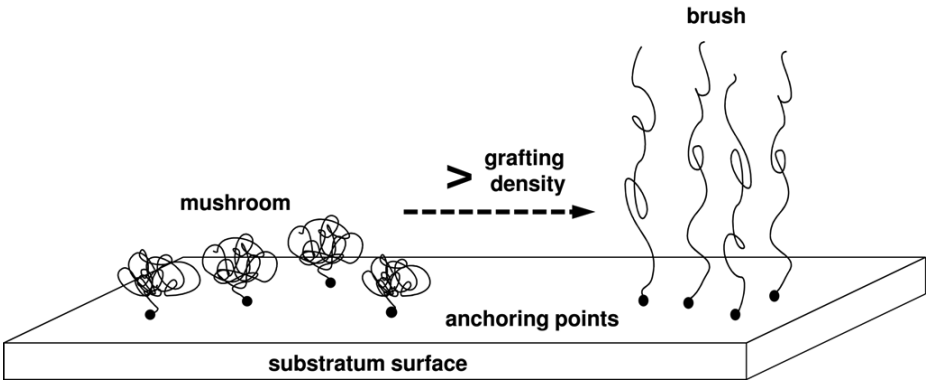

Figure 2. Conformations of hydrophilic polymer chains end-grafted on a surface in aqueous media from a mushroom conformation (left side) at low grafting densities to a brush conformation (right side) at high grafting densities.

Compression of such a structure upon bacterial approach gives rise to an osmotic pressure and decreases the mobility of the polymer chains, causing steric repulsion of approaching microorganisms, as illustrated in Figure 3. Thus, polymer brush coatings can act as a mechanical barrier for deposition of microorganisms on the surface of a biomaterial.

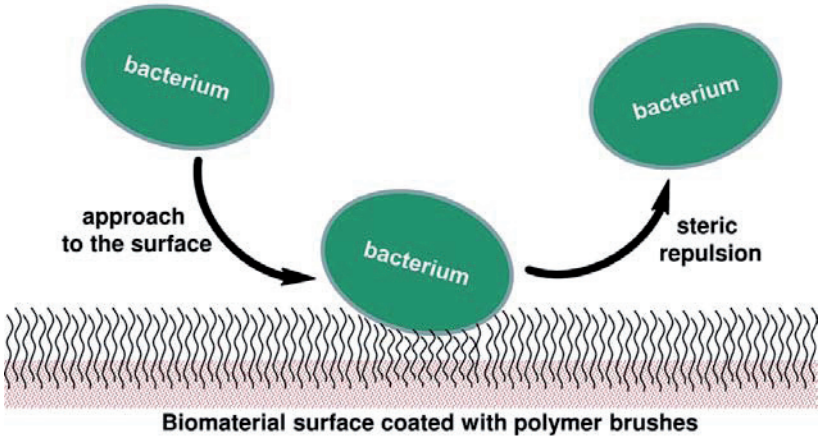

Figure 3. Mechanism of the anti-adhesive action of a polymer brush coating.

AIM OF THIS THESIS

There are numerous reports in the literature on non-adhesive properties of polymer brush coatings but none of them shows complete prevention of microbial adhesion. It is proven that even a few adhering bacteria are able to form a biofilm [35]. Hence, such coatings are simply not capable to prevent BAI. Another concern related to clinical applications is the fact that polymer brush coatings with strong anti-adhesive functionalities do not support tissue integration, impairing the wound healing process. The next logical steps to improve polymer brush coating functionalities for suppressing BAI is to introduce moieties in the brush layer that (a) prevent adhering bacteria from growing into a biofilm and (b) that stimulate good tissue integration.

The aim of this thesis is to develop and evaluate surface coatings in which anti-adhesive, antimicrobial and tissue integrating functionalities are combined. To this end, antimicrobial peptides (AMP) and tissue integrating peptides (RGD)

are covalently attached to poly(ethylene oxide) chains allowing the formation of a multi-functional brush coating, as illustrated in Figure 4.

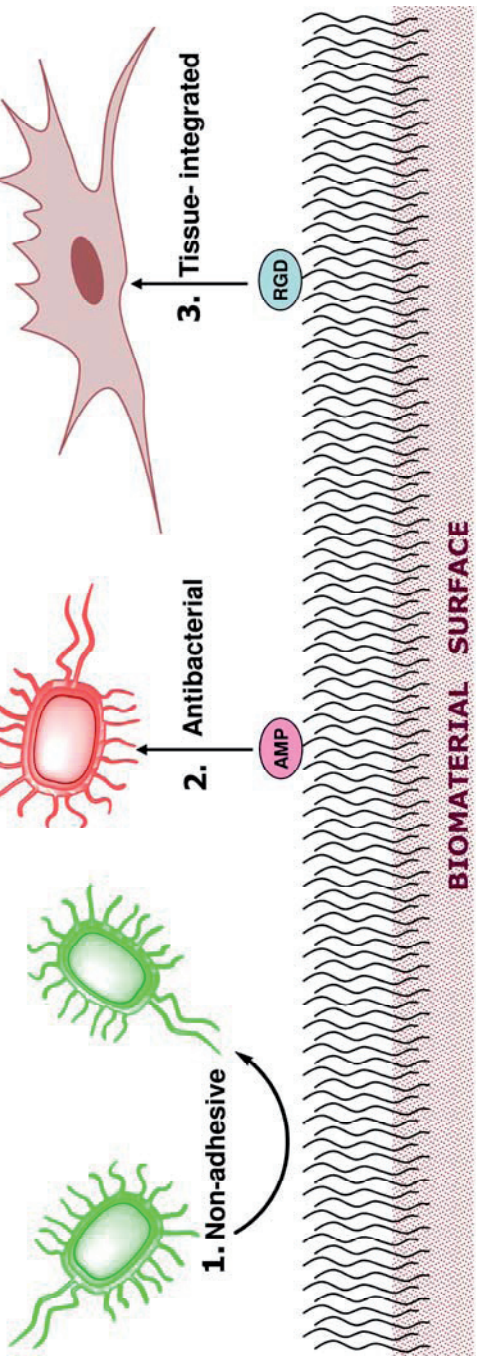

Figure 4. Multi-functional coating combining non-adhesive polymer chains (1), covalently attached antimicrobial peptides AMP (2) and integrin-binding RGD peptides promoting tissue integration (3).

REFERENCES:

1. Place ES, Evans ND, Stevens MM. Complexity in biomaterials for tissue engineering. Nat Mater 2009;8:457-470.

2. Editorial. Boom time for biomaterials. Nat Mater 2009;8:439.

3. Langer R, Tirrell DA. Designing materials for biology and medicine. Nature 2004;428:487-492.

4. Lutolf MP, Hubbell JA. Synthetic biomaterials as instructive extracellular microenvironments for morphogenesis in tissue engineering. Nat Biotechnol 2005;23:47-55.

5. Brochu ABW, Craig SL, Reichert WM. Self-healing biomaterials. J Biomed Mater Res A 2011;96:492-506.

6. Mark JE. Some novel polymeric nanocomposites. Acc Chem Res 2006;39:881–888.

7. Mark JE. Ceramic-modified elastomers. Curr Opin Solid State Mater Sci 1999;4:565–570.

8. Colas A, Curtis J. Silicone biomaterials: History and chemistry, medical applications of silicones. Biomaterials Science, 2nd edition, Elsevier/Academic Press, New York 2004.

9. Mata A, Fleischman AJ, Roy S. Characterization of polydimethylosiloxane (PDMS) properties for biomedical micro/nanosystems. Biomed Microdevices 2005;7:281-293.

10. Busscher HJ, Geertsema-Doornbusch GI, Van der Mei HC. Adhesion to silicone rubber of yeasts and bacteria isolated from voice prostheses: influence of salivary conditioning films. J Biomed Mater Res 1997;34:201-209.

11. Verkkala K, Eklund A, Ojajärvi J, Tiittanenb L, Hobornd J, Mäkeläb P. The conventionally ventilated operating theatre and air contamination control during cardiac surgery - bacteriological and particulate matter control garment options for low level contamination. Eur J Cardiothorac Surg 1998;14:206-210.

12. Darouiche RO. Device-associated infections: A macroproblem that starts with microadherence. Clin Infect Dis 2001;33:1567-1572.

13. Darouiche RO. Current concepts - Treatment of infections associated with surgical implants. New Eng J Med 2004;350:1422-1429.

14. Costerton JW, Stewart PS, Greenberg EP. Bacterial biofilms: A common cause of persistent infections. Science 1999;284:1318-1322.

15. Stewart PS, Costerton JW. Antibiotic resistance of bacteria in biofilms. Lancet 2001;358:135-138.

16. Costerton JW, Montanaro L, Acriola CR. Biofilm in implant infections: its production and regulation. Int J Artif Organs 2005;28:1062-1068.

17. Mack D, Rohde H, Harris LG, Davies AP, Horstkotte MA, Knobloch JK. Biofilm formation in medical device-related infection. Int J Artif Organs 2006;29:343-359.

18. Ayres N. Polymer brushes: Applications in biomaterials and nanotechnology. Polymer Chemistry 2010;1:769-777.

19. Neoh KG, Kang ET. Combating bacterial colonization on metals via polymer coatings: relevance to marine and medical applications. ACS Appl Mater Interfaces 2011;3:2808-2819.

20. Kingshott P, Wei J, Bagge-Ravn D, Gadegaard N, Gram L. Covalent attachment of poly(ethylene glycol) to surfaces, critical for reducing bacterial adhesion. Langmuir 2003;19:6912-6921.

21. Barentin C, Muller P, Joanny JF. Polymer brushes formed by end-capped poly(ethylene oxide) (PEO) at the air–water interface. Macromolecules 1998;31:2198-2211.

22. Eichler M, Katzur V, Scheideler L, Haupt M, Geis-Gerstorfer J, Schmalz G, Ruhl S, Müller R, Rupp F. The impact of dendrimer-grafted modifications to model silicon surfaces on protein adsorption and bacterial adhesion. Biomaterials 2011;32:9168-9179.

23. Konradi R, Pidhatika B, Mühlebach A, Textor M. Poly-2-methyl-2-oxazoline: A peptide-like polymer for protein-repellent surfaces. Langmuir 2008;24:613-616.

24. Chang Y, Liao SC, Higuchi A, Ruaan RC, Chu CW, Chen WY. A Highly stable nonbiofouling surface with well-packed grafted zwitterionic polysulfobetaine for plasma protein repulsion. Langmuir 2008;24:5453-5458.

25. Yoshimoto K, Hirase T, Madsen J, Armes SP, Nagasaki Y. Non-fouling character of poly[2-(methacryloyloxy)ethyl phosphorylcholine]-modified gold surfaces fabricated by the 'grafting to' method: comparison of its protein resistance with poly(ethylene glycol)-modified gold surfaces. Macromol Rapid Commun 2009;30:2136-2140.

26. Campoccia D, Montanaro L, Speziale P, Arciola CR. Antibiotic-loaded biomaterials and the risk for the spread of antibiotic resistance following their prophylactic and therapeutic clinical use. Biomaterials 2010;31:6363-6377.

27. Rojas IA, Slunt JB, Grainger DW. Polyurethane coatings release bioactive antibodies to reduce bacterial adhesion. J Control Release 2000;63:175-189.

28. Charville GW, Hetrick EM, Geer CB, Schoenfisch MH. Reduced bacterial adhesion to fibrinogen-coated substrates via nitric oxide release. Biomaterials 2008;29:4039-4044.

29. Wu P, Xie R, Imlay K, Shang JK. Visible-light-induced bactericidal activity of titanium dioxide codoped with nitrogen and silver. Environ Sci Technol 2010;44:6992-6997.

30. Visai L, De Nardo L, Punta C, Melone L, Cigada A, Imbriani M, Arciola CR. Titanium oxide antibacterial surfaces in biomedical devices. Int J Artif Organs 2011;34:929-946.

31. Baveja JK, Wilcox MDP, Hume EBH, Kumar N, Odell R, Poole-Warren LA. Furanones as potential anti-bacterial coatings on biomaterials. Biomaterials 2004; 25:5003-5012.

32. Kazemzadeh-Narbat M, Kindrachuk J, Duan K, Jenssen H, Hancock RE, Wang R. Antimicrobial peptides on calcium phosphate-coated titanium for the prevention of implant-associated infections. Biomaterials 2010;31:9519-9526.

33. Costa F, Carvalho IF, Montelaro RC, Gomes P, M. Martins MCL. Covalent immobilization of antimicrobial peptides (AMPs) onto biomaterial surfaces. Acta Biomater 2011;7:1431-1440.

34. Tan H, Peng Z, Li Q, Xu X, Guo S, Tang T. The use of quaternised chitosan-loaded PMMA to inhibit biofilm formation and downregulate the virulence-associated gene expression of antibiotic-resistant staphylococcus. Biomaterials 2012;33:365-377.

35. Nejadnik MR, Van der Mei HC, Norde W, Busscher HJ. Bacterial adhesion and growth on a polymer brush-coating. Biomaterials 2008;29:4117-4121.

36. Alexandridis P, Hatton TA. Poly(ethylene oxide)-poly(propylene oxide)-poly(ethylene oxide) block-copolymer surfactants in aqueous-solutions and at interfaces - thermodynamics, structure, dynamics, and modeling. Coll Surfaces A 1995;96:1-46.

37. Currie EPK, Norde W, Stuart MAC. Tethered polymer chains: surface chemistry and their impact on colloidal and surface properties. Adv Colloid Interf 2003;100:205-265.

38. Leckband D, Sheth S, Halperin A. Grafted poly(ethylene oxide) brushes as nonfouling surface coatings. J Biomat Sci Polyme Ed 1999;10:1125-1147.

39. Schroen CGPH, Stuart MAC, Maarschalk KV, Van der Padt A, Van't Riet K. Influence of preadsorbed block-copolymers on protein adsorption - surface properties, layer thickness, and surface coverage. Langmuir 1995;11:3068-3074.

Chapter 2

Bacterial adhesion forces with substratum surfaces and the susceptibility of biofilms to antibiotics

A.K. Muszanska, M.R. Nejadnik, Y. Chen, E.R. van den Heuvel, H.J. Busscher, H.C. van der Mei, W. Norde (2012) *Antimicrob Agents Chemother* 56:4961-4964.

ABSTRACT

Biofilms causing biomaterial associated infection (BAI) resist antibiotic treatment and usually yield replacement of infected implants. Here we relate bacterial adhesion forces and antibiotic susceptibility of biofilms on uncoated and polymer brush-coated silicone rubber. Adhesion forces were recorded using atomic force microscopy. Bacterial biofilms were grown on the substrata in a parallel plate flow chamber in absence or presence of gentamicin and subsequently analyzed using phase contrast and confocal laser scanning microscopy. Nine strains of *Staphylococcus aureus*, *Staphylococcus epidermidis* and *Pseudomonas aeruginosa* adhered more weakly ((-0.05 ± 0.03) – (-0.51 ± 0.62) nN) to brush-coated than to uncoated silicone rubber ((-1.05 ± 0.46) – (-5.1 ± 1.3) nN). Surface coverage by biofilms grown in the presence of gentamicin on polymer brush-coatings was significantly less than on uncoated silicone rubber, while also the percentage live organisms and amount of extracellular matrix produced was less. Consequently, biofilms on polymer brush-coatings remained susceptible to gentamicin, opposite to biofilms formed on uncoated silicone rubber, showing antibiotic resistance.

INTRODUCTION

Biomaterials-associated infections (BAI) remain the number one cause of failure of biomaterial implants or devices despite the development of various strategies to control BAI during implantation, like (*e.g.* modern, ventilated operating theatres and impermeable personnel clothing [1]. The occurrence of BAI for primary implants varies from 1 to 30 % with an associated mortality of up to 25 %, depending on the type of implant [2]. Common treatment procedures for patients suffering from BAI include long-term application of high doses of antibiotics, but frequently without success and the fate of an infected implant or device is replacement at great discomfort for the patient [3]. The costs of replacement, if the condition of a patient allows this at all, easily triple the costs of a primary implant or device and societal pressure to develop new preventive measures is huge. In the US, for instance, certain types of BAI are no longer covered by the Medicare program. At the same time, in an ageing society the use of biomaterials implants and devices is growing.

Microbial adhesion is considered to be the onset of BAI and can lead to formation of a biofilm, in which microorganisms embed themselves in a complex matrix of extracellular polymeric substances (EPS), which provides protection against antibiotic treatment and the host immune system [4,5]. Surface modifications can significantly reduce microbial adhesion and biofilm formation to biomaterial surfaces [6]. Polymer brush-coatings are currently the most promising non-adhesive coatings as they reduce the adhesion of various bacterial strains by orders of magnitude [7]. A polymer brush is formed when hydrophilic polymer chains are end-grafted to a surface in a high packing density, forcing the polymer chains to stretch away from the surface into the adjacent medium [8]. Compression of such a structure upon microbial approach gives rise to an osmotic pressure and decreased mobility of the polymer chains in the brush, which causes

repulsion of approaching microorganisms [9]. These coatings, however, do not completely suppress microbial adhesion and even the few bacteria adhering to a polymer brush have been demonstrated to be able to form a weakly adhering biofilm [7], albeit at a reduced rate when compared with uncoated substrata. In addition, we observed an alteration of biofilm structure from a thick compact layer on uncoated silicone rubber to scattered microcolonies on a polymer brush-coated substratum. Furthermore, a biofilm on brush-coated surfaces appeared to be more viable, probably because the bacteria in the microcolonies have better access to nutrients.

In this study we hypothesize that bacteria on polymer brush-coatings remain in a more or less planktonic state due to weak interaction forces with highly hydrated polymer brush-coatings and hence remain susceptible to antibiotics. This hypothesis, if proven right, would open a new pathway to combat BAI.

MATERIALS AND METHODS

Bacterial strains, growth conditions and harvesting

Nine bacterial strains, representing *Staphylococcus aureus* (799, 835, ATCC 12600), *Staphylococcus epidermidis* (ATCC 35984, HBH 276, 138) and *Pseudomonas aeruginosa* (#3, 6487, ATCC 19582) were used in this study. Strains were either established type strains or clinical isolates taken from patients with implant or device related infections. First bacteria were cultured aerobically overnight at 37^{o}C on blood agar plate from frozen stocks. Plates were kept at 4^{o}C and used no longer than 2 weeks. A single colony was inoculated in 10 ml tryptone soya broth (TSB, OXOID, England) and incubated at 37^{o}C for 24 h. This pre-culture was used to inoculate 200 ml of TSB and incubated for 16 h. Bacteria from the second culture were harvested by centrifugation for 5 min at 5000 × g

and washed twice with phosphate buffered saline solution (PBS buffer, 10 mM potassium phosphate, 150 mM NaCl, pH 6.8). To break up aggregates bacteria were sonicated whilst cooling on an ice-water bath for 3 × 10 s at 30 W (Vibra Cell model 375, Sonics and Materials, USA). This procedure was found not to cause cell lysis.

Substratum surface preparation

Implant grade silicone rubber sheets (thickness 0.5 mm, water contact angle 110 ± 1 degrees, Medin, Groningen, The Netherlands) were used as substrata. Prior to use, silicone rubber sheets were cut into small pieces, rinsed with ethanol (97%, Merck, Darmstadt, Germany) and demineralised water. Next, the sheets were sonicated for 3 min in 2% RBS 35 detergent (Omnilabo International BV, The Netherlands), subsequently rinsed with demineralised water, washed in methanol (Merck, Darmstadt, Germany) and again rinsed with demineralised water. Silicone rubber was exposed to a filter-sterilized solution of 0.5 mg/ml Pluronic F-127 (a copolymer of polyethylene oxide (PEO) and polypropylene oxide (PPO) with structure $PEO_{99}PPO_{65}PEO_{99}$, Mw 12600, Sigma-Aldrich, USA) in PBS at room temperature, as described before [7]. Non-attached polymers were removed by rinsing with PBS.

Atomic force microscopy (AFM)

Adhesion forces of all bacterial strains mentioned above on uncoated and polymer brush-coated silicone rubber were recorded using atomic force microscopy (AFM, BioScope Catalyst AFM with ScanAsyst Veeco, Camarillo, California, USA). Before each measurement, cantilevers were calibrated using the thermal tuning method and actual spring constants were always found to be close to the producer's specification of 0.06 N/m. Bacterial probes were prepared by

immobilizing single bacteria to a NP-O10 tipless cantilever using electrostatic attraction, mediated by positively charged poly-*L*-lysine adsorbed to the cantilever [10]. Briefly, calibrated cantilevers were mounted to the end of a micro-manipulator and under microscopic observation, the tip of a cantilever was dipped into a droplet of poly-*L*-lysine for 2 min. Following air-drying for 2 min, the end of the cantilever was carefully dipped into a droplet of freshly prepared bacterial suspension for another 2 min and dried in air, again for 2 min. Bacterial probes were always used immediately after the preparation. All adhesion force measurements were performed in PBS and at room temperature under a loading force of 5 nN and at three randomly chosen spots on uncoated and polymer brush-coated silicone rubber. For each bacterial strain, at least 15 retract force-curves were recorded on one spot, requiring a minimum of at least six bacterial probes for each strain.

Bacterial growth in parallel plate flow chamber

Bacterial growth and biofilm formation were monitored for one strain of each species, on uncoated and polymer brush-coated silicone rubber sheets, affixed to the polymethylmethacrylate bottom plate of a parallel plate flow chamber. Minimal inhibitory concentrations (MIC) of these strains against gentamicin were determined using the E-test (AB bioMérieux, Solna, Sweden) and all strains were found susceptible to gentamicin with an MIC below 4 μg/ml [11]. Bacteria were grown and harvested as described above, and finally suspended in 200 ml sterile PBS to a concentration of 3×10^8 per ml. After initial bacterial adhesion from this suspension for 30 min at room temperature under flow (shear rate 11 s^{-1}), flow was switched for 3.5 h to 10% TSB medium at 37^{o}C under reduced flow (shear rate 5 s^{-1}) to grow a biofilm. After that medium containing different concentrations (0.5, 5 and 50 μg/ml, i.e. below, at and above MIC) of gentamicin

sulfate (Sigma-Aldrich, USA) was perfused through the chamber for 16 h. Images were taken from the bottom plate of the flow chamber using phase-contrast microscopy throughout the entire course of an experiment and the surface coverage of uncoated and polymer brush-coated silicone rubber determined as a measure for the amount of biofilm formed. At the end of each flow experiment, 20 h old biofilms were removed from the substratum surfaces using a sterile cotton swab and suspended in demineralised water. Subsequently, 10 µl of the suspension was transferred onto a glass slide and stained for 30 min in the dark with a live/dead stain (*Bac*Light™, Molecular Probes Europe BV) to determine the percentage viability of the bacteria using fluorescence microscopy (Leica, Wetzlar, Germany). All experiments for quantitative biofilm analysis were done in duplicate, with separately grown bacterial cultures.

In a separate set of experiments, intact biofilms were visualized using a Leica TCS SP2 Confocal Scanning Laser Microscope (Leica Microsystems Heidelberg GmbH, Germany). 20 h old biofilms formed on the bottom plate of the parallel plate flow chamber, were stained with live/dead stain mixed with CalcoFluor White, a polysaccharide binding stain (Sigma-Aldrich, USA) applied to visualize EPS. Stacks of images were obtained with a 40 × water objective lens.

Statistics

All adhesion force measurements were analyzed per strain using a mixed effects model, taking absence or presence of the polymer brush-coating and probe employed as fixed effects and the spot chosen as a random one. The variance components were separately estimated for coated and uncoated surfaces. Maximum likelihood was used as estimation method and a type III test was applied to evaluate a significant effect of the polymer brush-coating on bacterial adhesion forces. For surface coverage and fraction of viable bacteria, an analysis

of variance was conducted for each bacterial strain after growth in the presence of the different antibiotic concentrations. If an overall effect of the surface coating on the outcomes was significant, Fisher's least significant difference test was applied to investigate the effect of the coating at each antibiotic concentration (including absence of antibiotic). All tests were conducted two-sided and at the significance level of 0.05.

RESULTS

Adhesion forces of all strains were less on polymer brush-coated silicone rubber ((-0.05 ± 0.03) to (-0.51 ± 0.62) Nn) than on uncoated silicone rubber ((-1.05 ± 0.46) to (-5.1 ± 1.3) nN), representing a significant (P < 0.05) reduction (see Figure 1).

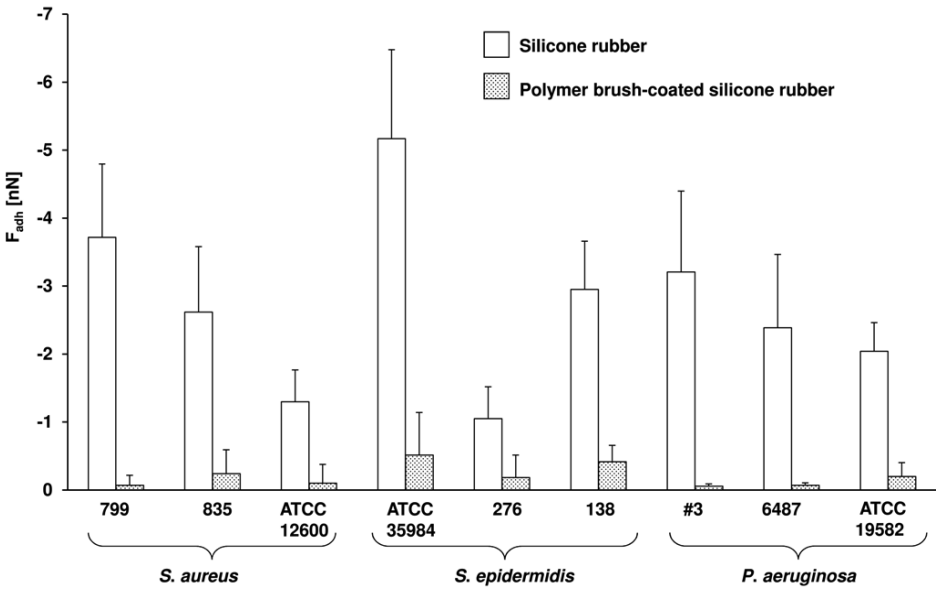

Figure 1. Bacterial adhesion forces (F_{adh}) to uncoated and polymer brush-coated silicone rubber, showing significant reductions in adhesion forces (P < 0.05) for all nine strains, after coating the silicone rubber surface with the polymer brush.

Biofilm formation of selected strains representing each of the three different species on uncoated silicone rubber was accompanied by the production of EPS in large amounts especially for the staphylococcal biofilms, while EPS production was virtually absent on polymer brush-coated silicone rubber (Figure 2).

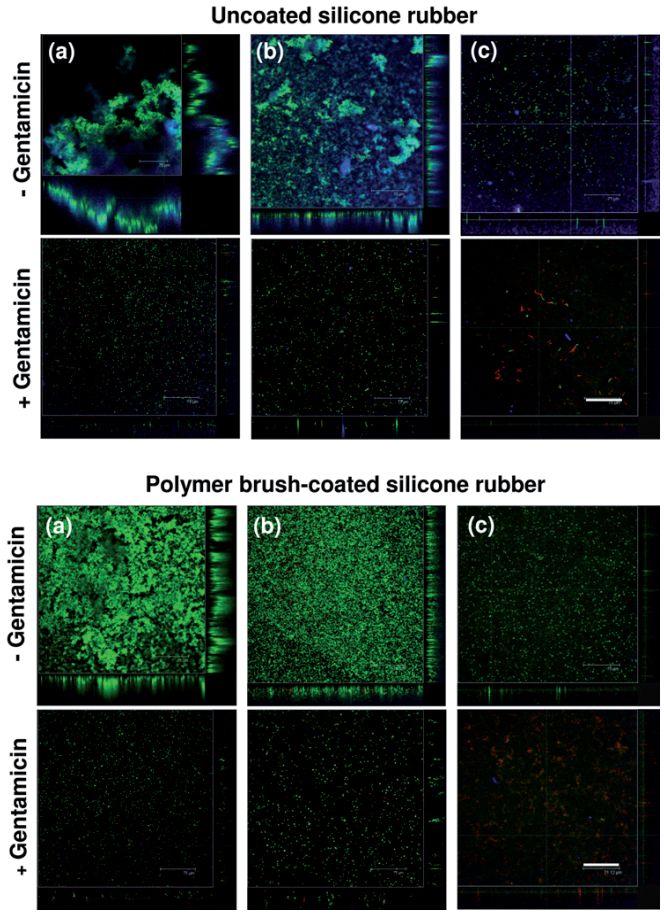

Figure 2. CLSM overlayer images and optical sections of 20 h old, intact biofilms grown in absence (-) and presence (+) of 50 µg/ml gentamicin for uncoated silicone rubber and polymer brush-coated silicone rubber. Live and dead bacteria appear green and red fluorescent, respectively while EPS yields blue fluorescent patches. Bar marker indicates 75 µm. (a) *S. aureus* ATCC 12600, (b) *S. epidermidis* 138 , (c) *P. aeruginosa* # 3.

For quantitative analysis, biofilm growth was monitored by phase-contrast microscopy as a function of time. Biofilms of both staphylococcal strains in the absence of antibiotics achieved full surface coverage on uncoated silicone rubber within 14 to 16 h, while on polymer brush-coated silicone rubber full coverage was not yet reached within 20 h (Figure 3).

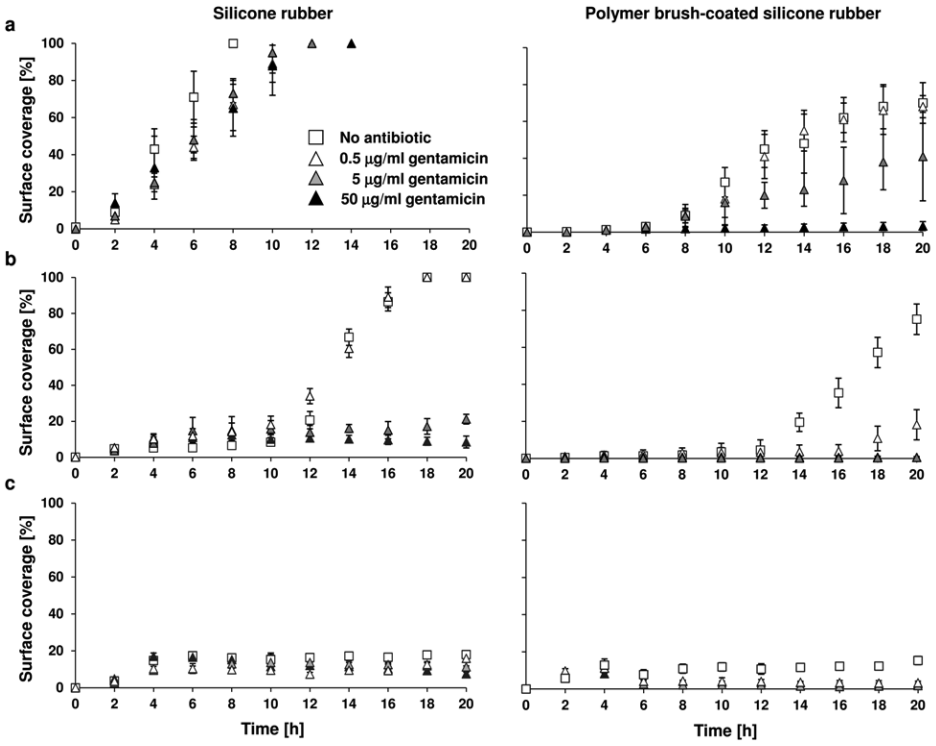

Figure 3. Surface coverage of as a function of time on uncoated silicone rubber and polymer brush-coated silicone rubber by biofilms grown in the absence and presence of varying concentrations of gentamicin. Gentamicin was introduced after 4 h of growth. Error bars represent standard deviations over two separate experiments. (a) *S. aureus* ATCC 12600, (b) *S. epidermidis* 138, (c) *P. aeruginosa* # 3.

Such a difference in growth kinetics was absent in case of *P. aeruginosa*, yielding less than 20% surface coverage. Importantly, biofilm growth in the presence of varying concentrations of gentamicin (0.5 μg/ml, 5 μg/ml and 50 μg/ml) was reduced significantly stronger on polymer brush-coatings than on uncoated silicone rubber. Surface coverage by *P. aeruginosa* remained similarly low in the presence of gentamicin than in its absence.

For further quantitative analysis of the percentage live and dead bacteria in the biofilms, 20 h old biofilms were dispersed, stained with *Bac*light live/dead stain and examined in a fluorescent microscope to derive the percentage of live and dead bacteria in the biofilms. Accordingly, Figure 4 separates the surface coverage by 20 h old biofilms into a live and dead component. In absence of antibiotics, the percentage live bacteria in the biofilms is higher on the polymer brush-coating than on uncoated silicone rubber. Interestingly, in the presence of gentamicin, we see a smaller percentage of live bacteria on the polymer brush-coating, with little or no efficacy of the antibiotic on biofilms formed on silicone rubber.

DISCUSSION

This study aims to verify the hypothesis that bacteria on polymer brush-coatings remain in a more or less planktonic state due to weak interaction forces with highly hydrated polymer brush-coatings and hence remain susceptible to antibiotics. Adhesion forces between the strains and polymer brush-coated silicone rubber showed significant reduction when compared to the uncoated surface. Surface coverage by biofilms grown in the presence of gentamicin on polymer brush-coatings was significantly less than on uncoated silicone rubber, while also the percentage live organisms was lower. Furthermore the amount of EPS produced was less on polymer brush-coatings, explaining the higher

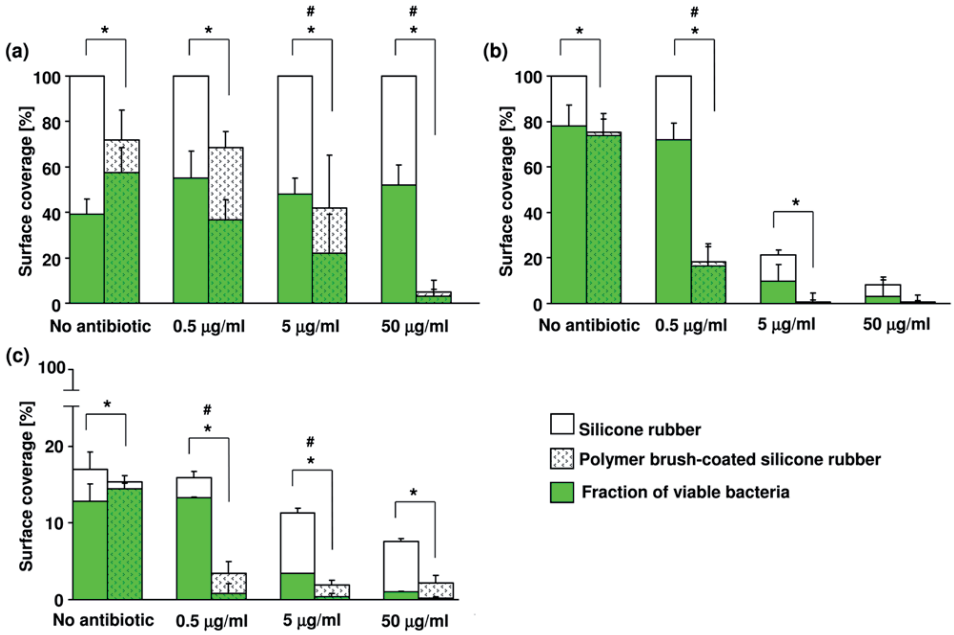

Figure 4. The percentage surface coverage by 20 h old biofilms of uncoated and polymer brush-coated silicone rubber, separated in live and dead bacteria. Error bars represent standard error over two separate experiments. (a) *S. aureus* ATCC 12600, (b) *S. epidermidis* 138, (c) *P. aeruginosa* # 3.

***** indicates a significant difference ($P < 0.05$) between uncoated silicone rubber and polymer brush-coated silicone rubber in surface coverage by biofilm after 20 h growth

# indicates a significant difference ($P < 0.05$) between silicone rubber and polymer brush-coated silicone rubber in numbers of viable bacteria in 20 h old biofilms.

susceptibility to gentamicin. Thus in addition to the known reduction in biofilm formation on polymer brush-coatings as compared with common biomaterials, this study is the first to demonstrate that bacterial biofilms on a polymer brush-coating remain susceptible to antibiotics, regardless of the molecular basis of the resistance mechanism. This phenomenon has enormous clinical implications, as it shows an original pathway toward biomaterials implant coatings that allows

antibiotic treatment to prevent biofilm formation and therewith reducing the risk of BAI.

Upon adhesion of bacteria, a cascade of genotypic and phenotypic changes are induced that results in a biofilm-specific phenotype [12-14]. Changes in gene regulation occur within minutes after bacterial attachment to a solid surface [15], suggesting that adhering bacteria may sense a solid surface leading to a signaling cascade that causes genes to be up- or down-regulated and the production of EPS [16], rendering the organisms more resistant to antimicrobial agents [14,17,18]. Recently it has been argued that in the absence of visual, auditory and olfactory perception, adhering bacteria react to membrane stresses arising from minor deformations due to the adhesion forces felt, to make them aware of their adhering state on a surface and change from a planktonic to a biofilm phenotype [19]. Adhesion forces of nine different bacterial strains are clearly much higher on silicone rubber than on the polymer brush-coating and in fact on the polymer brush adhesion forces are so low that it can be argued that bacteria, though weakly adhering, are unable to sense the surface as they do on silicone rubber. As a result, they remain in their antibiotic-susceptible state, whereas on silicone rubber they adopt a biofilm mode of growth with full protection against gentamicin concentrations of 50 μg/ml, far above the MIC.

CONCLUSIONS

This is the first study providing a link between bacterial adhesion forces and the susceptibility of bacterial biofilms, providing a clear clue as to why bacterial susceptibility of biofilms of the same strain may differ on different biomaterials. In fact, based on the current study, it can be concluded that the transition of microorganisms from a planktonic state towards their protected biofilm mode of growth is not merely dictated by the absence or presence of a substratum

material, but depends on the forces exerted on the organisms by the substratum surface. This is clinically relevant, as it suggests that antimicrobial treatment of BAI could be more effective in cases where infection occurs after implantation of a polymer brush-coated implant or device.

REFERENCES

1. Verkkala K, Eklund A, Ojajärvi J, Tiittanenb L, Hobornd J, Mäkeläb P. The conventionally ventilated operating theatre and air contamination control during cardiac surgery - bacteriological and particulate matter control garment options for low level contamination. Eur J Cardiothorac Surg 1998;14:206-210.

2. Darouiche RO. Device-associated infections: A macroproblem that starts with microadherence. Clin Infect Dis 2001;33:1567-1572.

3. Darouiche RO. Current concepts - Treatment of infections associated with surgical implants. New Eng J Med 2004;350:1422-1429.

4. Costerton JW, Stewart PS, Greenberg EP. Bacterial biofilms: A common cause of persistent infections. Science 1999;284:1318-1322.

5. Del Pozo JL, Patel R. The challenge of treating biofilm-associated bacterial infection. Clin Pharmacol Ther 2007;82:204-209.

6. Cheng G, Zhang Z, Chen SF, Bryers JD, Jiang S. Inhibition of bacterial adhesion and biofilm formation on zwitterionic surfaces. Biomaterials 2007;28:4192-4199.

7. Nejadnik MR, Van der Mei HC, Norde W. Busscher HJ. Bacterial adhesion and growth on a polymer brush-coating. Biomaterials 2008;29:4117-4121.

8. Schroen CGPH, Stuart MAC, Maarschalk KV, Van der Padt A, Van't Riet K. Influence of preadsorbed block-copolymers on protein adsorption - surface properties, layer thickness, and surface coverage. Langmuir 1995;11:3068-3074.

9. Currie EPK, Norde W, Stuart MAC. Tethered polymer chains: surface chemistry and their impact on colloidal and surface properties. Adv Colloid Interfac 2003;100:205-265.

10. Bolshakova AV, Kiselyova OI, Filonov AS, Frolova OYu, Lyubchenko YL, Yaminsky IV. Comparative studies of bacteria with an atomic force microscopy operating in different modes. Ultramicroscopy 2001;86:121-128.

11. Andrews JM. BSAC standardized disc susceptibility testing method (version 8). J Antimicrob Chemoth 2009;64:454-489.

12. Mah TFC, O'Toole GA. Mechanisms of biofilm resistance to antimicrobial agents. Trends Microbiol 2001;9:34-39.

13. Schachter B. Slimy business-the biotechnology of biofilms. Nat Biotechnol 2003;21:361-365.

14. Drenkard E, Ausubel FM. *Pseudomonas* biofilm formation and antibiotic resistance are linked to phenotypic variation. Nature 2002;416:740-743.

15. Davies DG, Geesey GG. Regulation of the alginate biosynthesis gene algC in *Pseudomonas aeruginosa* during biofilm development in continuous-culture. Appl Environ Microb 1995;61:860-867.

16. Jefferson KK. What drives bacteria to produce a biofilm? Fems Microbiol Lett 2004;236:163-173.

17. Mah TF, Pitts B, Pellock B, Walker GC, Stewart PS, O'Toole GA. A genetic basis for *Pseudomonas aeruginosa* biofilm antibiotic resistance. Nature 2003;426:306-310.

18. Whiteley M, Bangera MG, Bumgarner RE, Parsek MR, Teitzel GM, Lory S, Greenberg EP. Gene expression in *Pseudomonas aeruginosa* biofilms. Nature 2001;413:860-864.

19. Busscher HJ, Van der Mei HC. How do bacteria know they are on a surface and regulate their response to an adhering state? PLoS Pathog 2012;8:e1002440.

Chapter 3

Pluronic-lysozyme conjugates as anti-adhesive and antibacterial bifunctional polymers for surface coating

A.K. Muszanska, H.J. Busscher, A. Herrmann, H.C. van der Mei, W. Norde (2011) *Biomaterials* 32:6333-6341.

ABSTRACT

This paper describes the preparation and characterization of polymer-protein conjugates composed of a synthetic triblock copolymer with a central polypropylene oxide (PPO) block and two terminal polyethylene oxide (PEO) segments, Pluronic F-127, and the antibacterial enzyme lysozyme attached to the telechelic groups of the PEO chains. Covalent conjugation of lysozyme proceeded via reductive amination of aldehyde functionalized PEO blocks (CHO-Pluronic) and the amine groups of the lysine residues in the protein. SDS-PAGE gel electrophoresis together with MALDI-TOF mass spectrometry analysis revealed formation of conjugates of one or two lysozyme molecules per Pluronic polymer chain. The conjugated lysozyme showed antibacterial activity towards *Bacillus subtilis.* Analysis with a quartz crystal microbalance with dissipation revealed that Pluronic-lysozyme conjugates adsorb in a brush conformation on a hydrophobic gold-coated quartz surface. X-ray photoelectron spectroscopy indicated surface coverage of 32% by lysozyme when adsorbed from a mixture of unconjugated Pluronic and Pluronic-lysozyme conjugate (ratio 99:1) and of 47% after adsorption of 100% Pluronic-lysozyme conjugates. Thus, bifunctional brushes were created, possessing both anti-adhesive activity due to the polymer brush, combined with the antibacterial activity of lysozyme. The coating having a lower degree of lysozyme coverage proved to be more bactericidal.

INTRODUCTION

Biomaterials in the human body are prone to bacterial infections, which may lead to the formation of a biofilm. Biofilm formation is preceded by protein adsorption, deposition of cells and bacteria. The complex structure of a biofilm, containing slime and extracellular polymeric matrix, makes it resistant to the host immune system as well as to antibiotic treatment [1]. Infection of implanted biomaterials usually requires secondary surgery [2,3]. Various biomaterials surface modifications have been developed to improve their antibacterial properties of implant surfaces, such as applying bactericidal agents [4], a hydrogel coating releasing bioactive antibodies [5], nitric oxide releasing substrates [6], a coating with furanones [7], chalcones [8], or various polymers [9]. Especially the later polymer brush-coatings, have been proven in the past to reduce bacterial adhesion by one or two orders of magnitude [10-12], which makes them a promising tool for biomedical applications. A polymer brush is formed when highly soluble polymer chains are grafted to the surface at high packing density, forcing the polymer chains to extend into the surrounding aqueous medium. Thus, a highly hydrated polymer layer is formed at the surface, which acts as a barrier preventing deposition of particles, including bacteria [10]. Polymer chains can be grafted to the surface by simple physi-sorption, or by covalent bond formation. Chemical attachment makes the brush more stable but it is a complex and time-consuming procedure [13]. The grafting density plays a crucial role in the conformation of the adsorbed polymer layer. At low grafting densities, the polymer chains are coiled resulting in a so-called mushroom conformation of the adsorbed polymer molecule. At higher grafting densities, when the separation between the anchoring points is less than the hydrodynamic radius of the polymer coils, the polymer chains are forced to stretch into the surrounding medium forming a brush conformation [14]. In aqueous media, polyethylene oxide (PEO) is

most often used as the soluble polymer. Ethylene oxide (EO) moieties in the PEO chain have a good structural fit with water molecules enabling a strong hydrogen bond between the ether oxygen of PEO and the hydrogen of water. Thus the PEO brush-coating is highly hydrated. Compression of the PEO chains in the brush increases the osmotic pressure along with a reduction of their conformational entropy. This creates a strong repulsive force against deposition of indwelling particles, including bacteria [13,15,16].

The aim of this study is to design a bifunctional polymer brush-coating by conjugation of an antibacterial compound with the polymer molecules so that the brush attains bi-functionality i.e., resistance to particle deposition and selective lethal interaction with microorganisms. For our study, we chose Pluronic F-127 as the PEO-containing polymer. Pluronics are a family of synthetic non-toxic neutral triblock copolymers made up of a central hydrophobic polypropylene oxide (PPO) block that is connected to two hydrophilic PEO side blocks, PEO_n-PPO_m-PEO_n. In aqueous medium this triblock copolymer self-assembles into micelles. After exposure to a hydrophobic surface, the micelles disaggregate in favour of adsorption. It is inferred that the hydrophobic PPO block attaches spontaneously to the surface, whereas the two PEO segments extend into the water phase [17,18]. Lysozyme was chosen as the antimicrobial agent because of its well-known bactericidal properties [19,20], physiological abundance, high thermal stability with respect to structure [21], wide pH activity range [22], and well known structure [23,24]. Lysozyme is able to destruct bacterial cell walls by an enzymatic hydrolysis of 1,4-beta-linkages between N-acetylmuramic acid and N-acetyl-D-glucosamine residues of peptidoglycan in the bacterial cell wall, especially for Gram-positive bacteria [20]. Broadly directed activity makes lysozyme an important antimicrobial agent that can be used to prevent biomaterial associated infections by a wide variety of bacterial strains [25].

The use of polymer–protein conjugates is relatively new in biomedical research and has potential applications in drug delivery systems [26-28], and as novel biocompatible materials for e.g., implants and tissue engineering [29-32]. We used the protein-polymer conjugation approach [26] to synthesize lysozyme functionalized Pluronic molecules.

For lysozyme to exert enzymatic activity, it is desired, if not required, that it is exposed to the solution rather than being adsorbed to the surface. If the conjugate would adsorb with the lysozyme attached to the surface, the lysozyme would barely be accessible for the bacteria due to shielding by the polymer. Moreover, it has been reported that after adsorption on hydrophobic surfaces lysozyme looses its antimicrobial activity [33]. This implies that the conjugate should adsorb in a similar conformation as the unmodified Pluronic, i.e., via attachment of its PPO block, as shown in Figure 1. Surface coatings consisting of Pluronic-lysozyme conjugates were characterized in terms of thickness, viscoelastic properties, surface composition and their anti-adhesive and antibacterial properties.

MATERIALS AND METHODS

Aldehyde-end functionalization of Pluronic F-127

5 M excess of Dess-Martin periodinane (1,1,1-tris(acetyloxy)-1,1-dihydro-1,2-benziodoxol-3(1H)-one, 97%, Sigma Aldrich, Germany) was added to a solution of 200 mg of Pluronic F-127 (PEO_{99}-PPO_{65}-PEO_{99}), MW= 12.6 kDa (BASF, Sigma Aldrich, Germany) in 20 ml of dry dichloromethane (Sigma Aldrich, Germany) at room temperature and stirred overnight. Thereafter, the reaction mixture was treated with cold diethyl ether ~30 ml (Merck, Germany). The precipitated product was cooled on an ice-water bath for 1 h, filtered off, washed with cold diethyl ether (2 x 20 ml) and dried under vacuum. The conversion of the PEO

hydroxy end-groups into aldehyde functionalities and the degree of conversion was determined using the Purpald colorimetric assay [34]. First, a calibration curve was recorded, in order to convert measured UV-VIS absorbance into number of aldehyde groups, using formaldehyde (37 wt % in H_2O, Sigma Aldrich, Germany), as described elsewhere [34]. Aldehyde functionalized Pluronic was dissolved in ultrapure water in a known range of concentrations. Next, 100 μl of polymer solution was added to 100 μl of 30 mM Purpald (4-amino-3-hydrazino-5-mercapto-1,2,4-triazole, Sigma Aldrich, Germany) solution in 2 M NaOH. After 15 min equilibration, 100 μl of a 30 mM sodium periodate ($NaIO_4$, Sigma Aldrich, Germany) solution in 0.2 M NaOH was added and oxidation took place giving the mixture a purple colour. Changes in absorbance at 550 nm were measured by UV-VIS spectrophotometry.

Lysozyme conjugation

Lysozyme from chicken egg white (MW = 14.3 kDa, protein content ≥ 90%; Sigma Aldrich, Germany), was dissolved in 50 mM sodium nitrate ($NaNO_3$, Fluka, Germany) at pH 7.7, filtered over 0.22 μm pore size Acrodisc filter, to remove dust and minor impurities, and added dropwise to a stirred solution of aldehyde functionalized Pluronic (200 mg in 50 ml 50 mM $NaNO_3$ solution) at room temperature. After 20 min, 20 mg of sodium cyanoborohydride ($NaCNBH_3$, 95%; Sigma Aldrich, Germany) was added and the mixture was left stirring overnight at room temperature and pH 7.7. The molar ratio of lysozyme relative to aldehyde groups was chosen such that there was 10% molar excess of polymer aldehyde groups to amine groups from lysines in the lysozyme. Conjugation of protein to polymer was confirmed by sodium dodecyl sulphate polyacrylamide gel electrophoresis (SDS-PAGE) using NuPAGE Novex 4-12% Bis-Tris Gel (Molecular Probes, Invitrogen) stained with SimplyBlue™ safe stain (Molecular Probes,

Invitrogen, The Netherlands). Then, the reaction mixture was placed into a dialysis tube (MWCO 25 kDa) and dialyzed against 50 mM sodium nitrate ($NaNO_3$, Fluka, Germany) at pH 7.7 for 5 days changing the surrounding medium every 24 h in order to remove unreacted protein together with free polymer molecules. The purification process was monitored by SDS-PAGE and when no more free lysozyme molecules were detected, the reaction mixture was freeze-dried and kept at -20^{o}C. Molecular weight of obtained conjugates was determined using a Voyager-DE Pro (Applied biosystems, USA) MALDI-TOF mass spectrometer. Samples were prepared by plate spotting of tested compounds, mixed with a sinapinic acid matrix. Pure lysozyme was used as a reference sample.

Enzymatic activity assay

The enzymatic activity of Pluronic-lysozyme conjugates was determined and compared with that of free lysozyme using *Bacillus subtilis* 168. *B*. *subtilis* was selected to evaluate the applicability of Pluronic-lysozyme conjugates as an antibacterial surface coating, as a representative of the many strains sensitive to lysozyme, including strains involved in biomaterial associated infections. Lysozyme destructs the bacterial cell wall by catalyzing hydrolysis of 1,4-beta-linkages between N-acetylmuramic acid and N-acetyl-D-glucosamine residues of peptidoglycan in the bacterial cell membrane. As a result, the turbidity of the bacterial suspension decreases, which can be followed spectrophotometrically by measuring the change in absorbance. Bacteria were first grown aerobically overnight at 37^{o}C on blood agar plate from frozen stock. Plates were kept at 4^{o}C and used no longer than for 2 weeks. One colony was used to inoculate 10 ml tryptone soya broth (TSB, OXOID, England). The pre-culture was incubated at 37^{o}C for 24 h and used to inoculate another culture of 200 ml TSB that was incubated for 16 h. The culture was harvested by centrifugation for 5 min at

5000 x g and washed twice with phosphate buffered saline solution (PBS buffer, 10 mM potassium phosphate, 150 mM NaCl, pH 6.8). To break up aggregates bacteria were sonicated whilst cooling on an ice-water bath for 3 x 10 s at 30 W (Vibra Cell model 375; Sonics and Materials, USA). Finally, the bacteria were suspended in PBS buffer to an optical density at 600 nm (OD_{600}) of 0.500. For each enzymatic test, 1 ml of bacteria stock (OD_{600} = 0.500) was mixed with 100 μl of Pluronic-lysozyme conjugate of concentration 1 mg/ml or with free lysozyme at concentrations 0.05, 0.01, 0.005 mg/ml. Pluronic and PBS were used as control samples. Pure PBS buffer was used as a blank sample to calibrate the spectrophotometer. All measurements were done in triplicates at room temperature.

Quartz crystal microbalance with dissipation (QCM-D) measurements

Hydrated thickness and viscoelastic properties of adsorbed layers of unmodified Pluronic molecules, lysozyme conjugated Pluronic molecules and pure lysozyme molecules were studied using a QCM-D device, model Q-sense E4 (Q-sense, Sweden). Gold plated AT-cut quartz crystals, with a sensitivity constant of 17.7 ng/cm^2, were used as substratum. QCM-D has a distinctive advantage of elucidating interactions at a molecular level, by measuring the changes in frequency (*f*) and dissipation (*D*) of the gold crystal at 5 MHz oscillating frequency [35]. Prior to use, the gold surface of the crystals was cleaned by sonication in 2% SDS solution for 3 min, rinsed with ultrapure water, dried under a flow of filtered nitrogen gas and treated in a UV/ozone chamber for 10 min. These crystals were immersed in a heated (70^{o}C) mixture of ultrapure water, ammonia and hydrogen peroxide in a ratio 9:3:2 for 10 min. Next, they were rinsed with ultrapure water, again dried under a flow of filtered nitrogen gas and treated in a UV/ozone chamber for 10 min. The gold coated quartz crystals were stored overnight in PBS

buffer, yielding a hydrophobic gold surface with a water contact angle of 85 ± 1 degrees. Crystal stability with respect to changes in the base lines for *f* and *D* during the flow of PBS adhesion buffer was monitored. After crystal stability was established, solutions of pure CHO-Pluronic, pure lysozyme, and Pluronic-lysozyme conjugate were flown separately on different gold surfaces in the QCM chamber at a flow rate of 24 s^{-1} at 25°C and for 30 min. In a second set of experiments, CHO-Pluronic solution was flown over the 30 min old adsorbed pure lysozyme as well as pure lysozyme over the 30 min old adsorbed CHO-Pluronic in order to establish possible exchange between the two compounds at the surface. In a third set of experiments, the ratio of the Pluronic conjugated to lysozyme to unconjugated Pluronic, in the solution supplied to the surface, was varied (75%, 50%, 25%, 20%, 10%, 5%, 1%) and the corresponding solution was flown separately over the gold surface. All above-mentioned solutions were prepared in a concentration of 1 mg/ml of PBS adhesion buffer. At the end of each flow, all loosely adhered molecules were removed by rinsing with buffer.

During flow, changes in the frequency (*f*) and dissipation (D) were recorded and fitted using the Kelvin-Voight model, consisting of a spring and a dashpot assembly, at all overtones (3, 5, 7, 9 and 11) to evaluate the viscoelastic properties and the hydrated thickness of the adsorbed layer. The viscoelasticity was assessed in terms of relaxation time (τ), taken as a ratio of viscosity (η) and shear modulus (*G*). Viscosity and shear modulus of the adsorbed layers were calculated using software package Q-Tools 3.0.6, assuming that, in view of the low polymer fraction, the density of the adsorbed layer is 1000 kg/m^3. The viscosity of all solutions was measured and did not show a significant deviation from the viscosity of water, i.e. 1 m.Pa.s, which was used for all the calculations.

X-ray photoelectron spectroscopy measurements

Brushes on the gold plated crystal surfaces (see the above section) were subjected to surface chemical analysis, using X-ray photoelectron spectroscopy (XPS). Elemental compositions were measured using an S probe spectrophotometer (Surface Science Instruments, Mountain View, CA, USA) with X-rays (10 kV, 22 mA, spot size of 250 x 1000 μm) sourced from an aluminium anode with the analyzer placed at 35 degrees take-off angle. The binding energy of broad spectrum survey scans was in the range of 1 to 1100 eV recorded at low resolution (pass energy 150 eV). Peaks over 20 eV binding energy range were recorded at high resolution (pass energy 50 eV) for C_{1s}, O_{1s}, N_{1s} and Au_{4f}. The area under each peak was used to calculate peak intensities after correction using the sensitivity factor provided by the manufacturer. N_{1s} electron counts from a densely packed crystalline lysozyme filled trough were assumed to correspond with 100% surface coverage by proteins and used to estimate the lysozyme surface coverage for each sample.

Adhesion and growth of bacteria in a parallel plate flow chamber

Bacterial suspensions were prepared as described above for the enzymatic activity assay. For each experiment, 200 ml suspension in PBS buffer was prepared at a concentration of 3 x 10^8 cells/ml. Implant grade silicone rubber sheets (thickness 0.5 mm, water contact angle 110 ± 1 degrees, Medin, Groningen, The Netherlands) were used as substrata. Prior to use, they were cut into rectangular pieces (10 x 15 mm), rinsed with ethanol (97%, Merck, Darmstadt, Germany) and demineralised water. Next, they were sonicated for 3 min in 2% RBS 35 detergent (Omnilabo International BV, The Netherlands), subsequently rinsed with demineralised water, washed in methanol (Merck, Darmstadt, Germany) and again rinsed with demineralised water. The parallel plate flow chamber allows for

a stable laminar flow with a shear stress τ and a shear rate σ, that can be calculated from the volumetric flow rate *Q*, according to:

$$\tau = \eta\sigma = \frac{\eta 3Q}{2b^2 w} \quad (1)$$

where η is the absolute viscosity, and *b* and *w* are the flow chamber's depth and width, respectively [10]. Silicone rubber was fixed to the bottom plate of the chamber made of transparent thermoplastic poly(methyl methacrylate), whereas the top plate was made of glass. Before each experiment, the tubing and the chamber were filled with PBS buffer to remove air bubbles. Bottles containing bacterial suspension, buffer, polymer solution or bacterial medium were placed at a different height with respect to the chamber to create a hydrostatic pressure that allows the fluid to circulate through the chamber. Constant flow was maintained by recirculation, using a roller pump. A piece of silicone affixed at the bottom plate of the flow chamber was exposed for 30 min at room temperature to 1 mg/ml solutions of unconjugated Pluronic and Pluronic-lysozyme conjugates in varying ratios, i.e., 100%, and 1%, in separate sets of experiments. Non-attached molecules were removed by PBS buffer flow for 5 min. Then, the flow was switched from buffer to a bacterial suspension and bacteria were allowed to adhere for 2h at room temperature under a shear rate 11 s^{-1}. Bacterial adhesion in PBS buffer was monitored real-time during the experiment using a fire wire CCD camera, mounted on the phase-contrast microscope and coupled to PC image analysis software. Each image was obtained from summation of 15 subsequent images with time intervals of 0.25 s to eliminate moving organisms from the analysis. From the images, numbers of bacteria adhering per unit area were determined as a function of time as a measure for the anti-adhesive functionality of the coatings.

Subsequently, unattached bacteria were flushed out by rinsing with PBS buffer for 5 min after which the flow was switched to 10% TSB medium to allow growth of adhering bacteria. The temperature was raised to 37^{o}C and the shear rate was decreased to 5 s^{-1} for 20 h. Since the biofilm arising after growth of the adhering bacteria was too thick for enumeration of individual bacteria, 20 h old biofilms were removed from the substratum surfaces using a sterile cotton swab and suspended in 1 ml demineralised water. A dilution series of the bacterial suspension was plated on TSB agar to determine the absolute number of cultivable, live organisms (colony forming units or CFUs) on each surface. 10 µl of the suspension was transferred onto a glass slide and stained with live/dead stain (*Bac*Light^{TM}, Molecular Probes Europe BV) to determine percentage viability of the bacteria using fluorescence microscopy (Leica, Wetzlar, Germany) as a measure for the antibacterial functionality of the coatings.

RESULTS

Pluronic – lysozyme conjugation.

The preparation of Pluronic-lysozyme conjugates is outlined in Figure 1. The first step (A) involving Pluronic oxidation, was confirmed using Purpald colorimetric assay analysis, indicating 30% conversion of the hydroxyl end-groups (OH) into aldehyde functionalities (CHO). In the next step (B), the activated Pluronic molecules were coupled to lysine residues of lysozyme via reductive amination. Conjugate formation was confirmed by gel electrophoresis (Figure 2A). Lane 1 shows the protein molecular weight marker, which is a mixture of purified proteins resolving in sharp bands from 10 to 140 kDa. This marker is used to compare the molecular weight of the obtained conjugates. Lane 2 in Figure 2A shows Pluronic-lysozyme conjugates with molecular weights of 27 kDa and 41 kDa, respectively, and lane 3 represents free lysozyme. Since the average

molecular weight of Pluronic F-127 is 12.6 kDa and that of lysozyme 14.3 kDa, a conjugate of one Pluronic molecule with one lysozyme molecule corresponds to MW 27 kDa and one Pluronic molecule coupled with two lysozyme molecules to MW 41 kDa. Moreover, lane 2 indicates the presence of remaining uncoupled lysozyme molecules, which were effectively removed by dialysis, as can be seen in lane 4.

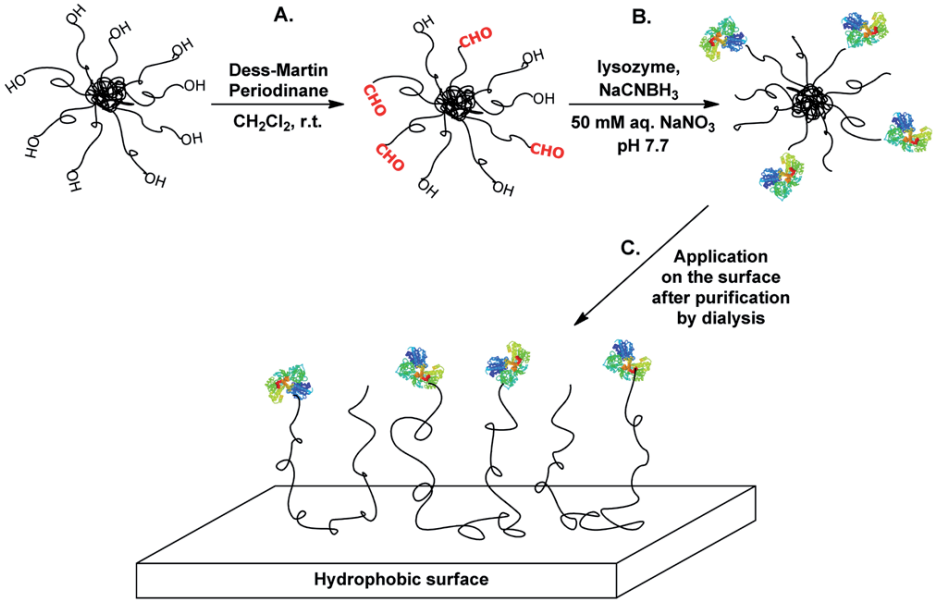

Figure 1. Reaction scheme for the oxidation of Pluronic (A) and conjugation with lysozyme (B) forming micelles in aqueous medium, and adsorption on a hydrophobic surface into the brush conformation (C).

Molecular weights of the obtained conjugates were confirmed by MALDI-TOF mass spectrometry (see Figure 2B). The mass spectrum of the purified sample shows characteristic peaks of the 1:1 Pluronic-lysozyme conjugate of MW 27 kDa (indicated as a in Figure 2B) and the 1:2 Pluronic-lysozyme conjugate of MW 41 kDa (indicated as b in Figure 2B). The strong peak to the left of 20 kDa peak, is

expected to be a conjugate of one Pluronic with two lysozymes, appearing as a doubly charged molecular ion. Moreover, the mass spectrometric analysis confirms the effectiveness of the dialysis purification step since no free lysozyme molecules were detected.

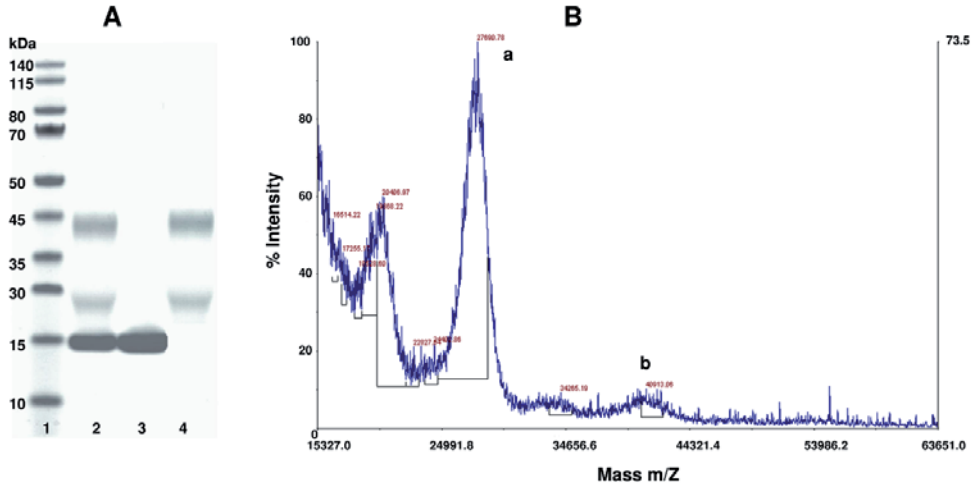

Figure 2. (A) SDS-PAGE analysis, lane 1-molecular weight marker, lane 2- Pluronic coupled with lysozyme before purification (mixture of ~27 kDa conjugates, ~41 kDa conjugates and free lysozymes ~14 kDa), lane 3- free lysozyme, lane 4- Pluronic coupled with lysozyme after dialysis (mixture of ~27 kDa conjugates and ~41 kDa conjugates), and (B) MALDI-TOF mass spectrum of Pluronic-lysozyme conjugates revealing successful coupling of one Pluronic molecule with one (a) and two lysozyme molecules (b).

Enzymatic activity assay of Pluronic-lysozyme conjugates

Data presented in Figure 3 show that Pluronic-lysozyme conjugates of 1 mg/ml concentration exhibit similar antibacterial activity as free lysozyme in a concentration of 0.005 mg/ml. The optical density of bacterial suspensions of Pluronic-lysozyme conjugates (1 mg/ml) was reduced from 0.50 to 0.16 ± 0.01, whereas for free lysozyme (0.005 mg/ml) the reduction was from 0.50 to 0.18 ± 0.02. Furthermore, a decrease in optical density from 0.50 to 0.35 ± 0.02

and 0.37 ± 0.02 was observed for bacterial suspensions exposed to pure phosphate buffer saline (PBS) and uncoupled Pluronic (1 mg/ml), respectively.

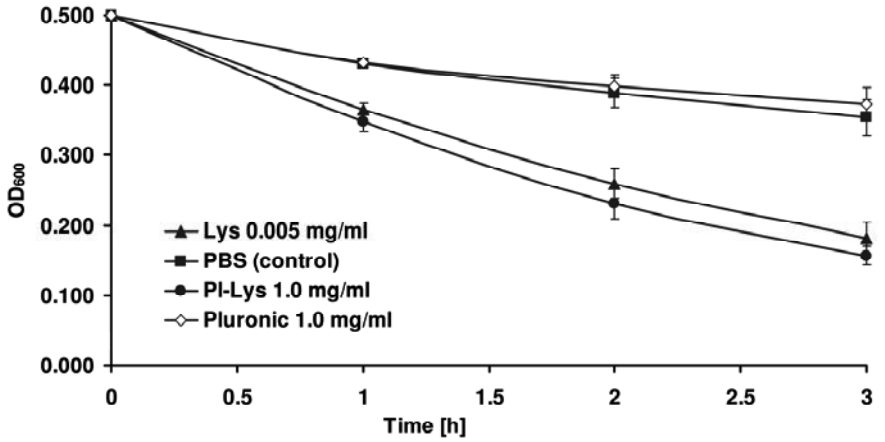

Figure 3. Enzymatic activity of Pluronic-lysozyme (Pl-Lys) conjugates as a function of time, compared to the free lysozyme (Lys) activity, shown as a decrease in optical density OD_{600} of *B. subtilis* 168 caused by lysis of the bacterial cell wall. Error bars indicate standard deviation over three separate experiments.

Properties of adsorbed Pluronic-lysozyme conjugates quartz crystal microbalance with dissipation measurements

Figure 4 shows the hydrated thickness (A) and relaxation time (B) upon exposure of the gold-coated quartz crystal to the various adsorbed compounds, i.e., (a) the uncoupled CHO-Pluronic, (b) lysozyme, (c) lysozyme after CHO-Pluronic, (d) CHO-Pluronic after lysozyme and (e) Pluronic-lysozyme conjugate 100%. The thickness of the 100% Pluronic-lysozyme conjugate is 14.3 ± 1.4 nm, which is greater than the sum of those calculated for CHO-Pluronic (5.8 ± 0.5 nm) and lysozyme (3.6 ± 0.5 nm). The relaxation time of the conjugate ((7.9 ± 0.2) x 10^{-3} s) does not significantly differ from that of the uncoupled CHO-Pluronic ((7.5 ± 1.5) x 10^{-3} s), whereas it is much less than the relaxation time of adsorbed lysozyme ((12.6 ± 2.9) x 10^{-3} s). Furthermore, both the thicknesses and relaxation times of lysozyme

supplied to pre-adsorbed CHO-Pluronic (6.9 ± 0.4 nm and (8.5 ± 1.9) x 10^{-3} s, respectively) as well as CHO-Pluronic after lysozyme (5.8 ± 2.3 nm and (9.0 ± 1.5) x 10^{-3} s, respectively), resemble those recorded for exposure to only uncoupled CHO-Pluronic.

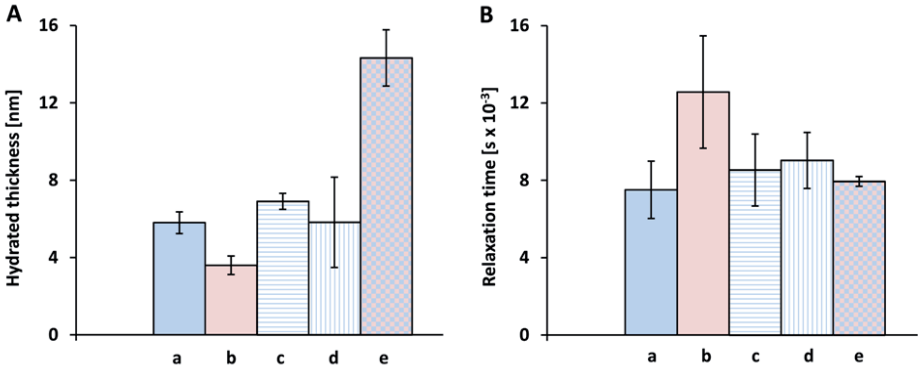

Figure 4. Hydrated thickness (A) and relaxation time (B) determined by QCM-D of the adsorbed layers of (a) CHO-Pluronic, (b) lysozyme, (c) lysozyme after CHO-Pluronic, (d) CHO-Pluronic after lysozyme, (e) Pluronic-lysozyme conjugate 100%. Error bars indicate standard deviation over three separate experiments.

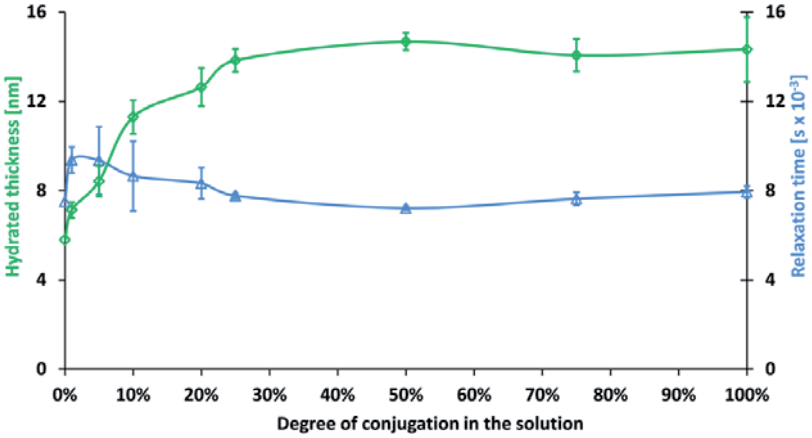

Figure 5. Hydrated thickness and relaxation time of adsorbed layers of Pluronic-lysozyme conjugates as a function of the degree of conjugation (100% corresponds to one Pluronic chain coupled to one or two lysozyme molecules). Error bars indicate standard deviation over three separate experiments.

Increasing the ratio of Pluronic conjugated with lysozyme to uncoupled Pluronic in the solution exposed to the surface, yields a change in the hydrated thickness from 7.1 ± 0.3 nm for 1% conjugation to 13.8 ± 0.5 nm for 25% conjugation, as presented in Figure 5. Beyond a conjugation ratio of 25%, the hydrated thickness reached saturation. No significant changes in the relaxation time with different degree of conjugation were observed for either of the adsorbed compounds.

X-ray photoelectron spectroscopy measurements

Table 1 presents observed N_{1s} electron counts for each sample. Based on the number of counts, the gold-coated surface with only adsorbed lysozyme resulted in 50% protein coverage, whereas adsorption form a solution with 100% or 1% Pluronic-lysozyme conjugation yielded 47% and 32% coverage by lysozyme, respectively.

Table 1. N_{1s} electron counts of a lysozyme filled trough taken as a reference for 100% surface coverage by lysozyme and N_{1s} electron counts and surface coverages by lysozyme calculated for lysozyme on a gold surface and Pluronic-lysozyme (Pl-Lys) conjugates with different degrees of conjugation on silicone rubber.

Sample	N_{1s} counts	Surface coverage by lysozyme [%]
Trough filled with lysozyme (reference)	4268	100
Lysozyme deposited on gold	2110	50
100% Pl-Lys	2017	47
1% Pl-Lys	1349	32

Bacterial adhesion and growth

Figure 6 gives the number of adhering bacteria in the absence of growth on uncoated silicone rubber, on a coating of unmodified Pluronic and of Pluronic-lysozyme conjugates (1% and 100% conjugation ratios) as a function of time. Adhesion of *B. subtilis* 168 after 2 h was reduced from (1.3 ± 0.5) x 10^5 /cm^2 on uncoated silicone rubber to (0.2 ± 0.1) x 10^5 /cm^2 on an unconjugated Pluronic brush. Adhesion to 100% and 1% Pluronic-lysozyme conjugated brush-coated surfaces resulted in (1.1 ± 0.2) x 10^5 and (0.8 ± 0.0) x 10^5 bacteria adhering per cm^2, respectively, attesting to their anti-adhesive functionality.

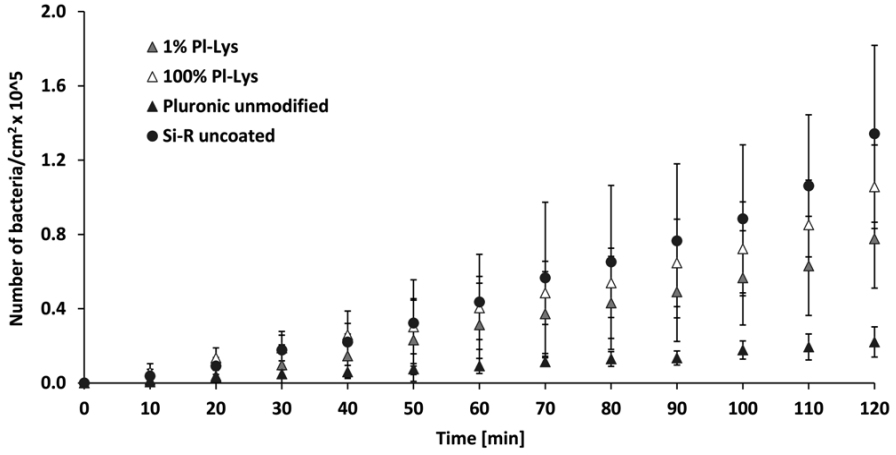

Figure 6. Initial adhesion of *B. subtilis* 168 to uncoated (Si-R uncoated) and coated silicone rubber when adsorbed from a mixture of uncoupled Pluronic and Pluronic lysozyme conjugate in 99:1 ratio (1% Pl-Lys) and 100 % Pluronic-lysozyme conjugates (100% Pl-Lys) as a function of time. Error bars indicate standard deviation over four separate experiments.

Figure 7 shows that the total number of cultivable bacteria or CFUs present on the surfaces after 20 h growth is highest after coating with unconjugated Pluronic molecules, followed by uncoated silicone rubber. The number of CFUs present on a surface coated with a 100% Pluronic-lysozyme conjugate is reduced to about

30% and to 15% for 1% Pluronic-lysozyme conjugate, as compared with a coating consisting of unconjugated Pluronic molecules. After 20 h of growth, however, there are both cultivable, live bacteria as well as dead bacteria, as presumably killed by the coating, present.

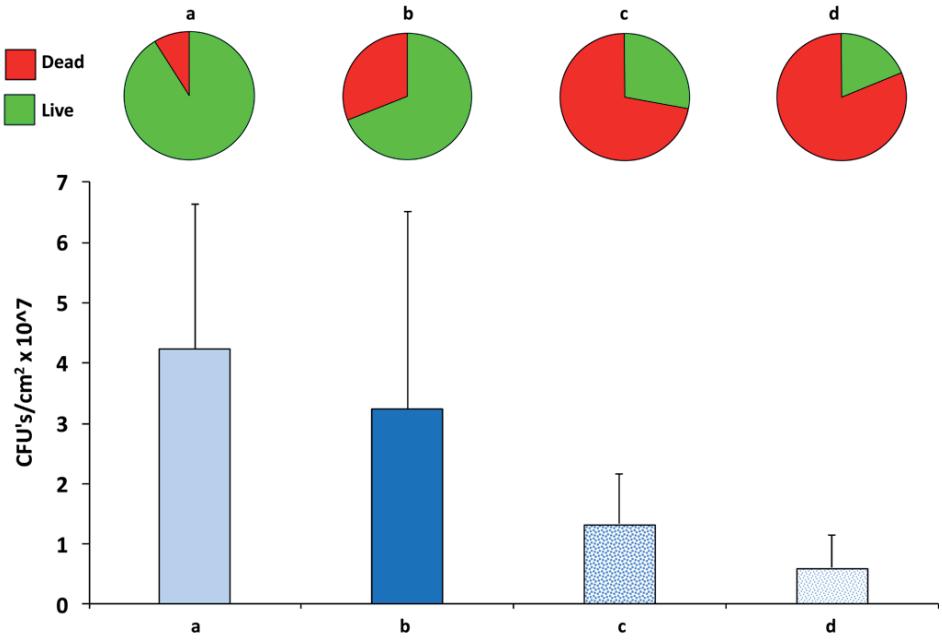

Figure 7. CFUs per unit area of *B. subtilis* 168 after 20 h of growth on (a) Pluronic unmodified coating (b) uncoated silicone rubber (c) 100% Pluronic-lysozyme and (d) 1% Pluronic-lysozyme coated silicone rubber together with the percentage viability of the biofilms, represented by the pancakes. Error bars indicate standard deviation over four separate experiments. Live/dead percentage of bacteria represented by the pancakes include an average standard deviation of 5% over four separate experiments.

The fraction of live bacteria (see Figure 7) on the uncoated silicone rubber is 69% and even 91% on unmodified Pluronic brush. However, in case of the lysozyme containing conjugates, the viability drops to 28% and 19% for coatings with 100% and 1% Pluronic-lysozyme conjugates, respectively. These finding attest to the antibacterial functionality, in addition to an anti-adhesive functionality.

DISCUSSION

Anti-adhesive properties of polymer brush-coatings have been reported in literature before [10,36], but interactions between bacteria and functionalized brushes have not received much attention so far. In this study, we present an approach for bioconjugate formation using a synthetic polymer, i.e. Pluronic and the protein lysozyme, in a two-step reaction. The resulting conjugates were characterized by SDS-PAGE gel electrophoresis, MALDI-TOF mass spectrometry and enzymatic activity assay. Physico-chemical properties of surfaces coated with Pluronic-lysozyme conjugates were determined using QCM-D and XPS techniques. Anti-adhesive and antibacterial functionalities of the modified coatings were determined against *B. subtilis* in a parallel plate flow chamber in terms of the number of initially adhering bacteria per unit area and the number of viable bacteria after growth for 20 h.

Preparation and activity of Pluronic-lysozyme conjugates

The conjugation reaction of lysozyme molecules to the Pluronic F-127 polymer requires only a simple procedure, is reproducible, and cost effective without the need of substrate recovery. Therefore, the coupling strategy involving two steps, i.e. alcohol oxidation followed by protein attachment by reductive amination, can be applied for other peptides and proteins as well. However, with lysozyme there is a risk of multi-conjugate formation because each lysozyme molecule contains six lysine residues, which gives the possibility of multiple couplings. Such a hybrid, where lysozyme is completely surrounded by polymer chains would be rather inactive due to reduced accessibility to the bacterial cell wall. To suppress the formation of multi-conjugates, the pH of the reaction mixture should be well controlled and maintained at ~7.7. For pH < 7 protonation of the $-NH_2$ groups of all six lysine residues makes the coupling reaction impossible to proceed and for

pH > 8 all $–NH_2$ groups are deprotonated and, hence, available for coupling with the PEO blocks. Analysis of obtained conjugates shows the absence of multi-conjugates. SDS-PAGE together with mass spectrometry clearly showed the presence of conjugates composed of Pluronic molecules with one and two lysozymes per chain. The compound with a MW 20 kDa, which was detected by MALDI-TOF, but not by SDS-PAGE, is expected to be a conjugate of one Pluronic with two lysozymes, appearing as a doubly charged molecular ion. MALDI-TOF is a soft ionization method where the singly protonated molecular ions are usually the dominant species. However, they can be accompanied by doubly charged species at approximately half the m/z value [37], which explains in our case the presence of a peak with half the Mw of 41 kDa. The partial loss of lysozyme activity after coupling to the polymer chain may be caused by conformational changes in the protein structure and/or reduction in the enzyme-substrate contact.

Based on the molecular weights of both Pluronic and lysozyme, we estimate how much protein is present in 1 mg conjugate. Having a mixture of Pluronic coupled with one and Pluronic coupled with two lysozymes in an assumed ratio 1:1, we calculate that 1 mg contains 0.4 mg of Pluronic and 0.6 mg of lysozyme. This indicates activity loss of the conjugated proteins by a factor of 120 compared to free lysozyme. Although, this is a severe loss, the adhesion and growth data together with biofilm viability displayed in the Figure 6 and 7, prove strongly remaining lysozyme activity in the conjugates when applied as a surface coating.

Conformation of Pluronic-lysozyme conjugates at a hydrophobic surface

Pluronic molecules adsorb at a hydrophobic surface by attachment of their hydrophobic PPO block, whereas their PEO chains protrude in the aqueous solution [17]. Pluronic F-127 adsorption is dictated by the hydrophobicity of the

substrate surfaces and adsorbs on different hydrophobic surfaces in the same conformation and with comparable thickness [39]. Hence, the structural information on the coating derived from QCM-D experiments using hydrophobic gold substrates may be correlated to the bacterial adhesion and viability tests performed in the parallel plate flow chamber on a hydrophobic silicone rubber biomaterial. After attachment of lysozyme to the terminal ends of the PEO chains, the adsorption behaviour of the conjugate may deviate from that of unmodified Pluronic. Lysozyme also has a tendency to adsorb to hydrophobic surfaces [38], and hence it may compete with the PPO block to attach to the surface. Obviously, the adsorbed Pluronic-lysozyme conjugate can adopt a brush or a pancake conformation (see Figure 8a and b), depending on the adsorption affinity of lysozyme, relative to that of PPO, and on the loss of conformational entropy of the conjugate when it attaches via lysozyme at its terminal ends.

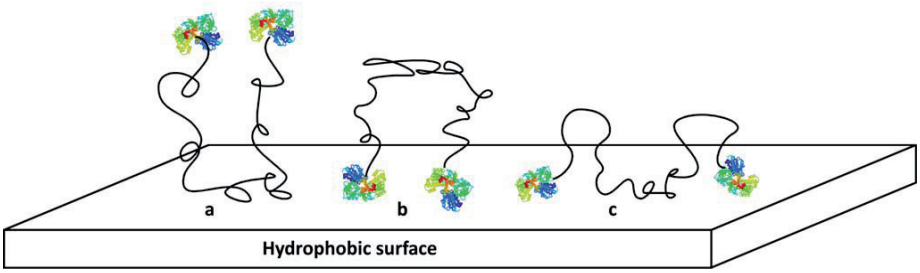

Figure 8. Possible conformations of Pluronic-lysozyme conjugates adsorbed as (a) a brush with the Pluronic with its PPO block attached to the surface and the PEO chains with the lysozyme in the solution (b) a pancake with lysozyme adsorbed on the surface or (c) a structure where both lysozyme and the PPO of the Pluronic attach to the surface.

It may also be possible that the conjugate anchors to the surface by both its PPO and lysozyme moieties as shown in Figure 8c. The conformation of the layer of Pluronic-lysozyme conjugates on the surface was investigated by comparing values of their thickness and relaxation time with those of uncoupled lysozyme

and Pluronic, obtained using QCM-D. The thickness of the uncoupled CHO-Pluronic (5.8 ± 0.5 nm) is in agreement with the thickness of a Pluronic brush of the same type [39]. The thickness of adsorbed lysozyme (3.6 ± 0.5 nm) corresponds to a monolayer with side-on adsorbed unperturbed lysozyme molecules having dimensions of 3.0 nm x 3.0 nm x 4.5 nm [22]. The thickness of the Pluronic-lysozyme conjugate is larger than the sum of those of CHO- Pluronic and lysozyme, suggesting that the lysozyme coupling forces the Pluronic to stretch out further into the solution. The observation that beyond a Pluronic-lysozyme: CHO-Pluronic ratio of 25% in solution, the thickness of the coating does not increase any further suggests preferential adsorption of the Pluronic-lysozyme conjugate. The relaxation time of this conjugate resembles that of CHO-Pluronic rather than that of lysozyme, showing that the polymer part and not the protein part determines the viscoelastic properties. Adsorption of lysozyme after pre-adsorption of CHO-Pluronic, as well as sequential adsorption in the reversed order, yields values for thickness and relaxation time resembling those obtained for CHO-Pluronic and deviating from the values obtained for lysozyme. These observations provide strong evidence that in sequential adsorption, CHO-Pluronic does displace lysozyme from the surface, but that lysozyme is not able to displace adsorbed CHO-Pluronic. Apparently, the affinity of Pluronic for the hydrophobic gold surface is much higher than the affinity of lysozyme for that surface. From those data, we infer that the conjugate adsorbs by attaching its PPO block to the surface and the PEO chains with the attached lysozyme molecules are exposed to the solution. The strong attachment of the PPO block to the hydrophobic surface is in line with the high stability of Pluronic layers adsorbed at such a surfaces [40,41].

The occurrence of the adsorbed Pluronic-lysozyme conjugates in a brush-like conformation is further supported by the results from the bacterial adhesion

and growth experiments, although adhesion of *B*. *subtilis* 168 is higher on a functionalized brush than on an unconjugated Pluronic brush-coating, which might be ascribed to favourable electrostatic interaction between the positively charged lysozyme molecules and the negatively charged bacteria. This on its turn, is supported by the observation of an increased fraction of dead bacteria in the biofilm grown on coatings with Pluronic-lysozyme conjugated brushes.

Composition of the coating with respect to anti-adhesive and antibacterial functionalities

Varying the ratio between Pluronic-lysozyme conjugates and unmodified Pluronic in a brush, enables determination of the optimal composition of the coating. Results obtained by XPS analysis clearly show that the content of lysozyme in 100% Pluronic-lysozyme conjugated coating is almost the same as when the surface is coated only with uncoupled lysozyme, corresponding to 47% surface coverage by lysozyme. Even for the coating formed after exposing the surface to a solution containing only 1% Pluronic-lysozyme conjugate, lysozyme coverage remains remarkably high, i.e., 32%. Again, this points to preferential adsorption of the conjugate relative to CHO-Pluronic. As expected, a lower surface coverage by lysozyme yields less bacterial adhesion, indicating that the anti-adhesive functionality of the Pluronic coating is preserved. The most viable biofilm was found on the unconjugated Pluronic brush-coating, in line with previous work [10], in which it was found that bacteria growing on Pluronic brush-coatings were less thick than on uncoated silicone rubber allowing more nutrients to penetrate into the adhering biofilm, yielding more viable bacteria. In fact, these observations prompted us to design a Pluronic brush-coating with conjugated lysozyme, to reduce the viability of the few bacteria that managed to adhere and grow on a Pluronic brush-coating. This requires an optimal amount of lysozyme in

these coatings based on the preservation of anti-adhesive versus the development of bactericidal properties. However, and unexpectedly, the coating with the lower surface coverage by lysozyme is more effective in killing (i.e. causing lysing in this particular case) the bacteria than the brush prepared of a 100% Pluronic-lysozyme conjugate. One might wonder whether the efficacy of the surface coating changes when the surface first comes in contact with a protein-containing solution, such as most biofluids are (*e.g.* blood or saliva). If proteins would adsorb on the coated surface, this would most likely influence bacterial adhesion and/or viability. However, Norde and Gage [42] showed that a very similar Pluronic, $(PEO)_{100}$-$(PPO)_{56}$-$(PEO)_{100}$, exposed to a hydrophobic surface adopts a brush conformation having a sufficiently high density to strongly suppress protein adsorption. Hence, anti-adhesive and antibacterial functions of our coating are not expected to be lost after exposure to a protein containing biofluid.

CONCLUSIONS

We presented a successful approach for preparing bioconjugates of synthetic polymers with natural proteins to be applied as functional coatings. Thus, brush-coatings consisting of Pluronic and Pluronic-lysozyme conjugates were applied that exert bi-functionality, i.e. an anti-adhesive activity due to the polymer brush together with the antibacterial activity of the lysozyme. The work described in this paper contributes to a better understanding of the behaviour and surface properties of functionalized polymers, which may help to future development of more complex multi-functional coatings for application in biological systems, including coating of biomaterials implant surfaces.

REFERENCES

1. Gristina AG. Implant failure and the immune-incompetent fibro-inflammatory zone. Clin Orthop Relat R 1994;298:106-118.

2. Gristina AG. Biomaterial-centered infection - microbial adhesion versus tissue integration. Science 1987;237:1588-1595.

3. Stickler DJ, Mclean RJC. Biomaterials associated infections - the scale of the problem. Cells Mater 1995;5:167-182.

4. Zhao LZ, Chu PK, Zhang YM, Wu ZF. Antibacterial coatings on titanium implants. J Biomed Mater Res B 2009;91:470-480.

5. Rojas IA, Slunt JB, Grainger DW. Polyurethane coatings release bioactive antibodies to reduce bacterial adhesion. J Control Release 2000;63:175-189.

6. Charville GW, Hetrick EM, Geer CB, Schoenfisch MH. Reduced bacterial adhesion to fibrinogen-coated substrates via nitric oxide release. Biomaterials 2008;29:4039-4044.

7. Baveja JK, Wilcox MDP, Hume EBH, Kumar N, Odell R, Poole-Warren LA. Furanones as potential anti-bacterial coatings on biomaterials. Biomaterials 2004;25:5003-5012.

8. Sivakumar PM, Iyer G, Natesan L, Doble M. 3 '-Hydroxy-4-methoxychalcone as a potential antibacterial coating on polymeric biomaterials. Appl Surf Sci 2010;256:6018-6024.

9. Leckband D, Sheth S, Halperin A. Grafted poly(ethylene oxide) brushes as nonfouling surface coatings. J Biomat Sci-Polym E 1999;10:1125-1147.

10. Nejadnik MR, Van der Mei HC, Norde W, Busscher HJ. Bacterial adhesion and growth on a polymer brush-coating. Biomaterials 2008;29:4117-4121.

11. Raynor JE, Capadona JR, Collard DM, Petrie TA, Garcia AJ. Polymer brushes and self-assembled monolayers: Versatile platforms to control cell adhesion to biomaterials. Biointerphases 2009;4:FA3-FA16.

12. Ayres N. Polymer brushes: Applications in biomaterials and nanotechnology. Polymer Chemistry 2010;1:769-777.

13. Currie EPK, Norde W, Stuart MAC. Tethered polymer chains: surface chemistry and their impact on colloidal and surface properties. Adv Colloid Interf 2003;100:205-265.

14. Sofia SJ, Premnath V, Merrill EW. Poly(ethylene oxide) grafted to silicon surfaces: Grafting density and protein adsorption. Macromolecules 1998;31:5059-5070.

15. FreijLarsson C, Nylander T, Jannasch P, Wesslen B. Adsorption behaviour of amphiphilic polymers at hydrophobic surfaces: Effects on protein adsorption. Biomaterials 1996;17:2199-2207.

16. Alexandridis P, Hatton TA. Poly(Ethylene Oxide)-Poly(Propylene Oxide)-Poly(Ethylene Oxide) block-copolymer surfactants in aqueous-solutions and at interfaces - thermodynamics, structure, dynamics, and modeling. Coll Surfaces A 1995;96:1-46.

17. Schroen CGPH, Stuart MAC, Maarschalk KV, Van der Padt A, Van't Riet K. Influence of preadsorbed block-copolymers on protein adsorption - surface properties, layer thickness, and surface coverage. Langmuir 1995;11:3068-3074.

18. Otsuka H, Nagasaki Y, Kataoka K. Self-assembly of poly(ethylene glycol)-based block copolymers for biomedical applications. Curr Opin Colloid In 2001;6:3-10.

19. Masschalck B, Michiels CW. Antimicrobial properties of lysozyme in relation to foodborne vegetative bacteria. Crit Rev Microbiol 2003;29:191-214.

20. Arnheim N, Inouye M, Law L, Laudin A. Chemical studies on enzymatic specificity of goose egg-white lysozyme. J Biol Chem 1973;248:233-236.

21. Czeslik C, Winter R. Effect of temperature on the conformation of lysozyme adsorbed to silica particles. Phys Chem Chem Phys 2001;3:235-239.

22. Vertegel AA, Siegel RW, Dordick JS. Silica nanoparticle size influences the structure and enzymatic activity of adsorbed lysozyme. Langmuir 2004;20:6800-6807.

23. Prager EM, Arnheim N, Wilson AC, Mross GA. Amino-acid sequence studies on bobwhite quail egg-white lysozyme. J Biol Chem 1972;247:2905-2916.

24. Strynadka NCJ, James MNG. Lysozyme revisited - crystallographic evidence for distortion of an N-acetylmuramic acid residue bound in site-D. J Mol Biol 1991;220:401-424.

25. Yuan S, Wan D, Liang B, Pehkonen SO, Ting YP, Neoh KG, Kang ET. Lysozyme-coupled poly(poly(ethylene glycol) methacrylate-stainless steel hybrids and their antifouling and antibacterial surfaces. Langmuir 2011;27:2761-2774.

26. Danial M, Klok HA, Norde W, Stuart MAC. Complex coacervate core micelles with a lysozyme-modified corona. Langmuir 2007;23:8003-8009.

27. Tao L, Liu JQ, Xu JT, Davis TP. Synthesis and bioactivity of poly(HPMA)-lysozyme conjugates: the use of novel thiazolidine-2-thione coupling chemistry. Org Biomol Chem 2009;7:3481-3485.

28. Yi X, Batrakova E, Banks WA, Vinogradov S, Kabanov AV. Protein conjugation with amphiphilic block copolymers for enhanced cellular delivery. Bioconjug Chem 2008;19:1071-1077.

29. Chung HJ, Go DH, Bae JW, Jung IK, Lee JW, Park KD. Synthesis and characterization of Pluronic® grafted chitosan copolymer as a novel injectable biomaterial. Curr Appl Phys 2005;5:485-488.

30. Thordarson P, Le Droumaguet B, Velonia K. Well-defined protein-polymer conjugates-synthesis and potential applications. Appl Microbiol Biotechnol 2006;73:243-254.

31. Shachaf Y, Gonen-Wadmany M, Seliktar D. The biocompatibility of Pluronic (R) F127 fibrinogen-based hydrogels. Biomaterials 2010;31:2836-2847.

32. Gonen-Wadmany M, Oss-Ronen L, Seliktar D. Protein-polymer conjugates for forming photopolymerizable biomimetic hydrogels for tissue engineering. Biomaterials 2007;28:3876-3886.

33. Schmidt CF, Zimmermann RM, Gaub HE. Multilayer adsorption of lysozyme on a hydrophobic substrate. Biophys J 1990;57:577-588.

34. Quesenberry MS, Lee YC. A rapid formaldehyde assay using purpald reagent: Application under periodation conditions. Anal Biochem1996;234:50-55.

35. Voinova MV, Rodahl M, Jonson M, Kasemo B. Viscoelastic acoustic response of layered polymer films at fluid-solid interfaces: Continuum mechanics approach. Phys Scr 1999;59:391-396.

36. Brittain WJ, Minko S. A structural definition of polymer brushes. J Pol Sci Pol Chem 2007;45:3505-3512.

37. Gross JH. Mass Spectrometry. A textbook. Springer-Verlag 2005: p. 507-560.

38. Wertz CF, Santore MM. Adsorption and reorientation kinetics of lysozyme on hydrophobic surfaces. Langmuir 2002;18:1190-1199.

39. Nejadnik MR, Olsson ALJ, Sharma PK, Van der Mei HC, Norde W, Busscher HJ. Adsorption of Pluronic F-127 on surfaces with different hydrophobicities probed by quartz crystal microbalance with dissipation. Langmuir 2009;25:6245-6249.

40. Liu X, Wu D, Turgman-Cohen S, Genzer J, Theyson TW, Rojas OJ. Adsorption of a nonionic symmetric triblock copolymer on surfaces with different hydrophobicity. Langmuir 2010;26:9565-9574.

41. Hellmich W, Regtmeier J, Duong TT, Ros R, Anselmetti D, Ros A. Poly(oxyethylene) based surface coatings for poly(dimethylsiloxane) microchannels. Langmuir 2005;21:7551-7557.

42. Norde W, Gage D. Interaction of bovine serum albumin and human blood plasma with PEO-tethered surfaces: influence of PEO chain length, grafting density and temperature. Langmuir 2004;20:4162-4167.

Chapter 4

Simulating bacterial response to a bifunctional polymer brush-coating using BioScape computer modeling

A. K. Muszanska, V. Sharma, A. Compagnoni, M. Libera, J. Sjollema, W. Norde, H.C. van der Mei, H.J. Busscher

ABSTRACT

The development of new, antimicrobial biomaterials or coatings consists traditionally of designing a surface and evaluating its properties experimentally. This trial and error approach is limited because of the resources and time required to provide a representative number of configurations in a complex experimental set-up. Therefore, computational modeling is of paramount importance in identifying optimal materials properties to prevent biomaterial-associated infections. To address this issue, we used BioScape, a concurrent agent-based modeling and simulation language for bacteria-materials interactions to build a computational model simulating properties of antimicrobial, bifunctional polymeric coatings. These bifunctional polymeric coatings are composed of anti-adhesive polymer chains (Pluronic) and an antimicrobial protein (lysozyme), covalently attached at the Pluronic ends. Our computational model was built to simulate bacterial responses to the three different surfaces namely, Pluronic unmodified, 1% Pluronic-lysozyme and 100% Pluronic-lysozyme (see also Chapter 3) for both the initial bacterial adhesion and growth phase. The output of the model not only plots the number of live and dead bacteria over time as a function of surface coverage by lysozyme over a much wider range of coverages than can be obtained experimentally, but it also produces 3D-rendered videos of bacteria-surface interactions enhancing the visualization of the system's behavior.

INTRODUCTION

The occurrence of biomaterial-associated infections (BAI) is a major clinical problem for which no solution has been found yet [1,2]. Detailed understanding of the various interactions between microorganisms and the biomaterial surface is required to design new biocompatible materials resistant to colonization by pathogenic bacteria [3-5]. Computational modeling may be helpful to assess these interactions. One of the formalisms that have been successfully used to model complex biological systems is process algebra, which is an alternative to models based on sets of differential equations [6-8]. Process algebras are particularly attractive because of their ability to accommodate multiple objects and different behavioral characteristics. In such a model the information is exchanged through communication channels and elements can interact simultaneously and influence each other simulating a real complex biological system [9,10]. Currently, however, existing modeling languages based on concurrent synchronization lack adequate design allowing to study complex interactions including movements in three-dimensional space and stochastic interactions. Modeling languages like SPiM [11], Kappa [12], Petri-Nets [13], BioAmbients [14] and BioPEPA [15] lack spatial attributes, SpacePi [16] and BioShape [17] lack stochasticity. To solve this problem we used a new, recently developed modeling language, called BioScape. BioScape incorporates both stochasticity and 3D spatial characteristics to simulate biological systems where all processes can happen at the same time in a reactive environment [18]. A stochastic simulation provides random variations to reflect natural processes. Unlike deterministic simulations, where every execution of the system gives an identical result, a stochastic process can always evolve in many different ways even if the initial conditions are the same [19,20]. BioScape allows us to model objects that are placed in 3D space, and it also raises the issue of shape and size of reactants, as well as the area within which they can move.

All these features are crucial to model the behavior of bacteria at a surface to which they may adhere, detach, multiply, get killed by an antimicrobial agent, grow into a biofilm, and where all these processes are occurring at the same time.

The aim of this study was to design a specific program that would allow to predict the surface response towards bacteria based on our previous work where we developed a bifunctional polymer brush-coating [21]. Such a coating combines two activities as presented in Figure 1; an anti-adhesive functionality due to the polymer chains and an antimicrobial one due to the lysozyme attached at the end of the chains able to kill bacteria on contact. To test the bacterial response towards each coating one must run at least a 20 h experiment. Taking into account all preparations prior to the appropriate experimental run followed by evaluation of the outcomes, one can do only two separate experiments per week. Computer programs that could predict bacterial response on differentially coated surfaces would allow to reduce the time spent on the experiments and help to validate obtained results. Development of new biomaterials and coatings is a slow and time-consuming process requiring very often endless laboratory experiments and evaluations proving its properties. A computer program that could predict these characteristics, when given right input information, would be a critical tool highly desired in the field of biomaterial surface engineering allowing to minimize the time and costs of bringing new products to the market. Here we present the development of a three dimensional computational model using BioScape [18], an agent-based modeling and simulation language. An agent, like a bacterium, reacts to its environment and is able to send or receive information through a communication channel (for example, kill or attach). The model addresses two different experimental phases: initial bacterial adhesion and growth, and it takes as input experimental results of three different coatings studied previously (see Chapter 3), namely, Pluronic unmodified, 1% Pluronic-lysozyme, and 100%

Pluronic-lysozyme. The ability to simulate bacterial responses towards varying configurations of surface coatings, both during the adhesion and growth phases, allowed us to find percentages of the coating constituents which would lead to optimal antimicrobial efficacy.

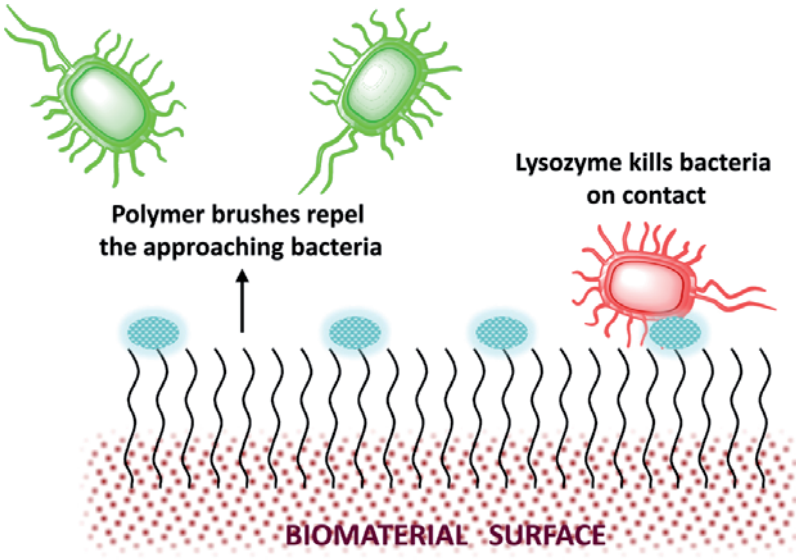

Figure 1. Scheme representing a bifunctional polymer brush-coating combining anti-adhesive properties due to the polymer chains and antimicrobial properties due to the lysozyme conjugated at the end of the chains having direct contact with adhering bacteria.

METHODS

Wet-lab experiments

Pluronic-lysozyme conjugates were synthesized as described previously [22]. The coating was formed by exposing the surface to a solution of unmodified Pluronic and Pluronic-lysozyme conjugates in varying ratios and allowing them to attach. The concentrations of the two components in the solution used for the wet-lab experiments were Pluronic unmodified, 1% conjugated Pluronic-lysozyme (1% Pluronic-lysozyme : 99% Pluronic unmodified) and 100% conjugated Pluronic-

lysozyme (100% Pluronic-lysozyme : 0% Pluronic unmodified). Surfaces coated with 1% Pluronic-lysozyme and 100% Pluronic-lysozyme were investigated by X-ray Photoelectron Spectroscopic analysis to determine the percentage surface coverage by lysozyme and yielded 32% and 47% coverage, respectively. In this study, we built the model to determine bacterial response towards surface coated with Pluronic unmodified, 1% Pluronic-lysozyme and 100% Pluronic-lysozyme.

***In silico*: BioScape language characteristics**

BioScape is a concurrent agent-based modeling language for the stochastic simulation of complex processes in a reactive environment and 3D space. The language characteristics listed below help in capturing the interactions at the interface between bacteria and biomaterials:

Concurrency: The processes we want to model are inherently concurrent like for example: bacteria adhere to the substratum surface, multiply, bacteria are being killed on contact with an antimicrobial molecule, bacteria diffuse into the solution, and it all can happen simultaneously.

Process algebra: Process algebras are formal languages originally designed to model complex reactive computer systems where heterogeneous agents interact concurrently, exchanging information through communication channels. Because of the similarities between reactive computer and biological systems, process algebras have recently been used to model various biological systems [22,23].

Stochastic simulation: A stochastic simulation provides for realistic variations and unforeseen event sequences to more faithfully reflect natural processes and wet-lab experiments, unlike deterministic simulations, where every execution of the system renders an identical result.

Simulation

The simulation algorithm has two phases: reaction and movement. The reaction phase is based on Gillespie's algorithm as implemented in SPiM, and instead of keeping only concentrations for each agent species, it also keeps 3D information – (x,y,z) – for each instance. Gillespie's algorithm produces two outputs in each iteration: a reaction to be executed next, and a time interval to update the simulation clock. If the selected reaction is an interaction between two agents (send/receive), then the algorithm uses 3D location information to identify two individual agents close enough to interact, and places the product in close proximity to the reagents avoiding collision/overlap. If there are not two such agents close enough to react and with adequate space to locate the product of the reaction (probabilistically impossible), it proceeds to the movement phase. If the selected reaction is a first order reaction (delay), the algorithm propagates 3D information to the product and resolves any overlap/collision generated by the reaction. The movement phase uses the time interval generated by Gillespie's algorithm and moves each agent in a random direction a distance proportional to the diffusion rate in that period of time. The movement phase takes into account collision/overlap detection.

From experimental data to computational model

In order to translate the experimental data into a computational model, we needed to introduce several input parameters such as binding sites, simulation time, reaction rates, and initial concentrations of unmodified Pluronic and lysozyme, which are listed and explained below:

Binding sites: There are 10^8 binding sites on 1 cm^2 surface. The size of the surface a single bacterium occupies is considered to be 1 μm^2. We calculate the number of binding sites as follows:

Total number of binding sites = total surface area/size of a single bacterium = 1 cm^2/1 μm^2 = 10^8 binding sites. In our *in silico* experimental set-up the size of the surface is 10,000 μm^2 resulting 10^4 binding sites, and each binding site is speculated to be either unmodified Pluronic or lysozyme.

Simulation time: One unit of simulation time corresponds to 10 min of a wet-lab. The adhesion phase consists of 12 units of simulation time and the growth phase consists of 108 units.

Reaction rate parameters: The conversions of bacterial attachment rates, for three different surfaces, Pluronic unmodified, 1% Pluronic-lysozyme and 100% Pluronic-lysozyme, and their replication rate from wet-lab experiments to their equivalents used *in silico* are presented in Table 1.

Table 1. Rate parameters employed for bacteria (Bac) when attached to Pluronic or lysozyme .

Name	Equation	Rates in wet-lab [bacteria/min per cm^2]	Rates *in silico* [bacteria/min at binding site]
Rate of attachment of bacteria to Pluronic	Bac + Pluronic --> Live	184	0.00000184
Rate of attachment of bacteria to lysozyme	Bac + lysozyme --> Dead	1671	0.00001671
Rate of replication of bacteria when attached to Pluronic	Bac --> Bac|Bac	100	0.000001

Initial concentrations: The calculated initial concentrations of Pluronic and lysozyme binding sites *in silico* based on the surface coverage by lysozyme from the wet-lab for the three surfaces are presented in Table 2.

Table 2. Surface coverage by lysozyme in the wet-lab and numbers of Pluronic and lysozyme binding sites *in silico*.

Name	Surface coverage by lysozyme [%] in wet-lab	No. of Pluronic binding sites *in silico*	No. of lysozyme binding sites *in silico*
Pluronic unmodified	0	10000	0
1% Pluronic-lysozyme	32	6800	3200
100% Pluronic-lysozyme	47	5300	4700

RESULTS

We used BioScape to build the computational model for evaluating the properties of anti-adhesive and antimicrobial bifunctional polymer coatings. Using Bioscape, we were able to obtain visual results as well as quantitative plots for the two experimental phases, initial bacterial adhesion and growth *in silico* mimicking the results from real, wet-lab experiments. Bioscape simulations help to better understand the complex responses of bacteria towards different surfaces and help to validate the results obtained from the wet-lab. After each phase, numbers of dead and live bacteria are measured.

Adhesion phase

During the adhesion phase, bacteria flow over the substratum surface and are allowed to move (vertically deposit onto the surface), attach or get killed by lysozyme. The unattached, free floating bacteria are flushed out. The total number of bacteria attached after 2 h adhesion phase in the wet-lab and their equivalents obtained *in silico* for three different surface coatings are presented in Table 3. The simulation results are shown in Figure 2 as visual snapshots of

bacteria adhering after 2 h (left column) and plots of numbers of bacteria adhering per unit surface area in time (right column). The simulation resulted in numbers of adhering bacteria matching to our wet-lab experiments for all three surface coatings: Pluronic unmodified, 1% Pluronic-lysozyme and 100% Pluronic-lysozyme. Additional to the experimental data, the results of BioScape simulations are separated in live (green) and dead (red) bacteria, resulting in only live bacteria on Pluronic unmodified through increased amounts of dead bacteria for surfaces coated with 1% Pluronic-lysozyme and 100% Pluronic-lysozyme.

Table 3. Numbers of bacteria adhering at the surface after two hours in the adhesion phase. The results obtained from the computational model are the average of five *in silico* experiments.

Name	**No. of bacteria per cm^2 in wet-lab**	**No. of bacteria per cm^2 *in silico***
Pluronic unmodified	0.22×10^5 ($\pm 0.08 \times 10^5$)	0.16×10^5 ($\pm 0.05 \times 10^5$)
1% Pluronic-lysozyme	0.78×10^5 ($\pm 0.26 \times 10^5$)	0.76×10^5 ($\pm 0.05 \times 10^5$)
100% Pluronic-lysozyme	1.06×10^5 ($\pm 0.22 \times 10^5$)	1.15×10^5 ($\pm 0.12 \times 10^5$)

Growth phase

After the adhesion phase, bacteria that are attached to the surface may replicate and form a biofilm during 18 h of experimental set-up. Bacteria that have contact with the killing site (lysozyme) get killed on contact. There is no movement allowed in the growth phase. Both vertical and horizontal growth of bacteria are allowed, however the rate of horizontal growth is higher than the vertical one.

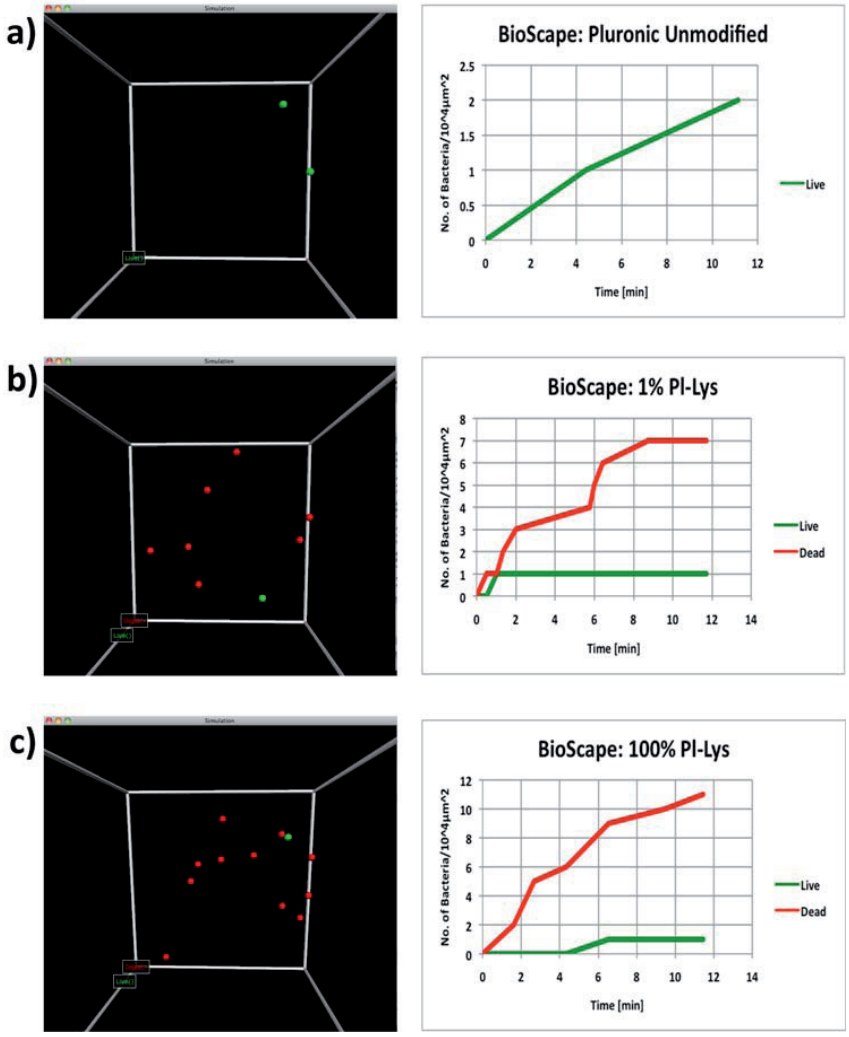

Figure 2. Simulation results of the initial bacterial adhesion phase, produced using BioScape showing a) Pluronic unmodified, b) 1% Pluronic-lysozyme conjugate, c) 100% Pluronic-lysozyme conjugate. Left column shows visualization as a snapshot and right column shows the plot of the number of adhering bacteria per unit area in time. Both visual snapshots and plots represent one out of five *in silico*, experimental runs.

Growth on the top of a dead bacterium as well as formation of multilayers of bacteria are allowed. The numbers of live bacteria expressed here as colony forming units (CFUs) and the percentages of dead bacteria after the 18 h growth phase are measured and shown in Table 4. The numbers of dead bacteria are both due to the presence of lysozyme (killing on contact) and apoptosis which is assumed to be 9% for all the surfaces. The results of the growth phase simulation for the three different surfaces are presented in Figure 3. Similarly as for the adhesion phase, the results are presented here both as visual snapshots (left column) and plots of the numbers of bacteria per unit surface area in time separated in live (green) and dead (red) cells. The simulations resulted in numbers of bacteria per unit surface area (Figure 3) as well as percentages live and dead bacteria (Figure 4), consistent with our wet-lab experiments for all three surface coatings.

Table 4. Numbers of bacteria (CFU's) after the growth phase in the wet-lab (n=3). The results obtained from the computational model are the average of five *in silico* experiments.

Name	**No. of bacteria (CFUs) per cm^2 in wet-lab**	**No. of bacteria (CFUs) per cm^2 *in silico***
Pluronic unmodified	4.22×10^7 ($\pm 2.40 \times 10^7$)	4.13×10^7 ($\pm 0.17 \times 10^7$)
1% Pluronic-lysozyme	0.6×10^7 ($\pm 0.56 \times 10^7$)	0.6×10^7 ($\pm 0.01 \times 10^7$)
100% Pluronic-lysozyme	1.33×10^7 ($\pm 0.83 \times 10^7$)	1.30×10^7 ($\pm 0.02 \times 10^7$)

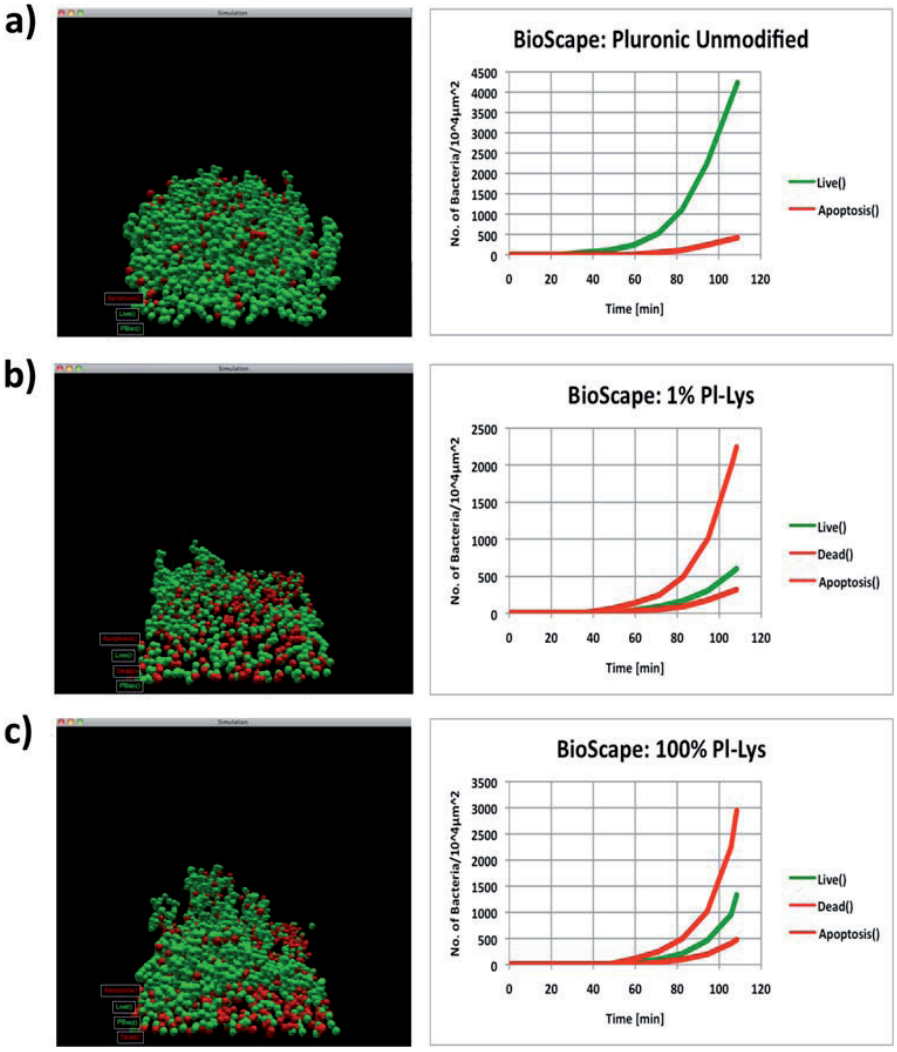

Figure 3. Simulation results of the growth phase, produced using BioScape showing a) Pluronic unmodified, b) 1% Pluronic-lysozyme conjugate, c) 100% Pluronic-lysozyme conjugate. Left column shows visualization as a snapshot and right column shows the plot of the number of bacteria per unit area in time. Both visual snapshots and plots represent one out of five *in silico*, experimental runs.

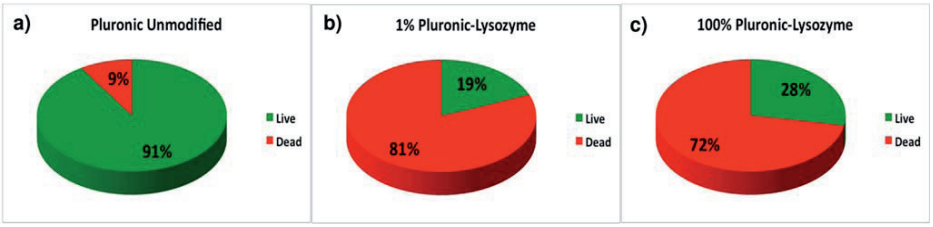

Figure 4. Simulation results of the growth phase, produced using BioScape showing the percentage live and dead bacteria for a) Pluronic unmodified, b) 1% Pluronic-lysozyme conjugate, c) 100% Pluronic-lysozyme conjugate.

DISCUSSION

By implementing our wet-lab experimental data the computational model described here could predict the ideal composition of the surfaces coatings. In the wet-lab experimental set up we usually can perform up to two experiments in one week to measure adhesion and bacterial growth on a specific surface. In order to optimize the composition of a bifunctional surface coating by doing experiments with 10% incremental increases in initial concentrations, it would involve 10 experiments in triplicates, with a total of 30 experiments in 15 weeks. This calculation ignores the time and cost to prepare the coatings, which can add up to 5 to 10 weeks and cost over $10,000 on its own. What we have concluded so far, is that our computational model can be built using nine experiments: three sets of 3 experiments for Pluronic unmodified, Pluronic-lysozyme (1%), and 100% Pluronic-lysozyme. The predictions of our model are then validated with two sets of 3 experiments around the predicted values.

The assumptions made for surface coverage by lysozyme for varying the degrees of Pluronic-lysozyme conjugations (10%, 20%, 30%, 40%, 50%, 60, 70%, 80% and 90%) *in silico* based on the results obtained for the surface coverage by lysozyme for 1% and 100% Pluronic-lysozyme conjugates in the wet-lab are listed in Table 5. The first column in Table 5 corresponds to the degree of conjugation

and the second column corresponds to the resulting surface coverage by lysozyme when applied as a surface coating.

Table 5. Surface coverage by lysozyme for varying concentrations of Pluronic-lysozyme conjugates, obtained by interpolation of X-ray Photoelectron Spectroscopic analysis results for 1% and 100% conjugation.

Name	Surface coverage by lysozyme [%]
Pluronic unmodified	0
1% Pluronic-lysozyme	32.0
10% Pluronic-lysozyme	33.5
20% Pluronic-lysozyme	35.0
30% Pluronic-lysozyme	36.5
40% Pluronic-lysozyme	38.0
50% Pluronic-lysozyme	39.5
60% Pluronic-lysozyme	41.0
70% Pluronic-lysozyme	42.5
80% Pluronic-lysozyme	44.0
90% Pluronic-lysozyme	45.5
100% Pluronic-lysozyme	47.0

The simulation of the adhesion and the growth phase produced using BioScape for varying degrees of Pluronic-lysozyme conjugation are presented in Figures 5a and b. For the adhesion phase, the output of the simulation shows the total number of bacteria (live and dead) adhered to the surface after 2 h.

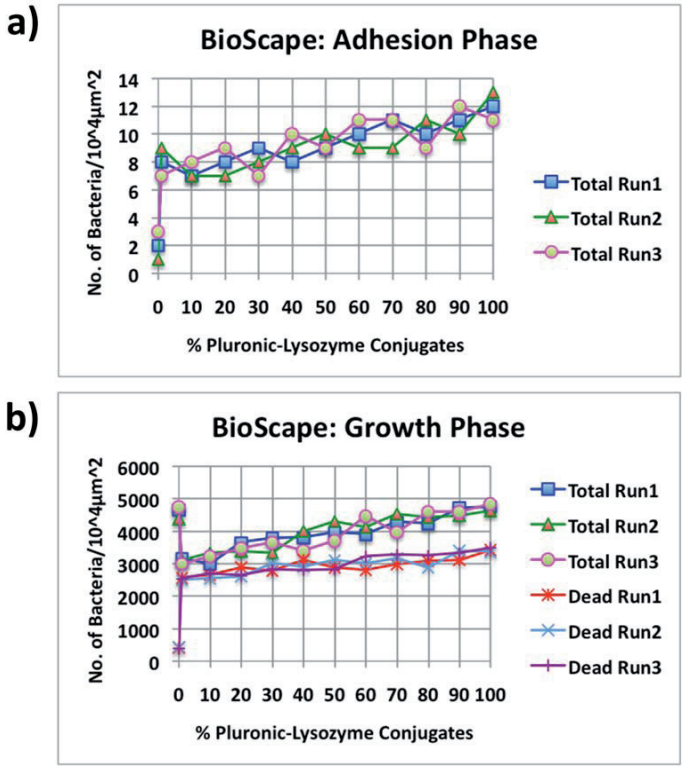

Figure 5. Simulation results for three runs of the a) adhesion phase and b) growth phase, produced using BioScape showing the total numbers of bacteria for varying percentage conjugation (0 - 100%) of Pluronic-lysozyme in solution.

For the growth phase the output of the simulation shows the total number of bacteria (live and dead) and percentage of dead bacteria present at the surface after 20 h of growth. The results of this simulations indicate that a degree of conjugation between 1% and 10% is optimal for its application as a bifunctional coating giving a minimal number of total bacteria present at the surface with the highest number of dead bacteria. Coatings with more than 10% conjugation of Pluronic-lysozyme result in higher numbers of live bacteria at the surface. This observation is consistent with our wet-lab experimental results where we showed that the coating with a lower concentration of lysozyme at the surface (1%)

resulted in higher fraction of dead bacteria in the biofilm compared to the coating with higher amount of lysozyme (100%). This is due to the strong attraction by positively charged lysozyme towards negatively charged bacteria. A higher concentration of lysozyme on the surface, meaning more positive charges, results in increased bacterial adhesion creating a layer of dead bacteria that block the antimicrobial lysozyme over which new bacteria can grow and multiply forming a biofilm.

CONCLUSIONS

We built a computational model to predict bacterial responses towards bifunctional polymer coatings which combine anti-adhesive and antimicrobial properties. *In silico* experiments using BioScape can greatly reduce the time and cost for wet-lab experiments and can accelerate an insight into reducing biomaterial-associated infections. Our model can predict the optimal composition of the surface in order to obtain a minimal number of bacterial surface coverage with the highest fraction of dead bacteria. The simulation results obtained from BioScape for both initial bacterial adhesion and growth phase on the coated surfaces are validated with wet-lab experiments for a limited numbers of conjugation degrees. Spatial information helped us to visualize the bacterial colonization on the surface in 3D. Thus, this study contributes in better understanding of designing an antimicrobial surface and evaluating its properties towards adhering and growing bacteria.

REFERENCES

1. Hasan J, Crawford RJ, Ivanova EP. Antibacterial surfaces: the quest for a new generation of biomaterials. Trends Biotechnol 2013;31:295-304.

2. Goodman SB, Yao Z, Keeney M, Yang F. The future of biologic coatings for orthopaedic implants. Biomaterials 2013;34:3174-3183.

3. Alves NM, Pashkuleva I, Reis RL, Mano JF. Controlling cell behavior through the design of polymer surfaces. Small 2010;6:2208-2220.

4. Brochu AB, Craig SL, Reichert WM. Self-healing biomaterials. J Biomed Mater Res A 2011;96:492-506.

5. Mitragotri S, Lahann J. Physical approaches to biomaterial design. Nat Mater 2009;8:15-23.

6. Machado D, Costa RS, Rocha M, Ferreira EC, Tidor B, Rocha I. Modeling formalisms in Systems Biology. AMB Express 2011;1:45-59.

7. Priami C, Quaglia P. Modelling the dynamics of biosystems. Brief Bioinform 2004;5:259-269.

8. Sumpter DJ, Blanchard GB, Broomhead DS. Ants and agents: a process algebra approach to modelling ant colony behaviour. Bull Math Biol 2001;63:951-980.

9. Cardelli L, Caron E, Gardner P, Kahramanoğulları O, Phillips A. A process model of Rho GTP-binding proteins. Theor Comput Sci 2009;410:3166-3185.

10. Ciocchetta F, Hillston J. Process algebras in systems biology. Lect Notes Comput Sc 2008;5016:265-312.

11. Phillips A, Cardelli L. Efficient, correct simulation of biological processes in the stochastic pi-calculus. Lect Notes Comput Sc 2007;4695:184-199.

12. Danos V, Feret J, Fontana W, Harmer R, Krivine J. Rule-based modelling and model perturbations. Lect Notes Comput Sc 2009;5750:116-137.

13. Peleg M, Rubin D, Altman RB. Using Petri Net tools to study properties and dynamics of biological systems. J Am Med Inform Assoc 2005;12:181-199.

14. Phillips A. An Abstract Machine for the Stochastic Bioambient calculus. Electron Notes Theor Comput Sci 2009;227:143-159.

15. Galpin V, Hillston J. A semantic equivalence for Bio-PEPA based on discretisation of continuous values. Theor Comput Sci 2011;412:2142-2161.

16. John M, Ewald R, Uhrmacher AM. A spatial extension to the π calculus. Electron Notes Theor Comput Sci 2008;194:133-148.

17. Buti F, Cacciagrano D, Corradini F, Merelli E, Tesei L. BioShape: a spatial shape-based scale-independent simulation environment for biological systems. Procedia Comput Sci 2010;1:827-835.

18. Compagnoni A, Sharma V, Bao Y, Libera M, Sukhishvili S, Bidinger P, Bioglio L, Bonelli E. Bioscape: A modeling and simulation language for bacteria-materials interactions. Electron Notes Theor Comput Sci 2013;293:35-49.

19. Versari C, Busi N. Efficient stochastic simulation of biological systems with multiple variable volumes. Electron Notes Theor Comput Sci 2008;194:165-180.

20. Mayer J, Schmidt V, Schweiggert F. A unified simulation framework for spatial stochastic models. Simulation Modelling Practice and Theory 2004;12:307-326.

21. Muszanska AK, Busscher HJ, Herrmann A, Van der Mei HC, Norde W. Pluronic-lysozyme conjugates as anti-adhesive and antibacterial bifunctional polymers for surface coating. Biomaterials 2011;32:6333-6341.

22. Cardelli L, Caron E, Gardner P, Kahramanoğulları O, Phillips A. A process model of Rho GTP-binding proteins. Theor Comput Sci 2009;410:3166-3185.

23. Priami C, Regev A, Shapiro E, Silverman W. Application of a stochastic name-passing calculus to representation and simulation of molecular processes. Inform Process Lett 2001;80:25-31.

Chapter 5

Anti-adhesive polymer brush-coating functionalized with antimicrobial and RGD peptides to reduce biofilm formation and enhance tissue integration

A.K. Muszanska, E.T.J. Rochford, A. Gruszka, A.A. Bastian, H.J. Busscher, W. Norde, H.C. van der Mei and A. Herrmann, submitted to *Biomaterials*

ABSTRACT

This paper describes the synthesis and characterization of polymer-peptide conjugates to be used as infection-resistant coating for biomaterial implants and devices. Anti-adhesive polymer brushes composed of block copolymer Pluronic F-127 were functionalized with antimicrobial peptides (AMP), able to kill bacteria on contact, and RGD peptides to promote the adhesion and spreading of host tissue cells. The anti-adhesive and antibacterial properties of the coating were investigated with three bacterial strains: *Staphylococcus aureus*, *Staphylococcus epidermidis* and *Pseudomonas aeruginosa*. The ability of the coating to support tissue integration was determined using human fibroblast cells. Coatings composed of the appropriate ratio of the three components: Pluronic, Pluronic functionalized with AMP and Pluronic functionalized with RGD proved to be tri-functional showing good anti-adhesive and bactericidal properties without hampering tissue integration.

INTRODUCTION

Bacterial contamination of biomedical implants and devices, leading to biomaterial-associated infection (BAI), is a major problem in hospitals worldwide [1]. It has been estimated that at least 50% of all nosocomial infections are implant-related and affect around two million patients each year in the United States alone [2]. Infection starts with the adhesion of pathogenic bacteria to an implant surface, after which they may multiply and form a biofilm [3]. The formation of biofilms can occur on essentially all currently used biomaterials causing infection and host tissue necrosis [4]. The most common method to treat BAI involves the use of antibiotics [5], the dose of which must be increased to influence bacteria located in protective biofilms compared with planktonic organisms [6]. The trend of emerging microbial resistance to current antibiotics creates the need to find alternatives, challenging material scientists to create a new class of infection-resistant biomaterials [7]. To date, progress in the development of various surfaces showing improved anti-adhesive or antimicrobial properties, has been reported [8-10]. However, the application of such materials is often hampered by poor tissue integration [11]. Designing a surface that resists biofilm formation and simultaneously shows good tissue integration remains a challenge, as it requires multiple conflicting properties to be united in one functional coating [7].

The most promising anti-adhesive surface modifications aim to prevent the initial adhesion of bacteria to a surface and include coating of a surface with a hydrophilic polymer brush [12]. Such a macromolecular architecture acts as a steric barrier between the surface and particles in the surrounding environment [13]. Unfortunately, to date, none of these coatings show complete prevention of bacterial adhesion, and it has been proven that even a few adhering bacteria are still able to form a mature biofilm on polymer brush-coatings [14]. Additionally,

one of the major drawbacks of polymer brush-coatings is the associated suppression of host tissue integration due to the strong anti-adhesive functionality present, thus restricting post-implantation wound healing for applications requiring integration. These features suggest that a polymer brush should be equipped with additional active antimicrobial components to kill the few adhering bacteria to prevent their colonization, as well as including a functionality that promotes tissue integration, thus forming a tri-functional surface [15,16]. Currently, several approaches to create bi-functional polymer brush-coatings have been described, such as by incorporating either antibacterial activity [17-18] or adhesive moieties for stimulated host tissue cell adhesion [19-20].

AMPs are considered to be natural alternatives for antibiotics due to the broad spectrum of their activity, very low toxicity levels and limited ability to create resistant phenotypes [21,22]. AMPs usually have both hydrophobic and hydrophilic regions that enable solubility in an aqueous environment and allow the molecule to pass through lipid-rich bacterial membranes [23,24]. The positively charged residues associated with these molecules interact electrostatically with negatively charged components of the microbial cell wall, such as lipopolysaccharides in Gram-negative and teichoic acids in Gram-positive bacteria, causing the disruption of bacterial membrane integrity [25]. This feature is especially appealing for the design of antimicrobial surfaces where killing bacteria on contact is desired. In tissue integration studies, peptides containing the short RGD sequence have been shown to promote host tissue cell attachment by binding to integrin receptors that are present on the cell surface [26,27]. Therefore, RGDs attached to the extended end of the polymer chain are expected to increase tissue cell adhesion. Unfortunately, RGDs do not only stimulate tissue cell adhesion, but also adhesion of selected bacterial pathogens [28]. Therefore,

these components should be combined into a tri-functional surface to investigate how each affects bacterial and host tissue cell interactions

However, so far these approaches have not been combined into a tri-functional coating and evaluated accordingly. The work presented in this publication describes the development of a tri-functional polymer brush-coating that combines anti-adhesive, bactericidal and tissue integrating properties. To create such a coating, polyethylene oxide chains of the triblock copolymer Pluronic F-127 were covalently conjugated at the terminal ends to an antimicrobial peptide (AMP) or to a short Arg-Gly-Asp (RGD) peptide moiety. We chose Pluronic F-127, as it is easily applied to hydrophobic materials. Despite the fact that this tri-block copolymer attaches solely through hydrophobic interactions, it binds quite strongly and it has been demonstrated that the anti-adhesiveness of a Pluronic F-127 coating on hydrophobic silicone rubber remains preserved despite bacterial adhesion and subsequent detachment [14]. Since bacteria are much smaller than tissue cells, a small number of RGDs may already suffice to promote cell adhesion, while not yet affecting bacterial adhesion [29]. Therefore, in the current study, Pluronic F-127 conjugated to AMPs and RGDs in varying ratios was attached to hydrophobic silicone rubber and investigated in terms of anti-adhesive and bactericidal properties as well as its ability to promote host tissue cell adhesion and spreading.

MATERIALS AND METHODS

Two peptides, AMP and RGD with the sequences ILPWRWPWWPWRR-NH_2 and Ac-GCGYGRGDSPG-NH_2 respectively, were synthesized by CASLO ApS, Denmark, and were provided with purity > 95%. All chemicals, if not otherwise stated, were purchased from Sigma-Aldrich and used without further purification.

Synthesis and characterization of Pluronic_AMP conjugate

First, the chain ends of Pluronic were transformed into carboxylic acids. Dry Pluronic F-127 (10.2 g, 0.8 mmol), succinic anhydride (1.78 g, 16.2 mmol) and pyridine (Pyr, 2 ml) were dissolved in anhydrous dioxane (100 ml) and refluxed for 10 h. Then most of the solvent was evaporated and the Pluronic-COOH was precipitated from ice-cold diethyl ether. 7.0 g of product was obtained (yield 68%). ^{1}H-NMR (400MHz, $CDCl_3$): δ ppm 1.11 (m, PPO C**H$_3$**), 2.62 (m, 4H, OC(O)C**H$_2$**C**H$_2$**COOH), 3.42 (m, PPO C**H**), 3.52 (m, PPO C**H$_2$**), 3.63 (m, PEG C**H$_2$**), 4.25 (m, 2H, ω-PEG CH_2C**H$_2$**O).

In the next step an activated ester was formed. Pluronic-COOH (1.12 g, 0.09 mmol) was dissolved in anhydrous dichloromethane (20 ml) and cooled down in an ice bath. Trifluoroacetic acid *N*-hydroxysuccinimide ester (0.37 g, 1.76 mmol) was added portion-wise and the reaction mixture was allowed to slowly warm up to room temperature. The product was precipitated from ice-cold dry diethyl ether after stirring for 24 h. 0.8 g of the product was obtained (yield 66%). The activation of Pluronic-COOH to Pluronic-*N*-hydroxysuccinimide ester (Pluronic-NHS) was confirmed by ^{1}H-NMR analysis. ^{1}H-NMR (400MHz, $CDCl_3$): δ ppm 1.12 (m, PPO C**H$_3$**), 2.76 (t, 2H, NOC(O)CH_2C**H$_2$**), 2.82 (s, 4H, C**H$_2$**C**H$_2$ (**NHS)), 2.95 (t, 2H, NOC(O)C**H$_2$**CH_2), 3.38 (m, PPO C**H**), 3.53 (m, PPO C**H$_2$**), 3.63 (m, PEG C**H$_2$**), 4.25 (m, 2H, ω-PEG CH_2C**H$_2$**O); 2.68 ppm residual peak from starting material.

In the last step, the activated Pluronic was coupled to the AMP. Pluronic-NHS (402 mg, 31.2 µmol) and *N,N*-diisopropylethylamine (DIPEA, 30 µl) were dissolved in anhydrous dimethylformamide (DMF, 2 ml) and mixed with AMP (5 mg, 2.5 µmol) dissolved in anhydrous DMF (200 µl). The reaction mixture was allowed to stir for 48 h at room temperature and was then dialyzed against demineralized water using a 3 kDa MWCO membrane. Finally, the resulting solution was freeze-dried. The conjugate was purified on Shimadzu VP series HPLC

system with PDA detector using Jupiter 4u Proteo 90A column 250 x 4 mm (Phenomenex®, The Netherlands). Linear gradient 0 – 65% B in 26 min was used (buffer A 0.1% trifluoroacetic acid and 5% CH_3CN in ultra-pure water, buffer B 0.1% trifluoroacetic acid in CH_3CN). Purification was monitored at a wavelength of 215 nm. The collected fraction was characterized by gel electrophoresis using NuPage® Bis Tris gel 12% in NuPage® MES SDS buffer (140 V, 45 min, Invitrogen, The Netherlands). Spectra Multicolor Low Range Protein Ladder (Thermo Scientific, USA) was used as a marker. The material was freeze-dried and kept at -20^{o}C prior to use. Molecular weight was determined using a Voyager-DE Pro (Applied Biosystems, USA) MALDI-TOF mass spectrometer. Samples were prepared by plate spotting employing a sinapinic acid matrix. Non-functionalized Pluronic was used as a reference sample.

Synthesis and characterization of Pluronic_RGD conjugate

The synthesis of Pluronic_RGD conjugate was performed according to the procedure described by Rehor et al. [30]. First, the Pluronic chain ends were functionalized with a Michael-acceptor. Dry Pluronic F-127 (10 g, 0.79 mmol) was dissolved in anhydrous toluene (200 ml) and cooled down in an ice-bath. Sodium hydride was added in 5 molar excess, relative to the hydroxyl groups of Pluronic, and the reaction mixture was stirred for 15 min. Subsequently, divinylsulfone was added in 15 molar excess and the reaction mixture was stirred at room temperature in the dark under nitrogen for 5 days. The reaction was terminated by filtering the solution through celite cake, concentrating it with a rotary evaporator to a small volume and precipitating the mixture in ice-cold diethyl ether. The product Pluronic-VS was dried *in vacuo* and stored at -20^{o}C prior to use. 6.2 g of the product was obtained (62% yield). The structure was confirmed by ^{1}H-NMR spectroscopy and elemental analysis. ^{1}H-NMR (400MHz, D_2O): δ ppm 1.19

(m, PPO C**H**$_3$), 3.58 (m, PPO C**H**C**H**$_2$), 3.73 (m, PEG C**H**$_2$), 6.36 (d, 1H, C**H**$_2$=CH-SO_2), 6.47 (d, 1H, C**H**$_2$=CH-SO_2), 6.95 (dd, 1H, CH_2=C**H**-SO_2). Elemental analysis: calculated: 56.52% C, 9.47% H, 33.51% O, 0.49% S; found: 55.28% C, 9.25% H, 35.08% O, 0.41% S.

In the second step, the peptide moiety was reacted with Pluronic. RGD-peptide (50 mg, 0.05 mmol) was dissolved in sodium phosphate buffer (18 ml, 0.1 M) at pH 8.3. Pluronic-VS (150 mg, 0.012 mmol) was added and the resulting solution was allowed to stir for 24 h. The reaction mixture was dialyzed against demineralized water using a 3.5 kDa MWCO membrane, freeze-dried and kept at -20^{o}C prior to use. The structure was confirmed by ^{1}H-NMR analysis. ^{1}H-NMR (400MHz, D_2O): δ ppm 1.20 (m, PPO C**H**$_3$), 1.66, 1.78, 1.98, 2.32, 2.69, 2.99, 3.1, 3.24 (m, RGD), 3.58 (m, PPO C**H**C**H**$_2$), 3.73 (m, PEG C**H**$_2$), 3.92, 3.99 (m, PEG C**H**$_2$$CH_2$O, RGD), 4.38, 4.46, 4.67 (m, RGD) 6.86 (m, RGD), 7.15 (m, RGD).

Immobilization of the conjugates to silicone rubber

Implant grade silicone rubber sheets (thickness 0.5 mm, water contact angle 110 ± 1 degrees, Medin, The Netherlands) were used as substrata. Prior to use, the sheets were cut into small pieces and rinsed with ethanol as well as demineralised water. Next, the sheets were sonicated for 3 min in 2% RBS 35 detergent (Omnilabo International BV, The Netherlands), subsequently rinsed with demineralised water, washed in methanol and again rinsed with demineralised water. Before each experiment, the silicone rubber was exposed to the filtered solution containing different composition of the three components Pluronic_RGD:Pluronic_AMP:Pluronic; 0:0:0, 100:0:0, 80:20:0, 50:50:0, 0:100:0 for testing bacterial adhesion and growth and 0:0:0, 100:0:0, 50:50:0, 95:0:5, 45:50:5 and 40:50:10 for the evaluation of host tissue cell adhesion and spreading.

Anti-adhesive and bactericidal properties of the Pluronic conjugates attached to silicone rubber

Three bacterial species were used in this study: *Staphylococcus aureus* ATCC 12600, *Staphylococcus epidermidis* 138 and *Pseudomonas aeruginosa* #3. Bacteria were grown and harvested as previously described [13]. A single bacterial colony from a blood agar plate was inoculated in 10 ml tryptone soya broth (TSB, OXOID, England) and incubated at 37^{o}C for 24 h. This pre-culture was used to inoculate 200 ml of TSB and incubated for 16 h. Bacteria were harvested by centrifugation at 5000 × *g* for 5 min and washed twice with phosphate buffered saline (PBS buffer, 10 mM potassium phosphate, 150 mM NaCl, pH 6.8). To break up aggregates, bacteria were sonicated on ice for 3 × 10 s at 30 W (Vibra Cell model 375, Sonics and Materials, USA). This established procedure did not cause cell lysis. Minimal inhibitory concentrations (MIC) of the strains against the AMP were determined using a micro-dilution method. In brief, wells of a sterile 96 tissue culture plate (BD Falcon, USA) were filled with 100 µl of different concentrations of AMP in TSB to which 100 µl of a diluted bacterial pre-culture was added. The plates were incubated at 37^{o}C for 24 h. The lowest concentration of the AMP that completely inhibited visual bacterial growth was defined as MIC.

Bacterial adhesion, subsequent growth and biofilm formation were monitored for each strain on coated and uncoated silicone rubber using a parallel plate flow chamber [17]. Silicone rubber was affixed to the bottom plate of the chamber and the constant laminar flow through the chamber was maintained by hydrostatic pressure, using a roller pump. Bacteria were grown and harvested as described above, and finally suspended in 200 ml sterile PBS to a concentration of 3×10^8 per ml. After initial bacterial adhesion from this suspension for 30 min at room temperature under flow (shear rate 11 s^{-1}), the flow was switched to 10% TSB medium at 37^{o}C at reduced rate (shear rate 5 s^{-1}) for 20 h to grow a biofilm.

From the images taken throughout the entire course of an experiment the surface coverage was determined as a measure for the amount of biofilm formed. At the end of each flow experiment, 20 h old biofilms were stained with live/dead stain (LIVE/DEAD® BacLight™ Bacterial Viability Kit, Invitrogen, The Netherlands) mixed with CalcoFluor White a polysaccharide binding stain (Sigma-Aldrich, USA) applied to visualize extracellular polymeric substances (EPS). Stacks of images were obtained with a 40 × water objective lens using a Leica TCS SP2 Confocal Scanning Laser Microscope (Leica Microsystems GmbH, Germany). The images were analysed by Matlab with COMSTAT software giving the mean biovolume separated in the amount of live and dead bacteria. All experiments for quantitative biofilm analysis were done in triplicate, with separately grown bacterial cultures.

Host tissue cell adhesion and spreading

Fibroblast cell-line CCD-1112Sk (ATCC: CRL2429) was routinely cultured in RPMI-1640 with L-glutamine containing Penstrep (penicillin 100 U/ml, streptomycin 100 µg/ml) and 10% fetal bovine serum (FBS). For each experiment the cells were harvested and plated at a density of 10^4 cells/ml in 24 well tissue culture plates containing the functionalized silicone rubber samples. The cell suspensions were incubated at 37°C in a 5% CO_2 humidified environment for 48 and 120 h. After incubation, the samples were washed, fixed and stained as described previously [31]. Briefly, the media was removed and the samples were gently rinsed in PBS. Following this wash, the cells were fixed using 3.7% paraformaldehyde in cytoskeleton stabilization buffer for 5 min. The samples were washed once more before being incubated in 0.5% TritonX-100 for 3 min. The TritonX-100 was removed and staining was achieved by incubating in PBS containing 0.0098% 4',6-diamidino-phenylindole (DAPI) and 2µg/ml tetramethylrhodamine-5-(and 6)-

isothiocyanate-phalloidin for 30 min at 37°C. The excess stain was removed by gentle washing and the samples were kept at 4°C in PBS until imaging. The surface coverage, cell density, and individual cell spreading were determined on 5 predetermined areas of each sample and the entire experiment was performed in triplicate. Cell spreading was quantified in Photoshop by calculating the number of pixels occupied by the phalloidin stained cells to yield the coverage of the surface by tissue cells. To calculate the individual cell spreading, this was divided by the number of cells present.

Statistical analysis

The results were analyzed by two-tailed Student's **T-** test, and **P** values of < 0.05 were considered statistically significant.

RESULTS

Synthesis and characterization of Pluronic_AMP and Pluronic_RGD conjugates

The synthesis of Pluronic_AMP conjugate was carried out in three-steps (Scheme 1a). After transforming the hydroxyl end groups of Pluronic F-127 into carboxylic acids these telechelic moieties were activated as N-hydroxysuccinimide esters and reacted with the NH_2-terminus of the AMP. The final conjugate formation was confirmed by gel electrophoresis and the molecular weight was analysed by MALDI-TOF mass spectrometry (Figure 1). A mass peak at around 14.6 kDa proves identity of our target compound since the molecular weight of Pluronic is around 12.6 kDa and that of AMP is 2 kDa. The synthesis of the Pluronic_RGD conjugate was accomplished by first modifying the hydroxyl chain ends of Pluronic with vinylsulfone groups and then coupling the peptide via a free cysteine thiol in a Michael addition (Scheme 1b). The reaction proceeded quantitatively and the full conversion of vinylsulfone groups was confirmed by ^{1}H-NMR spectroscopy.

Immobilization of the obtained conjugates on a silicone rubber surface by dip coating resulted in formation of a polymer brush-coating with three combined functionalities, (i) anti-adhesive, due to the protruding polymer chains, (ii) bactericidal, due to the presence of AMPs, and (iii) tissue integrating, due to the exposition of RGD's (Scheme 1c).

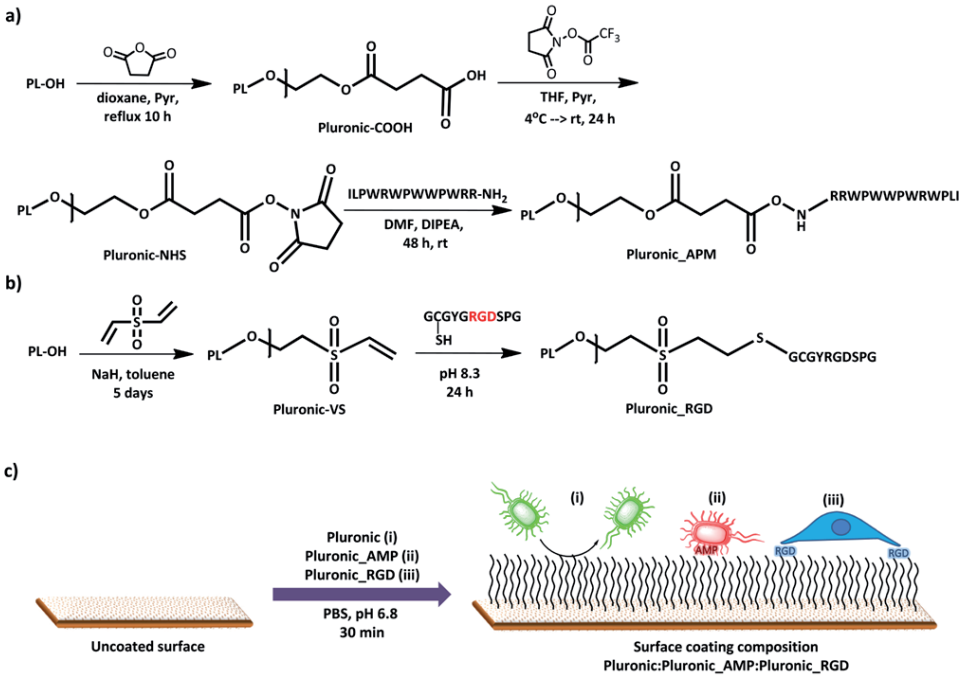

Scheme 1. Synthesis of polymer-peptide conjugates a) Pluronic_AMP b) Pluronic_RGD and c) immobilization of the conjugates on the surface of silicone rubber by dip-coating resulting in the triple activity of the coating, i.e. (i) anti-adhesiveness (ii) contact-killing and (iii) cell adhesion and spreading ("tissue integration").

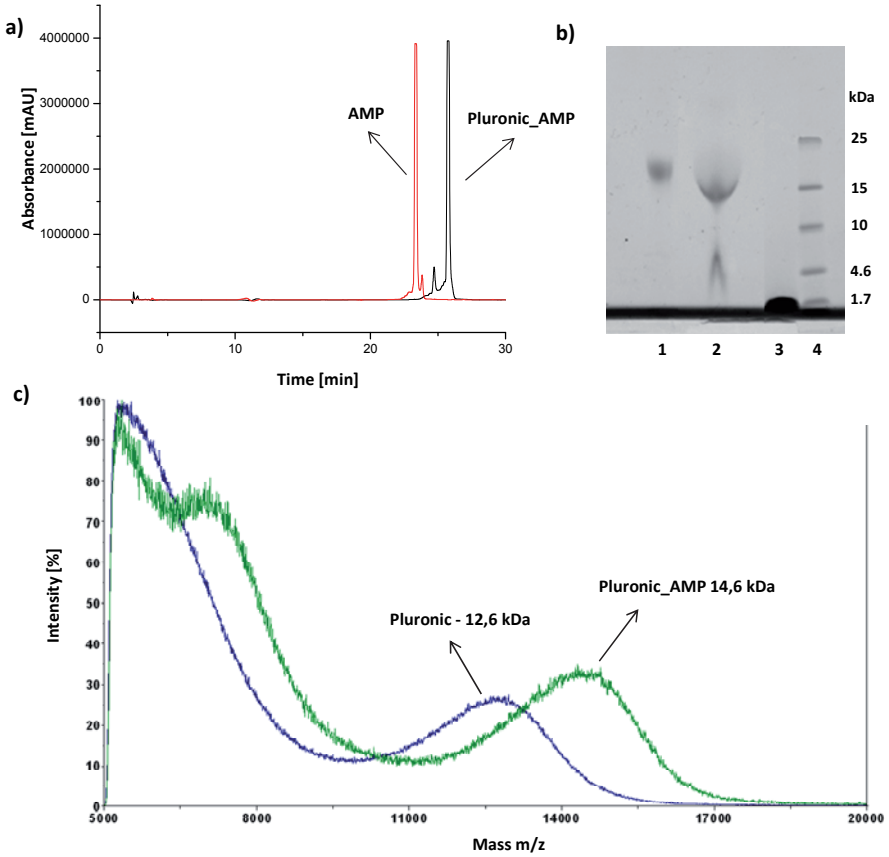

Figure 1. Characterization of Pluronic_AMP conjugate: a) HPLC analytical run of the conjugate purified by Reversed Phase Chromatography and pure AMP b) Characterization of the conjugate by SDS-PAGE: lane 1- Pluronic_AMP, lane 2- reaction mixture, lane 3- pure AMP, lane 4- marker c) MALDI-TOF mass spectrum confirming the expected molecular weight of the conjugate.

Anti-adhesive and antibacterial properties

The minimal inhibitory concentrations of the AMP in planktonic conditions amounted to 8 μg/ml for *S. aureus* ATCC 12600, 16 μg/ml for *S. epidermidis* 138 and > 125 μg/ml for *P. aeruginosa* #3.

The anti-adhesive and bactericidal properties of the coatings were investigated in an established flow displacement system [32]. The number of bacteria adhering to the coated and uncoated surfaces after 30 min are presented in Figure 2. Coating the silicone rubber surface (0:0:0) with Pluronic (100:0:0) resulted in nearly complete suppression of bacterial adhesion, but not to a zero level. After coating the surface with Pluronic_AMP conjugates, the numbers of adhering bacteria increased with increasing amount of AMPs, from 80:20:0 via 50:50:0 to 0:100:0, compared to the coating composed of pristine Pluronic (100:0:0). All bacterial strains responded similarly to the coatings in terms of their initial adhesion. However, after 20 h of growth to allow biofilm formation, the response to the coating was different for each bacterial strain, as illustrated in Figure 3.

In the case of *S. aureus* ATCC 12600 (Figure 3a), bacterial killing on contact was not enhanced by the peptide since the viabilities of the biofilm coated surfaces containing AMPs were not significantly different from the viability of the biofilm on the Pluronic coated surface. Nevertheless, the surface coverage by *S. aureus* on the coating with the composition 50:50:0 was reduced significantly when compared to all other surfaces, including the uncoated silicone rubber surface and the Pluronic coated one. For *S. epidermidis* 138 (Figure 3b), killing on contact with the coating was enhanced by the presence of AMPs when compared to coatings without AMPs, while here too the coating with composition 50:50:0 showed a significant reduction in surface coverage by live bacteria when compared to the uncoated (0:0:0) surface as well as to the surface coated with Pluronic (100:0:0) despite similar total surface coverages.

Contact-killing by the AMP-containing coating of adhering *P. aeruginosa* #3 was very strong (Figure 3c). Similarly as for both staphylococcal strains, the most effective coating against *Pseudomonas* was the one with composition 50:50:0.

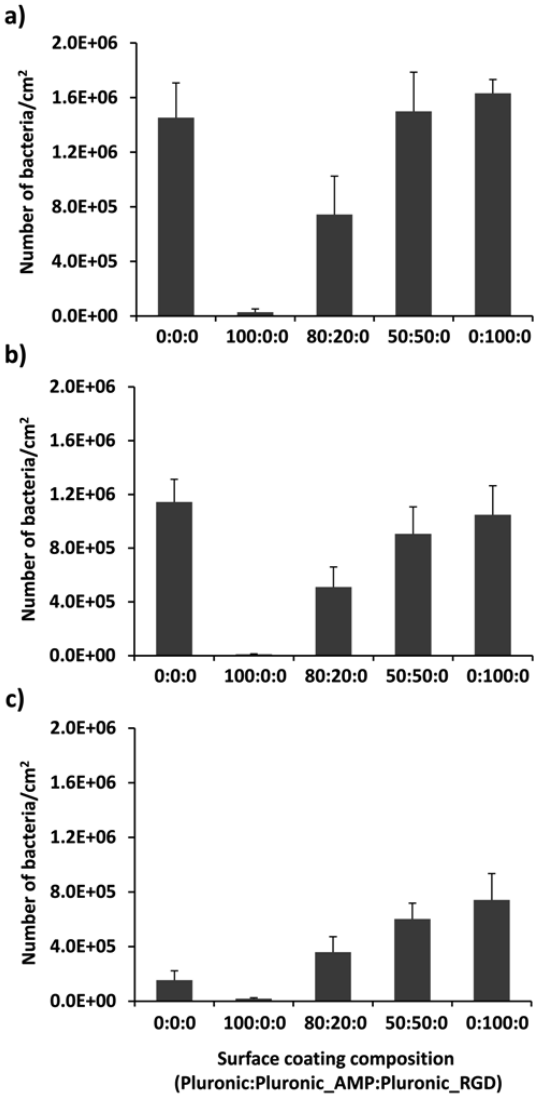

Figure 2. Numbers of bacteria per cm^2 adhering after 30 min on uncoated silicone rubber (0:0:0) and the surfaces coated with a ratio of elements Pluronic:Pluronic_AMP:Pluronic_RGD for a) *S. aureus* ATCC 12600, b) *S. epidermidis* 138, and c) *P. aeruginosa* #3. Error bars represent standard error over three separate experiments.

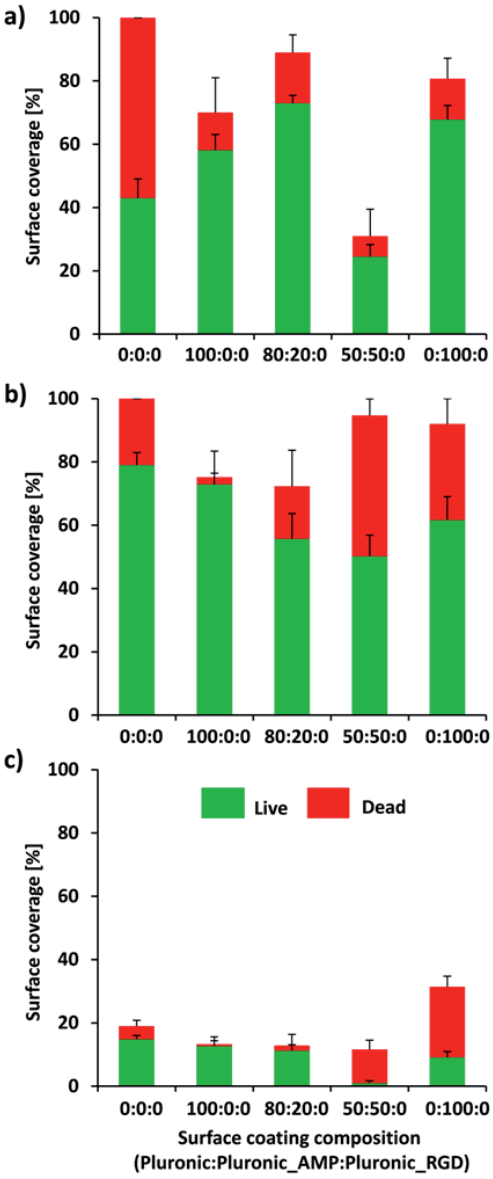

Figure 3. The percentage surface coverage by 20 h old biofilms of a) *S. aureus* ATCC 12600 b) *S. epidermidis* 138 and c) *P. aeruginosa* # 3 on a silicone rubber surface uncoated (0:0:0) and coated with a ratio of elements Pluronic:Pluronic_AMP:Pluronic_RGD, separated in the percentage of live and dead bacteria. Error bars represent standard error over three separate experiments.

Moreover, for each bacterial strain, extracellular polymeric substances (EPS) were absent on each of the coated surfaces opposite to the uncoated surface where, especially, staphylococcal biofilms produced EPS in large amounts, as shown in our previous study [13].

Tissue integration

The ability of the coatings to establish good tissue integration was investigated with human fibroblasts. Results presented in Figure 4 show evaluation of the surfaces in terms of surface coverage (Figure 4a), cell density (Figure 4b) and individual cell spreading (Figure 4c). As expected, surfaces coated with Pluronic (100:0:0) showing good anti-adhesive properties against bacteria, did not support fibroblast adhesion and spreading and consequently, surface coverage, as an overall indicator of tissue integration, was significantly lower after 120 h of growth compared to the uncoated surface (Figure 4a). Functionalizing the Pluronic brush-coating with only a small amount of RGDs (95:0:5) resulted in twice the surface coverage after 120 h compared to the uncoated surface and four times higher in relation to the Pluronic coated (100:0:0) or Pluronic_AMP coated (50:50:0) surfaces (Figure 4a). Pluronic brush-coatings functionalized with only AMP peptide (50:50:0) did not exhibit good tissue integration and surface coverage remained equally low as on a surface coated with Pluronic. On the tri-functional coating (45:50:5), fibroblasts were able to attach and spread over the surface resulting in a similar surface coverage as in the absence of AMP (95:0:5).

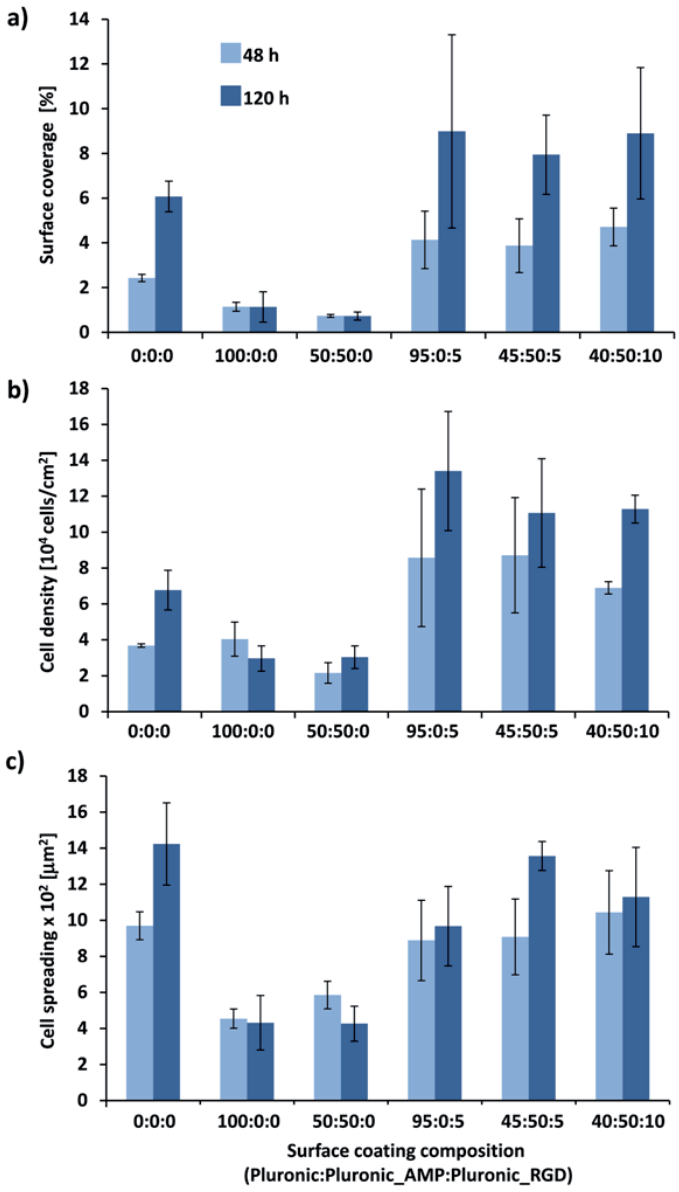

Figure 4. Tissue integration by human fibroblast cells of (un)coated silicone rubber surfaces according to a) surface coverage b) cell density and c) cell spreading. Error bars represent standard error over three separate experiments.

DISCUSSION

We have developed a tri-functional polymer brush-coating composed of anti-adhesive Pluronic molecules to repel adhering bacteria, Pluronic_AMP conjugates to kill bacteria on contact and Pluronic_RGD conjugates to enhance tissue integration. Antimicrobial cationic peptides AMPs, have been extensively described in the literature as potential therapeutic drugs against infection due to their broad activity spectrum and low chance of microbial resistance development [33]. However, despite the clear advantages of using these AMPs, there are still several limitations associated with clinical development of anti-infection-therapies using AMPs, such as enzymatic degradation in physiological fluids, possible toxicity of AMPs towards host tissue cells and high cost of production [34]. The antimicrobial peptide used in the present study consists of a relatively small number of amino acids with many hydrophobic residues and is active against both Gram-positive and Gram-negative bacteria. AMPs with a high content of hydrophobic amino acids and arginine show slightly different mechanisms of membrane permeabilization compared to others. Instead of forming pore complexes with hydrophilic membrane anions, they are transported across cellular membranes and act intracellularly [35]. Moreover, the amidation of the C-terminal end of the peptide used in this study might improve stability by protecting the molecule from proteolytic degradation. Normally, this peptide is poorly water soluble due to its hydrophobic character, a disadvantage common to many antimicrobial peptides that are considered for clinical application. However, after coupling the peptide with amphiphilic Pluronic, we obtained a water-soluble conjugate, which is crucial for its application as a biomaterial surface coating.

Anti-adhesive polymer brushes containing antimicrobial peptides have been previously described [18,36] and are mostly applied using surface activated polymerization methods followed by peptide coupling on the immobilized brush.

The approach presented herein consisting of non-covalent surface anchoring of prefabricated building blocks offers several advantages compared to methods involving grafting from polymerization techniques with subsequent peptide functionalization. The peptide-polymer conjugates are prepared in solution phase, which generally results in higher coupling yields compared to reactions on a solid substrate. Surface coatings with different compositions, e.g. ratio of AMP to RGD motif, can be generated by simply mixing the components and do not require a new polymerization or chemical coupling step. Moreover, characterization of the different conjugates of the coating is much simpler than assessing the chemical structure on a surface. Finally, the materials presented here can be easily stored and sterilized by filtration directly before immobilization on the surface. This set of properties allows the fabrication of surface coatings exhibiting different functionalities in a very controlled way in a minimal time effort.

The anti-adhesive properties as well as the ability of our tri-functional polymer brush-coating to kill bacteria on contact was proven against three bacterial strains known to cause BAI. Silicone rubber coated with Pluronic_AMP conjugates resulted in increased numbers of adhering bacteria compared to the surface coated with Pluronic, as expected due to the presence of positive charges [17]. The AMP used exhibits a net charge of +3, which results in electrostatic interactions with the under physiological conditions negatively charged cell walls present in nearly all bacterial strains. A coating composed of 50:50:0 ratio of the three components Pluronic_RGD:Pluronic_AMP:Pluronic was effective against all bacterial strains included in this study by either inhibiting their growth (*S. aureus*) or direct killing on contact (*S. epidermidis* and *P. aeruginosa*). In case of *S. aureus*, the coating was not able to kill all adhering bacteria upon contact, but did significantly delay their growth. The strain-dependence of contact-killing by our tri-functional coating might be due to different binding mechanisms and

interactions of the AMP with the bacterial cell walls [37]. AMPs interact selectively with hydrophilic anions in the cell membrane and due to structural variations the composition of hydrophilic ions in the membrane this interaction may differ between different strains as reported by Mai *et al* [38]. Surprisingly, the AMP was effective against *P. aeruginosa* only when conjugated to the polymer brush-coating, whereas the AMP in solution showed little antimicrobial activity against *P. aeruginosa* in the planktonic state. This phenomenon was observed previously by Tiller *et al.,* describing that conjugated, positively charged antimicrobials work differently than when free in solution [39], which may be highly beneficial for future applications of AMP_polymer conjugates as anti-infection coatings on biomaterial implants and devices.

Additional functionalization of the surface by RGD moieties with Pluronic or Pluronic_AMP yielded improved surface coverage by human fibroblasts. Silicone rubber surface with a tri-functional coating of Pluronic:Pluronic_AMP:Pluronic_RGD composed of an appropriate ratio of these components (45:50:5) demonstrated similar surface coverage as in the absence of AMP (95:0:5), most likely due to a more favorable spatial distribution of RGD on the material surfaces resulting from competition with AMP. This explanation is supported by a previous study, where the spatial arrangement and density of RGD moieties on a substratum surface affected cell spreading in a density-dependent manner [40]. The coating functionalized with only AMP (50:50:0) demonstrated optimal bacterial killing on contact, but poor tissue integration and may therefore still find applications as a bactericidal surface in applications where tissue integration is not needed, for instance in industrial or environmental settings or alternatively in specific medical applications as for example urinary catheters or voice prostheses, where tissue integration is not required.

CONCLUSIONS

The balance between infection risk and host healing is often described as a competition between contaminating pathogens and host cells to cover the material in what has been termed “the race for the surface” [41]. The novel tri-functional surface developed and presented in the current study represents a method by which biomaterial designers may be able to bias this competition in favor of the patient via simultaneous multiple approaches. Therewith it may provide an effective alternative to commonly used antibiotics for reducing the risk of BAI.

REFERENCES

1. Francolini I, Donelli G. Prevention and control of biofilm-based medical-device-related infections. FEMS Immunol Med Microbiol 2010;59:227-238.

2. Chitnis AS, Edwards JR, Ricks PM, Sievert DM, Fridkin SK, Gould CV. Device-associated infection rates, device utilization, and antimicrobial resistance in long-term acute care hospitals reporting to the National Healthcare Safety Network, 2010. Infect Control Hosp Epidemiol 2012;33:993-1000.

3. Arciola CR, Campoccia D, Speziale P, Montanaro L, Costerton JW. Biofilm formation in Staphylococcus implant infections. A review of molecular mechanisms and implications for biofilm-resistant materials. Biomaterials 2012;33:5967-5982.

4. Singhai M, Malik A, Shahid M, Malik MA, Goyal R. A study on device-related infections with special reference to biofilm production and antibiotic resistance. J Glob Infect Dis 2012;4:193-198.

5. Darouiche RO. Treatment of infections associated with surgical implants. N Engl J Med 2004;350:1422-1429.

6. Nikaido H. Multidrug resistance in bacteria. Annu Rev Biochem 2009;78:119-146.

7. Busscher HJ, Van der Mei HC, Subbiahdoss G, Jutte PC, Van den Dungen JJ, Zaat SA, Schultz MJ, Grainger DW. Biomaterial-associated infection: Locating the finish line in the race for the surface. Sci Transl Med 2012;4:153-164.

8. Muñoz-Bonilla A, Fernández-García M. Polymeric materials with antimicrobial activity. Prog Polym Sci 2012;37:281-339.

9. Follmann HD, Martins AF, Gerola AP, Burgo TA, Nakamura CV, Rubira AF, Muniz EC. Antiadhesive and antibacterial multilayer films via layer-by-layer assembly of TMC/heparin complexes. Biomacromolecules 2012;13:3711-3722.

10. Neoh KG, Kang ET. Combating bacterial colonization on metals via polymer coatings: relevance to marine and medical applications. ACS Appl Mater Interfaces 2011;3:2808-2819.

11. Bieser AM, Thomann Y, Tiller JC, Contact-active antimicrobial and potentially self-polishing coatings based on cellulose. Macromol Biosci 2011;11:111-121.

12. Kobayashi M, Terayama Y, Yamaguchi H, Terada M, Murakami D, Ishihara K, Takahara A. Wettability and antifouling behavior on the surfaces of superhydrophilic polymer brushes. Langmuir 2012;28:7212-7222.

13. Muszanska AK, Nejadnik MR, Chen Y, Van den Heuvel ER, Busscher HJ, Van der Mei HC, Norde W. Bacterial adhesion forces with substratum surfaces and the susceptibility of biofilms to antibiotics. Antimicrob Agents Chemother 2012;56:4961-4964.

14. Nejadnik MR, Van der Mei HC, Norde W, Busscher HJ. Bacterial adhesion and growth on a polymer brush-coating. Biomaterials 2008;29:4117-4121.

15. Ratner BD, Bryant SJ. Biomaterials: where we have been and where we are going. Annu Rev Biomed Eng 2004;6:41-75.

16. Holzapfel BM, Reichert JC, Schantz JT, Gbureck U, Rackwitz L, Noth U, Jakob F, Rudert M, Groll J, Hutmacher DW. How smart do biomaterials need to be? A translational science and clinical point of view. Adv Drug Deliv Rev 2013;65:581-603.

17. Muszanska AK, Busscher HJ, Herrmann A, Van der Mei HC, Norde W. Pluronic-lysozyme conjugates as anti-adhesive and antibacterial bifunctional polymers for surface coating. Biomaterials 2011;32:6333-6341.

18. Gao G, Lange D, Hilpert K, Kindrachuk J, Zou Y, Cheng JT, Kazemzadeh-Narbat M, Yu K, Wang R, Straus SK, Brooks DE, Chew BH, Hancock RE, Kizhakkedathu JN. The biocompatibility and biofilm resistance of implant coatings based on hydrophilic polymer brushes conjugated with antimicrobial peptides. Biomaterials 2011;32:3899-3909.

19. Shimoda A, Sawada S, Akiyoshi K. Cell specific peptide-conjugated polysaccharide nanogels for protein delivery. Macromol Biosci 2011;11:882-888.

20. Wohlrab S, Muller S, Schmidt A, Neubauer S, Kessler H, Leal-Egana A, Scheibel T. Cell adhesion and proliferation on RGD-modified recombinant spider silk proteins. Biomaterials 2012;33:6650-6659.

21. Hancock RE, Sahl HG. Antimicrobial and host-defense peptides as new anti-infective therapeutic strategies. Nat Biotechnol 2006;24:1551-1557.

22. Friedrich CL, Moyles D, Beveridge TJ, Hancock RE. Antibacterial action of structurally diverse cationic peptides on gram-positive bacteria. Antimicrob Agents Chemother 2000;44:2086-2092.

23. Rajanbabu V, Chen JY. Applications of antimicrobial peptides from fish and perspectives for the future. Peptides 2011;32:415-420.

24. Wimley WC. Antimicrobial Peptides: successes, challenges and unanswered questions. ACS Chem Biol 2010;5:905-917.

25. Pag U, Oedenkoven M, Sass V, Shai Y, Shamova O, Antcheva N, Tossi A, Sahl HG. Analysis of in vitro activities and modes of action of synthetic antimicrobial peptides derived from an α-helical sequence template. J Antimicrob Chemother 2008;61:341-352.

26. Yang F, Williams CG, Wang DA, Lee H, Manson PN, Elisseeff J. The effect of incorporating RGD adhesive peptide in polyethylene glycol diacrylate hydrogel on osteogenesis of bone marrow stromal cells. Biomaterials 2005;26:5991-5998.

27. Tugulu S, Silacci P, Stergiopulos N, Klok HA. RGD-Functionalized polymer brushes as substrates for the integrin specific adhesion of human umbilical vein endothelial cells. Biomaterials 2007;28:2536-2546.

28. Schwarz-Linek U, Höök M, Potts JR. Fibronectin-binding proteins of gram-positive cocci. Microbes Infect 2006;8:2291-2298.

29. Ponnuraj K, Bowden MG, Davis S, Gurusiddappa S, Moore D, Choe D, Xu Y, Höök M, Narayana SVL. A "dock, lock and latch" structural model for staphylococcal adhesion binding to fibrinogen. Cell 2003;115:217-228.

30. Rehor A, Schmoekel H, Tirelli N, Hubbell JA. Functionalization of polysulfide nanoparticles and their performance as circulating carriers. Biomaterials 2008;29:1958-1966.

31. Wang Y, Subbiahdoss G, Swartjes J, Van der Mei HC, Busscher HJ, Libera M. Length-scale mediated differential adhesion of mammalian cells and microbes. Adv Funct Mater 2011;21:3916-3923.

32. Busscher HJ, Van der Mei HC. Microbial adhesion in flow displacement systems. Clin Microbiol Rev 2006;19:127-141.

33. Christopher D. Fjell CD, Hiss JA, Hancock REW, Schneider G. Designing antimicrobial peptides: form follows function. Nat Rev Drug Discov 2012; 11:37-51.

34. Wimley WC. Antimicrobial Peptides: successes, challenges and unanswered questions. ACS Chem Biol 2010;5:905-917.

35. RokitskayaTI, Kolodkin NI, Kotova EA, Antonenko YN. Indolicidin action on membrane permeability: Carrier mechanism versus pore formation. Biochim Biophys Acta 2011;1:91-97.

36. Glinel K, Jonas AM, Jouenne T, Leprince J, Galas L, Huck WTS. Antibacterial and antifouling polymer brushes incorporating antimicrobial peptide. Bioconjugate Chem 2009;20:71-77.

37. Hilpert K, Elliot M, Jenssen J. Kindrachuk HJ. Fjell CD. Koerner J, et al. Screening and characterization of surface-tethered cationic peptides for antimicrobial activity. Chem Biol 2009;16:58-69.

38. Mai J, Tian X, Gallant JW, Merkley N, Biswas Z, Syvitski ZR, et al. A novel target-specific, salt-resistant antimicrobial peptide against the cariogenic pathogen *Streptococcus mutans.* Antimicrob Agents Chemother 2011;55:5205-5213.

39. Tiller JC, Liao CJ, Lewis K, Klibanov AM, Designing surfaces that kill bacteria on contact. Proc Natl Acad Sci USA 2001;98:5981-5985.

40. Maheshwari G, Brown G, Lauffenburger DA, Wells A, Griffith LG. Cell adhesion and motility depend on nanoscale RGD clustering. J Cell Sci. 2000;113:1677-1686.

41. Gristina AG. Biomaterial-centered infection: microbial adhesion versus tissue integration. Science 1987;237:1588-1595.

Chapter 6

General discussion

Bacterial infection remains the number one cause of implant failure despite various preventive strategies and antibiotic therapies. This problem seems to increase due to a rapid development of bacterial resistance to commonly used antibiotics [1]. Various biomaterials surface modifications have been introduced in order to prevent bacterial adhesion and their subsequent growth into a biofilm leading to implant infection. Anti-adhesive coatings, especially polymer brushes are one of the most promising solutions to prevent bacterial adhesion to the implant surface [2]. Polymer brushes form a compact structure that acts as a steric barrier between the surface of a biomaterial and approaching bacteria. However they are not able to reduce completely the adhesion of bacteria [3]. Therefore, inclusion of an antimicrobial agent is necessary to prevent mature biofilm formation. Moreover, eukaryotic cell adhesive motives need to be introduced in order to support tissue integration necessary for proper wound healing. However, there are very few known approaches that would combine anti-adhesiveness of a polymer brush with antimicrobial activity like killing on contact and enhanced adhesion of eukaryotic cells. In this thesis we described the development of such a functional polymer brush-coating that inhibits microbial adhesion, kills the few attached bacteria on contact and stimulates mammalian cell spreading and growth.

Polymer brush-coating immobilization

In our study we used physisorption from aqueous solution to immobilize polymer brushes at the surface. The main advantage of such an approach is that it is simple, does not require complicated specialized equipment and is not time consuming. The polymer brush-coating used for our study is composed of the triblock copolymer Pluronic F127 consisting of a central block of polypropylene oxide PPO_{65} (containing 65 monomer units) and two terminal polyethylene oxide blocks

PEO_{99} (each containing 99 monomer units). In aqueous environment PEO is highly hydrated and therefore very well soluble in water. PPO on the contrary is poorly water soluble. Hence, Pluronic F127 has an amphiphilic character and because of the relatively large PEO blocks it is water soluble. Due to its amphiphilicity it has a strong tendency to adsorb at surfaces. At a hydrophobic surface (having a water contact angle above 80 degrees) it anchors with its PPO block at the surface leaving the PEO parts dangling into the solution at such a high density that the PEO chains adopt a so-called brush conformation [4]. Despite the absence of a covalent bond between the substratum surface and the central PPO block, the polymer brush-coating used in this study has been proven to be stable against mechanical stress and for at least 20 h in contact with bacterial suspension [3]. Another advantage of Pluronic F127 polymer is the fact that it is non-toxic, does not cause irritation to skin or eyes, evokes minimal inflammatory response and is easy to sterilize by filtration from solution [5]. The simple immobilization by dip coating from the solution as well as the easy sterilization and storing methods make Pluronic F127 a great candidate for applications on biomedical materials.

Mono-functional polymer brush-coating

Using an established parallel plate flow system we demonstrated that the presence of the polymer brush strongly suppresses bacterial adhesion and atomic force microscopy (AFM) revealed that bacteria adhere much weaker to the polymer brush than to the uncoated surface irrespective of their morphology or cell wall composition. However, even the few attached bacteria are still able to grow into a biofilm (Chapter 2). Despite the great anti-adhesiveness of a brush-coating it requires additional antimicrobial activity to combat bacterial colonization. We observed that a biofilm on a brush-coated surface forms more open structures and is easy to penetrate by antibiotics since it is not protected by

a layer of extracellular polymeric substances (EPS), whereas a biofilm on an uncoated surface forms a thick contiguous layer resistant for antibiotic treatment due to the impenetrability of the EPS. Furthermore, low adhesion forces of bacteria towards a polymer brush-coating suggest that bacteria do not sense the surface and behave more planktonically thus remaining in an antibiotic susceptible state. Although this finding may open new successful pathways to fight biomaterial associated infections, the risk of antibiotic resistance is a major problem in hospitals nowadays and clinicians are seeking for new technologies of antibacterial therapies [6].

Bi-functional polymer brush-coating

One of the solutions for the rising problem of bacterial multidrug resistance as related with the use of biomaterials, may be the development of a bi-functional polymer brush-coating incorporating an antimicrobial agent. For that purpose we used the natural antimicrobial protein lysozyme, which was chemically linked to the terminal end of the PEO chains (Chapter 3). Using the Quartz Crystal Microbalance with Dissipation technique (QCM-D) we proved the desired brush-like conformation of the modified polymer chains with lysozyme extended into the solution. Such a coating is bi-functional as it combines two types of activities in one design, i.e., anti-adhesiveness due to the polymer chains and killing on contact due to the lysozyme. This approach allows direct bactericidal interactions and reduces the need of extensive usage of antibiotics associated with the development of bacterial resistance mechanisms. Varying the amount of lysozyme on the surface, we determined the coating composition that is antimicrobial but still preserves its anti-adhesive functionality. Interestingly the coating having a lower degree of lysozyme coverage proved to be more bactericidal. We speculate that the coating with a higher degree of lysozyme, which is positively charged,

attracts a high number of the negatively charged bacteria so that antimicrobial moieties become blocked and a layer of bacteria can be formed on top of which new bacteria can grow.

In order to determine the optimal lysozyme coverage on the surface, we additionally developed a computer modeling program that can simulate bacterial response towards the surface of a biomaterial when given right input information (Chapter 4). Using computer simulations we were able to extrapolate our data without doing additional time consuming experiments. Such a program able to predict antibacterial and anti-adhesive properties of a biomaterial and validate experimental data is highly desired in the field of surface engineering. However, one of the main limitations of the model is the fact that it does not take into account the fate of the dead bacteria, for instance the extent to which they are lysed or degraded and whether they detach from the surface, phenomena that may well occur in real lab-experiments. Thus, our model needs further improvements so that it can more precisely reflect complex processes of bacteria-surface interactions.

Based on the successful performance of a bi-functional Pluronic F127 coating modified with the natural protein lysozyme, we took a similar approach to introduce another antimicrobial compound, i.e., a synthetic antimicrobial peptide (AMP), into the brush (Chapter 5). AMPs are considered a class of new age antibiotics because of their limited ability to create resistance mechanisms and low toxicity levels towards mammalian cells [7]. Furthermore, AMPs are small synthetic molecules what makes them more stable and effective for a longer time compared to lysozyme, a natural enzyme which can be proteolytically degraded. AMPs, similarly to lysozyme, are able to kill bacteria on contact by disrupting their cell wall causing multiple stresses on the cytoplasmic membrane [8]. The coating of which 50% of the PEO polymer terminal ends were conjugated with AMPs

proved to have both anti-adhesive and antimicrobial activity and was the most effective against all bacterial strains evaluated in our study, i.e., *Sthaphylococcus aureus*, *Staphylococcus epidermidis* and *Pseudomonas aeruginosa*. Surprisingly in case of *Pseudomonas*, the coating displayed very high bactericidal activity despite bacterial resistance against AMPs in the solution proving its different mechanism of action when immobilized at a surface.

Tri-functional polymer brush-coating

Taking the modifications of polymer brush-coatings one step closer to clinical applications, we introduced another functionality by conjugating PEO polymer chains to RGD moiety containing peptides. These short peptides are responsible for eukaryotic cell adhesion and spreading which is crucial for proper wound healing (Chapter 5). As contact killing moieties for the tri-functional approach, we used antimicrobial peptides (AMPs) because their bactericidal activity is broader than lysozyme especially towards pathogenic organisms like *Staphylococci* or *Pseudomonas*. Both mono- and bi-functional coatings composed of Pluronic and Pluronic conjugated to AMPs, respectively, were not able to maintain good tissue integration. Here we demonstrated that functionalizing such a coating with very small amount of RDG peptide (5%) is already enough to promote adhesion and spreading of the human tissue cells without losing its antimicrobial activity. Such a tri-functional coating proved to combine anti-adhesive, antimicrobial and tissue integrating functionalities in one system and could be a well-suited future alternative to prevent infection associated with totally internal biomaterial implants and devices.

Conclusions and future research

Surface modifications of existing medical devices are essential to modern medicine since they save lives or improve the quality of life of millions of people around the world. Our results suggest that modifications of polymer brushes to include various functionalities could be a successful approach to develop new surface coatings in order to prevent biomaterial associated infections. Our design of a tri-functional coating combining PEO polymer chains with AMP and RGD peptides proved that such a coating can exert good antimicrobial properties without hampering tissue integration. The choice of a fibroblast as a cell type for evaluation and silicone rubber as a biomaterial points to the application of our coating for soft tissue implantation. However, it would be interesting to investigate how this design can be translated to other types of application, for example orthopedic or dental implants. Moreover, additional *in vitro* evaluations are needed, like pre-treating the surface with physiologically relevant proteins, before taking the new systems to *in vivo* evaluation. Furthermore, the stability and effectiveness of the coating in complex physiological fluids rich in several kinds of surface active substances still has to be determined. The stability and shelf life of the antimicrobial agents used in our design has also not been investigated and, hence, it would be interesting to determine whether the antimicrobial molecules are being degraded over time or otherwise deactivated. Also the fate of killed bacteria on contact by lysozyme or AMPs is not fully understood. Both antimicrobial molecules are able to damage bacterial cell walls, but we can only speculate whether in the human body dead bacteria will be completely lysed or removed by immune cells exposing the antimicrobial spot again or whether the antimicrobial site will remain blocked by a layer of a dead bacteria on top of which other bacteria will be able to stay alive since they have no direct contact with the killing site anymore. However, whether or not the

number of bacteria arriving at the implant surface after implantation will be high enough to form bi-layers of bacteria, greatly depends on the application aimed for.

In order to address the discussion points and uncertainties presented here, *in vitro* methodology should be progressed towards conditions more closely mimicking those in the human body, taking into account the host immune system as well. Additionally, time consuming and complicated *in vitro* experiments combining inclusion of tissue cells and bacteria in one system as well as bacterial multispecies biofilm formation experiments are needed in order to validate our monoculture studies. Further animal experiments are required to validate *in vitro* results and to correlate them to clinical performance.

Creating surfaces with multiple functionalities (see Figure 1) able to prevent bacterial colonization and integrate with the host tissue is still a big challenge. Our approach of a multifunctional surface coating combined with other novel technologies, such as tissue engineering and controlled drug delivery may finally bring effective solutions in creating biomedical materials that resist bacterial infections.

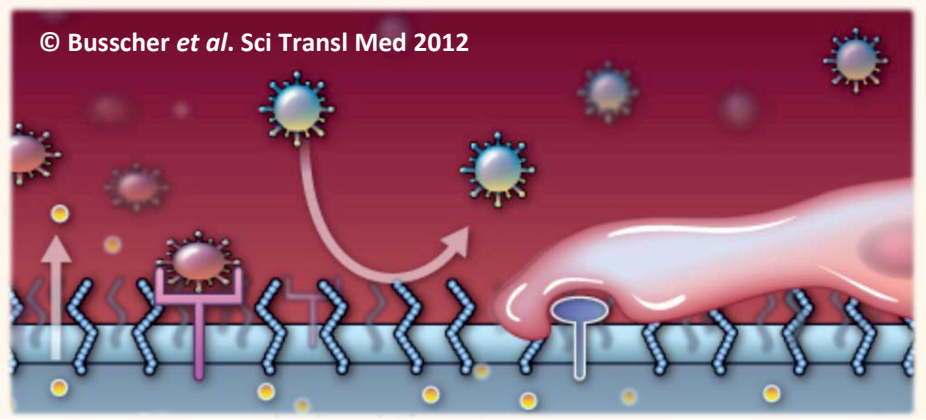

Figure 1. A schematic representation of a multi-functional coating for biomaterials [9].

REFERENCES

1. Nikaido H. Multidrug resistance in bacteria. Annu Rev Biochem 2009;78:119-146.

2. Kingshott P, Wei J, Bagge-Ravn D, Gadegaard N, Gram L. Covalent attachment of poly(ethylene glycol) to surfaces, critical for reducing bacterial adhesion. Langmuir 2003;19:6912-6921.

3. Nejadnik MR, Van der Mei HC, Norde W, Busscher HJ. Bacterial adhesion and growth on a polymer brush-coating. Biomaterials 2008;29:4117-4121.

4. Nejadnik MR, Olsson ALJ, Sharma PK, Van der Mei HC, Norde W, Busscher HJ. Adsorption of Pluronic F-127 on surfaces with different hydrophobicities probed by quartz crystal microbalance with dissipation. Langmuir 2009;25:6245-6249.

5. Khattak SF, Bhatia SR, Roberts SC. Pluronic F127 as a cell encapsulation material: utilization of membrane-stabilizing agents. Tissue Eng 2005;11:974-983.

6. Defoirdt T, Boon N, Sorgeloos P, Verstraete W, Bossier P. Alternatives to antibiotics to control bacterial infections: luminescent vibriosis in aquaculture as an example. Trends Biotechnol 2007;25:472–479.

7. Hancock RE, Sahl HG. Antimicrobial and host-defence peptides as new anti-infective therapeutic strategies. Nat Biotechnol 2006;24:1551-1557.

8. Wimley WC. Describing the mechanism of antimicrobial peptide action with the interfacial activity model. ACS Chem Biol 2010;5:905–917.

9. Busscher HJ, Van der Mei HC, Subbiahdoss G, Jutte PC, Van den Dungen JJ, Zaat SA, Schultz MJ, Grainger DW. Biomaterial-associated infection: Locating the finish line in the race for the surface. Sci Transl Med 2012;4:153-164.

Summary

We live in the era of rapid developments in the field of biomaterial application and regenerative medicine to save lives and improve the quality of life of millions of people around the world. However, one of the main drawbacks associated with increasing use of implanted biomaterials is the occurrence of microbial infections, which is considered to be the number one cause of biomaterial implant failure. Currently the most common treatments used in the clinic to combat biomaterial-associated infections are often long-lasting at great discomfort of the patient. They require large doses of antibiotics with an uncertain outcome. The growing risk of multidrug resistance development by pathogenic bacteria may make the antibiotic therapy unsuccessful so that the infected implant has to be removed, while bringing greater risk of infection during revision surgery.

Chapter 1 gives an overview of several preventive methods that have been proposed to reduce bacterial adhesion to biomaterial surfaces, considered to be the onset of biofilm development causing implant infection. Non-adhesive coatings such as polymer brushes are currently one of the most promising surface modifications of existing biomaterials to prevent implant infection. Despite the impressive anti-adhesive activity of polymer brush-coatings, reducing bacterial adhesion up to 95%, as shown by many studies, they are not able to fully suppress biofilm formation. Therefore, the aim of this thesis is to develop a polymer brush-coating that combines three activities: 1) anti-adhesive to repel approaching microorganisms, 2) antimicrobial to kill the few adhering ones and 3) tissue integrating to promote mammalian cell adhesion and spreading as a protective means to prevent microbial adhesion. To produce a non-adhesive polymer brush-coating, we used the triblock copolymer Pluronic F127 composed of a central polypropylene oxide block PPO_{65} which is hydrophobic and two terminal polyethylene oxide blocks PEO_{99} that are hydrophilic. The amphiphilic character of

Pluronic allows it to spontaneously adsorb to hydrophobic surfaces, like silicone rubber having a water contact angle of 112°, chosen for our study. Polymer brushes were immobilized at the surface by a simple dip coating method.

The anti-adhesive properties of the coating were investigated in **chapter 2** by measuring the adhesion forces between bacteria and the surface using atomic force microscopy. We demonstrated that nine strains of *Staphylococcus aureus*, *Staphylococcus epidermidis* and *Pseudomonas aeruginosa* adhered more weakly to polymer brush-coated than to uncoated silicone rubber. However, as shown before, a few adhering bacteria appeared to be able to grow into a biofilm, but on a polymer brush-coated surface this biofilm was less compact and had a more open structure compared to the one formed on uncoated surfaces. Using an established parallel plate flow system we investigated the growth of bacteria in the absence and presence of the antibiotic gentamicin, introduced to kill the few bacteria adhering to the polymer brush-coating. We showed that the surface coverage by biofilms grown in the presence of gentamicin on polymer brush-coated silicone rubber was significantly lower than on uncoated silicone rubber. At the same time, the percentage of live organisms and amount of extracellular matrix produced was much less on the brush-coated surface. Therefore, weakly adhering bacteria on polymer brush-coatings remained in a planktonic state susceptible to gentamicin, opposite to biofilms formed on uncoated silicone rubber, showing antibiotic resistance.

We proved in the previous chapter, that biofilm formation on polymer brush coatings can be effectively reduced by gentamicin treatment. However, due to the growing development of bacterial resistance towards antibiotics, there is a trend in the clinic to avoid extensive antibiotic therapies and seek for alternatives.

Taking this issue into account, we designed in **chapter 3**, a bi-functional polymer brush by conjugating the antibacterial enzyme lysozyme to the telechelic groups of the Pluronic PEO chains. Conjugate formation was confirmed by SDS-PAGE gel electrophoresis together with MALDI-TOF mass spectrometry. We investigated the conformation of the adsorbed layer of the Pluronic-lysozyme conjugates at the surface using a quartz crystal microbalance with dissipation and demonstrated that the polymers adsorb in a brush-like conformation with lysozymes extending into the surrounding medium and allowing them to have direct contact with bacteria that managed to adhere to the coating. The anti-adhesive and antimicrobial properties of the coating were investigated using a parallel plate flow system against *Bacillus subtilis.* Data indicated that such a coating exerts bi-functionality, i.e. anti-adhesive activity due to the polymer brush, combined with the antibacterial activity of lysozyme.

To create a bi-functional coating with the optimal amount of lysozyme at the surface, a wide range of coating compositions have to be evaluated, which is time consuming and tedious. In **chapter 4** we describe the development of a computer modelling program able to predict surface response towards bacteria. As input information, we used the data obtained for our bi-functional coating against *B. subtilis*. By doing computer simulations, we were able to predict which coating composition shows minimal coverage of the surface by bacteria with the highest number of dead bacteria, thus escaping the need of performing additional, lengthy experiments to determine optimal coating formulations.

The development of a bi-functional polymer brush coating can provide alternatives for antibiotic therapies and contributes to future applications of multifunctional coatings. One of the crucial properties that needs to be

implemented in such a design, depending on the application aimed for, is the ability of a coating to support tissue integration. In **chapter 5** we show the development of a tri-functional coating composed of Pluronic, Pluronic conjugated to antimicrobial peptides (AMPs) and Pluronic conjugated to RGD peptides. The properties of the coating were investigated in a parallel plate flow chamber against three common, infection causing bacterial strains: *S. aureus*, *S. epidermidis* and *P. aeruginosa*. A coating where 50% of the polymer ends were conjugated to AMP, showed antimicrobial activity against each bacterial strain tested. The ability of the coating to maintain good tissue integration was investigated with human fibroblast cells. We demonstrated that functionalizing the coating with only 5% RGD peptides resulted in its ability to promote cell adhesion and spreading opposite to the mono-functional coating composed of Pluronic only and the bi-functional coating composed of Pluronic with AMPs. The coating presented in our study combines three activities in one design, i.e., anti-adhesive to repel the approaching bacteria, antimicrobial to kill bacteria on contact and tissue integrating to promote adhesion and spreading of eukaryotic cells.

In the general discussion presented in **chapter 6,** we emphasize the advantages of our designs for the development of future applications and discuss the limitations of our methodology. Finally, the main conclusions of the project are presented together with suggestions for future research.

Samenvatting

We leven in een tijdperk van snelle ontwikkelingen op het gebied van biomaterialen en regeneratieve geneeskunde om levens te redden en de kwaliteit van leven van miljoenen mensen op de wereld te verbeteren. Echter, één van de grootste nadelen van het toenemende gebruik van geïmplanteerde biomaterialen is het optreden van microbiële infecties, de nummer één oorzaak van het falen van een biomedisch implantaat. De huidige klinische methoden om deze biomateriaal geassocieerde infecties te behandelen zijn vaak langdurig van aard en veroorzaken veel ongemak bij de patiënt. Ook vereist de behandeling hoge doseringen antibiotica met daarbij een onzekere uitkomst. Het toenemende risico van pathogene bacteriën die resistentie ontwikkelen tegen meerdere antibiotica maakt dat het toedienen van antibiotica niet altijd succesvol is, met als gevolg dat het geïnfecteerde implantaat verwijderd moet worden, waarna een groter risico op infectie optreedt tijdens de revisie-operatie.

Hoofdstuk 1 geeft een overzicht van een aantal preventieve methoden die zijn voorgesteld om de hechting van bacteriën, die wordt gezien als het begin van biofilmvorming die implantaatinfecties veroorzaakt, aan het oppervlak van biomaterialen te reduceren. Niet-hechtende coatings zoals polymere borstel-coatings zijn tegenwoordig één van de meest veelbelovende oppervlaktemodificaties van bestaande biomaterialen om implantaatinfecties te voorkomen. Ondanks de indrukwekkende anti-hechting activiteit van polymere borstel-coatings, die in veel studies tot wel 95% verlaging van hechtende bacteriën laat zien, zijn ze niet in staat om biofilmvorming volledig tegen te houden. Daarom is het doel van dit proefschrift om een polymere borstel-coating te ontwikkelen die drie verschillende functionaliteiten bezit: 1) anti-hechting om naderende micro-organismen af te stoten, 2) antimicrobieel om de enkele bacteriën die wel weten te hechten te doden, 3) weefselintegratie om de adhesie

en spreiding van weefselcellen te promoten waarna ze bescherming bieden tegen microbiële hechting. Om een polymere borstel-coating te produceren die hechting tegengaat hebben we de tri-blok copolymeer Pluronic F127 gebruikt, bestaande uit een centraal polypropyleen oxide blok PPO_{65} met hydrofobe eigenschappen en twee terminale polyethyleen oxide blokken PEO_{99} die hydrofiel zijn. Het amfifiele karakter maakt het voor Pluronic mogelijk om spontaan op hydrofobe oppervlakken te adsorberen, zoals het siliconenrubber gekozen voor onze studie dat een water randhoek heeft van 112°. Polymere borstels werden op het oppervlak geïmmobiliseerd door een simpele dip-coat methode.

De anti-hechting eigenschappen van de coating werden onderzocht in **hoofdstuk 2** door het meten van de hechtingskrachten tussen bacteriën en het oppervlak met behulp van atomaire kracht-microscopie. We toonden aan dat negen stammen van *Staphylococcus aureus*, *Staphylococcus epidermidis* en *Pseudomonas aeruginosa* minder sterk hechtten aan siliconenrubber met een polymere borstel-coating, dan niet gecoat siliconenrubber. Echter, zoals eerder aangetoond, het kleine aantal hechtende bacteriën was desondanks in staat uit te groeien tot een biofilm, hoewel op een polymere borstel-coating deze biofilm minder compact was en een meer open structuur had, vergeleken met de biofilm die zich vormde op niet gecoate oppervlakken. Met behulp van de parallelle plaat stroom kamer hebben we de groei van bacteriën in de aan- en afwezigheid van het antibioticum gentamicine onderzocht, om hiermee de bacteriën die in staat waren te hechten op de polymere borstel-coating te doden. We lieten zien dat het totale oppervlak dat bedekt werd door biofilms in de aanwezigheid van gentamicine significant lager was op siliconenrubber met een polymere borstel-coating dan op niet gecoat siliconenrubber. Op hetzelfde moment was ook het aantal levende organismen en de hoeveelheid extracellulaire matrix die

geproduceerd was veel lager op oppervlakken met polymere borstel-coatings. Zwak hechtende bacteriën op een polymere borstel-coating bleven in de planktonische staat en gevoelig voor gentamicine, in tegenstelling tot biofilms die vormden op niet gecoat siliconenrubber, welke antibiotica resistentie lieten zien.

In het vorige hoofdstuk lieten we zien dat biofilmvorming op polymere borstel-coatings effectief verminderd kan worden door behandeling met gentamicine. Echter, vanwege de toenemende resistentie van bacteriën tegen antibiotica, is het een trend in de kliniek om uitgebreide antibioticatherapieën te vermijden en te zoeken naar alternatieven. Hier rekening mee houdend hebben we in **hoofdstuk 3** een bi-functionele polymere borstel-coating ontworpen door conjugatie van het antibacteriële enzym, lysozym, aan de PEO groepen van Pluronic. Succesvolle conjugatie werd bevestigd door SDS-PAGE gel-elektroforese en MALDI-TOF massaspectrometrie. We onderzochten de conformatie van de geadsorbeerde laag van het Pluronic-lysozym conjugaat met behulp van een quartz crystal microbalance met dissipatie en toonden aan dat het polymeer adsorbeert in een borstelconformatie waarbij lysozym uitsteekt in het omliggende medium, waardoor het in direct contact kan komen met bacteriën die in staat zijn te hechten op de coating. De anti-hechting en antimicrobiële eigenschappen van de coating ten opzichte van *Bacillus subtilis* werden onderzocht met de parallel plaat stroom kamer. De data toonde dat een dergelijke coating bi-functionele eigenschappen vertoond, t.w. antihechting dankzij de polymere borstel, gecombineerd met de antibacteriële activiteit van lysozym.

Om een bi-functionele coating te creëren met het optimale aantal lysozym moleculen op het oppervlak zou een groot aantal coatings met verschillende percentages lysozym aan het oppervlak getest moeten worden, iets dat eentonig

en tijdrovend is. In **hoofdstuk 4** beschrijven we de ontwikkeling van een computermodel dat het mogelijk maakt de oppervlakterespons ten opzichte van bacteriën te voorspellen. Als input-informatie hebben we de data van onze bi-functionele coating tegen *B. subtilis* gebruikt. Door middel van computersimulaties konden we voorspellen welk percentage lysozym het minst aantal bacteriën hecht en het hoogste aantal dode bacteriën laat zien, waardoor het doen van extra, langdurige experimenten om de optimale coatingsamenstelling te vinden, niet nodig waren.

De ontwikkeling van een bi-functionele polymere borstel-coating kan alternatieven bieden voor antibioticatherapie en bijdragen aan toekomstige toepassingen voor multifunctionele coatings. Eén van de cruciale eigenschappen die in een dergelijk ontwerp, afhankelijk van de toepassing, moet worden meegenomen is de mogelijkheid van een coating om weefselintegratie te ondersteunen. In **hoofdstuk 5** tonen we de ontwikkeling van een tri-functionele coating bestaande uit Pluronic, Pluronic geconjugeerd met antimicrobiële peptiden (AMPs) en Pluronic geconjugeerd met RGD peptiden. De eigenschappen van de coating werden onderzocht in een parallelle plaat stroom kamer tegen drie veelvoorkomende, infectie veroorzakende bacteriën: *S. aureus*, *S. epidermidis* en *P. aeruginosa.* Een coating waarbij 50% van het polymeer met AMPs was geconjugeerd, liet antimicrobiële activiteit zien tegen elke geteste stam. Het vermogen van de coating om weefselintegratie te bevorderen werd onderzocht met humane fibroblastcellen. We toonden aan dat 5% RGD peptide functionaliteit resulteerde in de mogelijkheid om celhechting en spreiding te bevorderen, ten opzichte van de monofunctionele coating bestaande uit alleen Pluronic en de bio-functionele coating bestaande uit Pluronic met AMPs. De coating gepresenteerd in ons onderzoek combineert drie verschillende functionaliteiten in één ontwerp,

i.e., anti-hechting om naderende bacteriën af te stoten, antimicrobieel om bacteriën bij contact te doden en weefselintegratie om de hechting en spreiding van eukaryote cellen te promoten.

In de algemene discussie in **hoofdstuk 6** benadrukken we de voordelen van onze ontwerpen voor de ontwikkeling van toekomstige toepassingen en bespreken we de beperkingen van onze methodologie. Ten slotte worden de belangrijkste conclusies van het project gepresenteerd met daarbij suggesties voor toekomstig onderzoek.

Podsumowanie

Inżynieria Biomedyczna to bardzo interdyscyplinarna dziedzina nauki. Jest mieszanką medycyny, biologii, chemii, fizyki i nauk technicznych. Uważana jest za siłę napędową współczesnej medycyny. Głównym zadaniem tej dziedziny nauki jest ciągle udoskonalanie wszelakich technik używanych w dzisiejszej medycynie jak np. ulepszanie sprzętu medycznego lub wytwarzanie nowych materiałów dla potrzeb inżynierii regeneracyjnej. Wszystko po to, aby skuteczniej leczyć, skracać proces rekonwalescencji czy poprawiać komfort życia po zabiegach szpitalnych. Jest to relatywnie nowa, dynamicznie rozwijająca się dziedzina nauki a jednym z głównych jej działów są powszechnie używane biomateriały.

Biomateriały stają się z dnia na dzień wręcz niezbędnym elementem rozwijającej się medycyny. Wraz z rozwojem medycyny wzrasta oczekiwana długość życia człowieka. Przewidywane jest, że do 2050 odsetek ludności powyżej 60 roku życia wzrośnie do 2 miliardów. Liczba osób powyżej 80 roku życia zwiększy się w tym czasie czterokrotnie. Problem starzejacych się społeczeństw to prawdziwe wyzwanie dla medycyny, w tym szczególne dla inżynierii biomedycznej. Starzejące się ludzkie ciało z wiekiem traci wiele funkcji, które są ponad możliwością naturalnej regeneracji. W takiej sytuacji pomocne są właśnie biomateriały, z których wytwarzane są różne implanty, sztuczne organy czy protezy medyczne. Zastosowanie biomateriałów w medycynie gwarantuje częściową lub całkowitą regenerację utraconej funkcji ciała, co polepsza, jakość życia jak np. popularne implanty stawu biodrowego, sztuczne serce, bajpasy, implanty zębów, implanty piersi po chorobie nowotworowej, bądź w celu poprawy urody. Inzynieria medyczna skupia się, zatem na wytwarzaniu coraz to nowych biomateriałów nietoksycznych dla ludzkiego ciała, czyli biokompatybilnych i odpornych na bardzo częste infekcje bakteryjne.

Zakażenia bakteryjne biomateriałów stanowią ciągły problem w szpitalach na całym świecie i są jednym z głównych powodów niepowodzenia zabiegu i odrzucenia wszczepu. Zakażenia te najczęściej są wynikiem bakteryjnej kontaminacji biomateriału w momencie jego implantacji. Najczęstszymi czynnikami etiologicznymi zakażenia miejsca operowanego są bakterie typu *Staphylococcus aureus, Staphylococcus epidermidis, Esherihia coli, Pseudomonas aeruginosa,* czy grzyby z rodzaju *Candida albicans.* Adhezja (czyli przyleganie) bakterii do powierzchni biomateriałów jest pierwszym etapem powstawania infekcji zapoczątkowanym czesto w miejscu zetknięcia się biomateriału ze skórą. Przylegające bakterie mnożą się, rosną w kolonie i wytwarzają śluz, który ułatwia im przyleganie do powierzchni i umożliwia przeżycie w organizmie gospodarza. Śluz stanowi barierę przed składnikami układu odpornościowego, stanowi też swoistą tarczę ochronną, przez co utrudnia penetrację antybiotyków czy innych środków bakteriobójczych. Taka kompleksowa struktura, zbudowana z komórek bakterii, połączonych zewnątrzkomórkowym śluzem nazywana jest biofilmem. Biofilm jest odporny na działanie antybiotyków, dlatego jedynym rozwiązaniem w takiej sytuacji jest usunięcie zakażonego implantu oczyszczenie i dezynfekcja rany oraz reimplantacja, co wiąże się ze zwiększonym ryzykiem ponownej infekcji.

Zapobieganie zakażeniom biomateriałów związanych z powstawaniem biofilmu wiąże się z wprowadzeniem odpowiedniej antyseptyki jak odpowiedniej wentylacji sali operacyjnej, jałowego sprzętu i właściwych technik chirurgicznych. Jednak mimo wielu starań niemożliwością jest utrzymanie 100% sterylnego otoczenia a długoterminowa antybiotykoterapia wiąże się z możliwością wykształcenia odporności u bakterii. Dlatego zadaniem naukowców jest udoskonalanie i tworzenie nowych biomateriałów które będą odporne na infekcje bakteryjne i tym samym nietoksyczne dla ludzkiego organizmu. Literatura

naukowa prezentuje coraz to nowsze rozwiązania, które mają za zadanie pomagać w walce z uporczywymi infekcjami materiałów. Znane są różnorodne modyfikacje powierzchni biomateriałów mające za zadanie np. redukcje adhezji zbliżających się bakterii lub uwalnianie srodków bakteriobójczych. Materiał, zatem może być pokryty warstwą anty-adhezyjną bądź zaimpregnowany odpowiednim antybiotykiem.

W mojej pracy skupiłam się na rozwoju i ulepszeniu materiałów powierzchniowych, jakim są szczotki polimerowe. Szczotki polimerowe składają się z łańcuchów polimerów, które przyczepione do powierzchni materiału w odpowiedniej gęstości i w środowisku wodnym tworzą strukturę przypominającą szczotki. Tak zmodyfikowana powierzchnia zapobiega adhezji bakterii, co jest pierwszym krokiem prowadzącym do infekcji biomateriału.

Rozdział pierwszy (chapter 1) opisuje ogólne wprowadzenie do tematu modyfikacji powierzchni biomateriałów, przedstawia główne problemy z jakimi zmaga się ten obszar badań oraz uzasadnia cel i założenia tej pracy.

Rozdział drugi (chapter 2) opisuje właściwości antyadhezyjne szczotek polimerowych w kontakcie ze zbliżającymi się bakteriami odpowiedzialnymi za powstawanie infekcji w porównaniu z materiałem niepokrytym takimi polimerami. Udowodniliśmy ze biomateriały pokryte szczotkami polimerowymi ułatwiają penetrację antybiotyków, co pozwala na łatwiejszą eliminacją zakażenia. Biofilm powstały na szczotkach jest rzadszy i nie posiada osłonowego śluzu w porównaniu z biofilmem utworzonym na materiałach niepokrytych szczotkami który jest odporny na działanie antybiotyków.

Rozdział trzeci (chapter 3) opisuje modyfikacje szczotek poprzez bezpośrednie przyłączenie do łańcucha polimerowego naturalnego środka antybakteryjnego jakim jest lysozym. Daje to możliwość dwu-funkyjnosci powierzchni poprzez

połączenie właściwości anty-adhezyjnych szczotek i antybakteryjnych lysozymu. Taka modyfikacja pozwala na bezpośrednią eliminację bakterii które stykają się z powierzchnią i redukuje potrzebę dodatkowej ingerencji antybiotyku z zewnątrz.

Rozdział czwarty (chapter 4) opisuje rozwój programu komputerowego, który modeluje reakcje bakterii na zmodyfikowane powierzchnie biomateriałów. Poprzez odpowiednie symulacje komputerowe uzyskaliśmy informacje o optymalnej kompozycji materiałów powłokowych bez konieczności przeprowadzania długotrwałych eksperymentów w laboratorium.

Rozdział piąty (chapter 5) przedstawia dodatkową modyfikację szczotek polimerowych, dzięki czemu uzyskaliśmy trój-funkcyjność powierzchni. Do szczotek zostały przyłączone krótkie peptydy antybakteryjne AMP o silniejszych właściwościach bakteriobójczych niż lyzozym. Szczególną zaletą peptydów AMP jest rzadkość występowania bakteryjnej odporności na ich działanie. Kolejną modyfikacją szczotek polimerowych było przyłączenie do łańcucha krótkich peptydów zawierających sekwencje RGD (czyli R: arginina, G: glicyna, D: kwas asparaginowy) odpowiedzialne za poprawną integracją komórek tkankowych, czyli proces gojenia rany. W ten sposób uzyskaliśmy funkcjonalny materiał powłokowy o właściwościach anty-adhezyjnych dzięki szczotkom polimerowym, bakteriobójczy dzięki obecnym peptydom AMP oraz zdolny do adhezji komórek eukariotycznych dzięki peptydom RGD.

Rozdział szósty (chapter 6) to ogólna dyskusja gdzie podkreślamy zalety naszych projektów w celu dalszego rozwoju do przyszłych zastosowań oraz omawiamy ograniczenia w naszej metodologii. Przedstawiamy także główne wnioski pracy oraz sugestie do przyszłych badań.

Acknowlegdements

Completing this PhD thesis wouldn't be possible without help and support I received from many people during this past four years.

Willem, I respect your professionalism, experience, knowledge and wisdom. I was very lucky to have you as my advisor and I appreciate all the liberty, trust and confidence invested in me. I have developed various skill sets necessary to be a good scientist under your mentorship.

Henk and Henny, thank you for giving me the opportunity to start this PhD. I have always received an extensive scientific feedback from both of you during my research. Thank you for your positive attitude and convincing capability without which it would be difficult to finish this PhD work. I admire you both and appreciate that I got the chance to continue my research adventures with you.

Andreas, I think I would need four more years of a PhD to execute all your creative ideas. Thank you for the scientific support, guidance and enthusiasm.

Ton, thank you for very careful revisions of my thesis. I appreciate to get the opportunity of working with you.

Wya, thank you for help with all the financial paper work.
Ina and Willy thank you for all the administrative support and for help with formatting this book.

My collaborators: Agnieszka, Andreas, Yun, Ed thank you for being involved in my projects, I enjoyed working with you. The quality of this thesis wouldn't be the same without your contribution.

Jan, thank you for taking the time to translate my summary into Dutch.
Ed, thank you for designing the cover of my thesis.

My dear paranimfen Lucja and Agnieszka thank you for all your support and for being next to me on this important day.

Gesinda, Betsy, Minnie, Jelly, Marja, Rene, Marianne thank you for all the help and advices with my experiments and for making the lab a pleasant place to work in.

All BME friends especially Katja, Sara, Rebbecca, Brandon, Prashant, Joop, Jan, Akshay, Ed, Joanna, Jesse, Raquel, Arina, Otto, Sharifi, Anton, Stefan, Jenny, Adam thank you for all the fun and unforgettable moments we shared during my PhD time.

Leeman, Lanus, Rhodium, Edje, Davide & Gini, Laura, Joost, Wesley, Hans you made my first two years in Groningen a very memorable time. Thank you for all the crazy parties. I am very happy to have you as my friends.

Drodzy przyjaciele na emigracji Ola, Gosia, Joanna, Magda, Marta, Gosia i Pawel, Kasia i Antek dziekuję za wszystkie wspólne imprezy, pogaduchy, wyjazdy. O wiele milej się tu mieszka mając tak świetne towarzystwo!

Drodzy rodzice dziekuję za wszystko zwłaszcza cierpliwość i ogromne zaufanie. Dziekuję za wsparcie moralne i inne czary mary które przyczyniły sie do ukończenia przeze mnie tego doktoratu.
Dziekuję moim wszystkim przyjaciołom i całej rodzinie w Polsce.

Deepak thank you for all your patience, motivation and optimism. I am grateful to have you in my life and I wish we share many happy moments together.

Agnieszka Muszanska was born on September 14th, 1982 in Rymanów, Poland. In 2006 she obtained her MSc degree in Biotechnology (Department of Chemistry) at the Wroclaw University of Technology, Poland. After graduation she joined the Leonardo Da Vinci European programme and did her internship at Chemtura (Polymer Chemistry) in Herentals, Belgium. To pursue her career in Industry she moved to Groningen, the Netherlands and worked at Syncom BV as a research chemist. In March 2009 she started her PhD in University of Groningen. She worked in the department of Biomedical Engineering under the supervision of Willem Norde, Henk Busscher and Henny van der Mei. Her PhD work emphasizes the development of polymer brush-coatings for biomaterials to prevent implant infections. She continues her work at the University of Groningen as a post-doctoral researcher on the development of antimicrobial coatings for biomaterials under supervision of Ton Loontjes.